Simulations of Idealized Solid Electrolytes for Solid State Battery Designs*

N. A. W. Holzwarth**

Department of Physics

Wake Forest University, Winston-Salem, NC, USA, 27109

*Supported by NSF Grant DMR-1507942, WFU's DEAC cluster, and Center for Energy, Environment, and Sustainability.

**With help from: Nicholas Lepley (WFU Ph. D., Dec. 2015) , Ahmad Al-Qawasmeh, Jason Howard, and Larry Rush (WFU graduate students), Dr. Yaojun Du (former Postdoc), colleagues from the WFU chemistry department – Dr. Keerthi Senevirathne (currently at Florida A & M U.), Dr. Cynthia Day, Professor Michael Gross, Professor Abdessadek Lachgar, and Zachary Hood (currently at Georgia Tech and ORNL), and Professor Jennifer Aitken from Duquesne U.

Outline

- **Motivation – Why solid electrolytes?**
- **Computational tools & reality checks; "first principles" calculations**
- **Some examples based on crystalline materials**
  - **Li phosphorus oxynitrides (first developed at Oak Ridge National Laboratory)**
  - **Li thiophosphates**
  - **Other examples**
- **Summary and remaining challenges**

Motivation –
Why solid electrolytes?

Materials components of a Li or Na ion battery

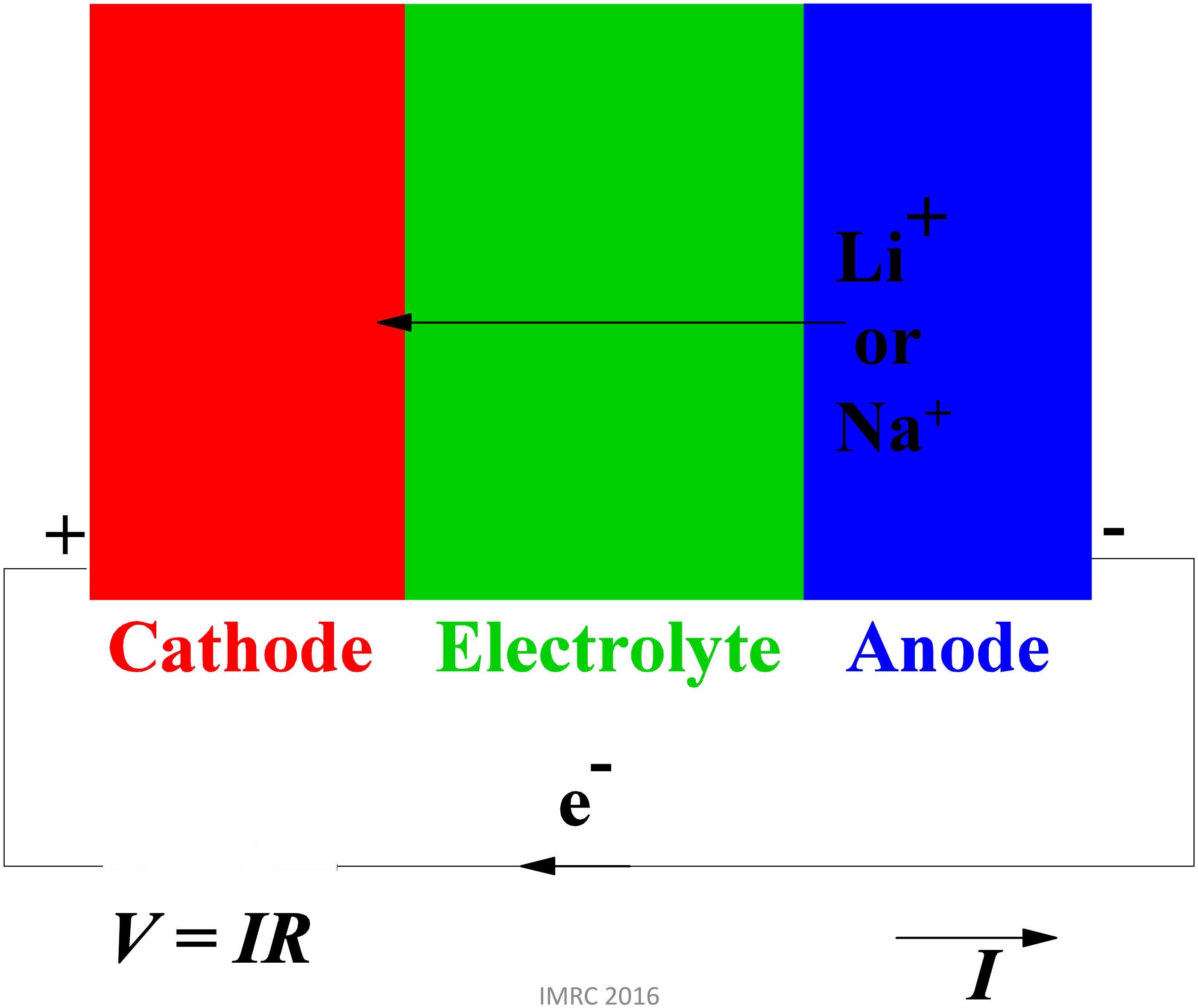

From Toyota Motor Company Website:

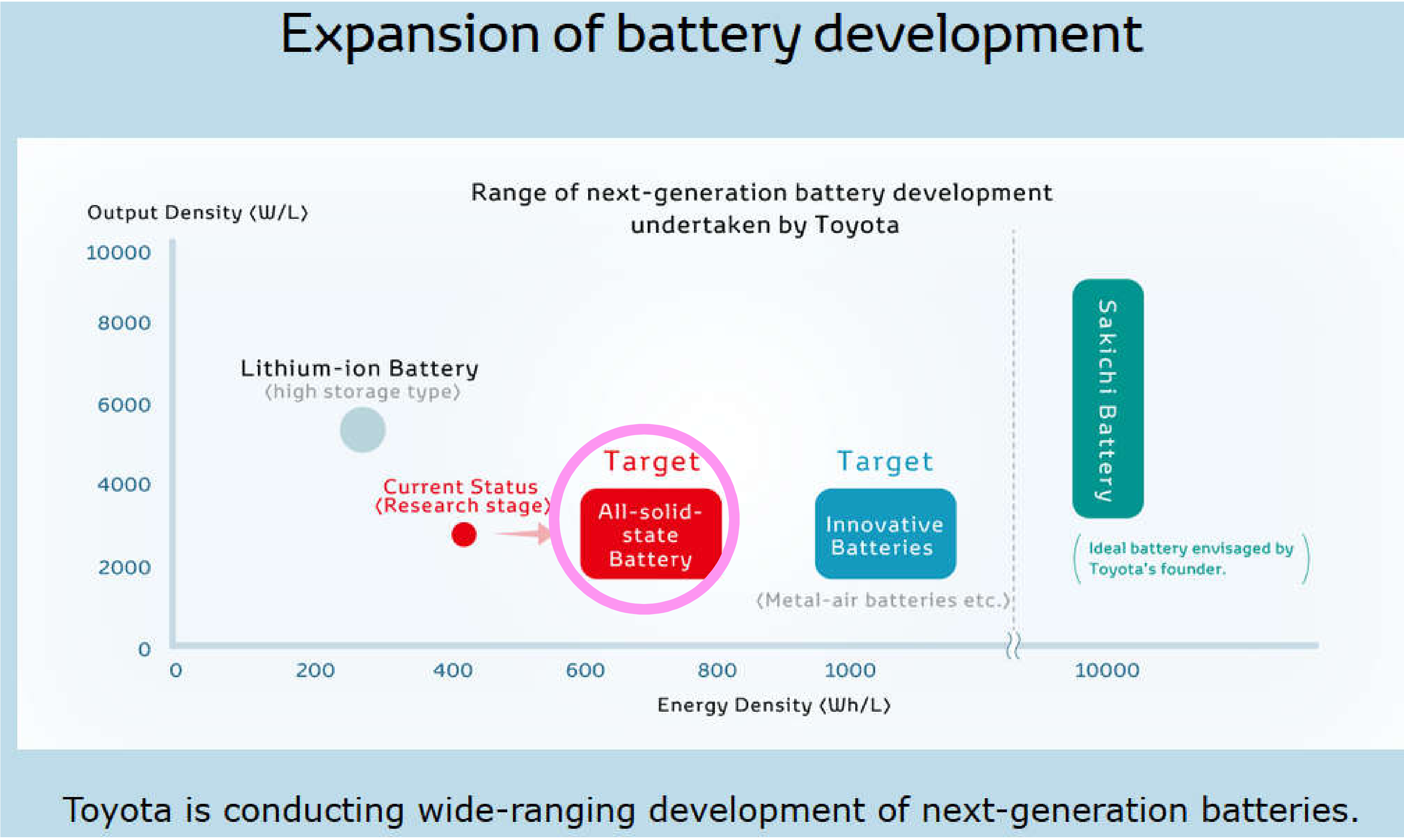

http://www.toyota-global.com/innovation/environmental_technology/keytech/

From Oak Ridge National Laboratory:

WAKE FOREST UNIVERSITY

Materials Views www.MaterialsViews.com
Adv. Energy Mater. 2015, 5, 1401408
ADVANCED ENERGY MATERIALS www.advenergymat.de
DOI: 10.1002/aenm.201401408

Solid Electrolyte: the Key for High-Voltage Lithium Batteries

Juchuan Li, Cheng Ma, Miaofang Chi, Chengdu Liang, and Nancy J. Dudney**

Advantages

- **Compatible and stable with high voltage cathodes and with Li metal anodes**

Disadvantages

- **Relatively low ionic conductivity (Compensated with the use of less electrolyte?)**
- **Lower total capacity**

Demonstrated for $LiNi_{0.5}Mn_{1.5}O_4$/LiPON/Li

- **10^{-6} m LiPON electrolyte layer achieved adequate conductivity**
- **10,000 cycles* with 90% capacity retention**

***1 cycle per day for 27 years**

Motivation: Paper by N. Kayama, *et. al* in ***Nature Materials*** **10**, 682-686 (2011)

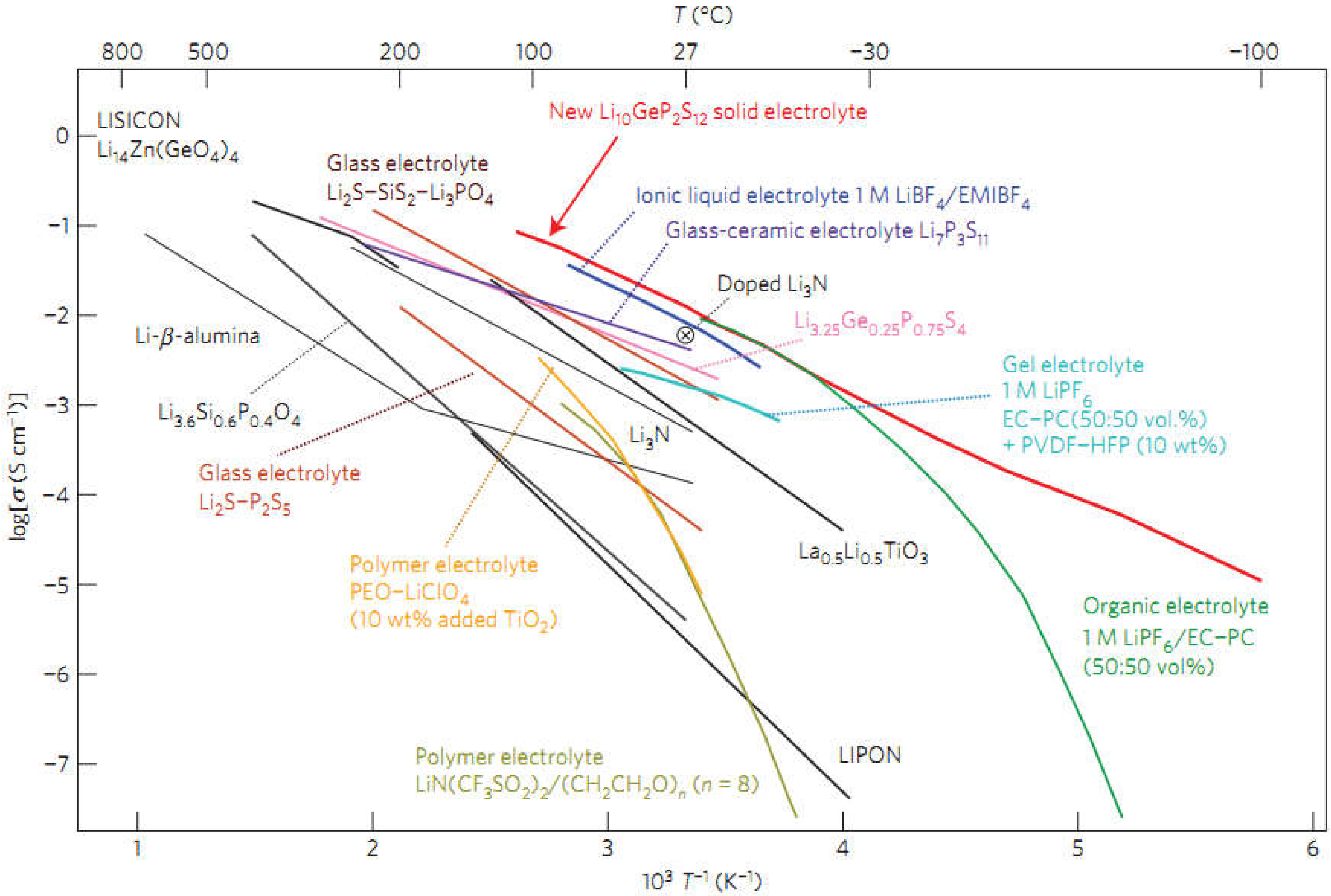

Figure 3 | Thermal evolution of ionic conductivity of the new $Li_{10}GeP_2S_{12}$ phase, together with those of other lithium solid electrolytes, organic liquid electrolytes, polymer electrolytes, ionic liquids and gel electrolytes[3-8,13-16,20,22]. The new $Li_{10}GeP_2S_{12}$ exhibits the highest lithium ionic conductivity ($12\ m\ S\ cm^{-1}$ at 27 °C) of the solid lithium conducting membranes of inorganic, polymer or composite systems. Because organic electrolytes usually have transport numbers below 0.5, inorganic lithium electrolytes have extremely high conductivities.

Motivation: Paper by N. Kamaya, *et. al* in ***Nature Materials* 10**, 682-686 (2011)

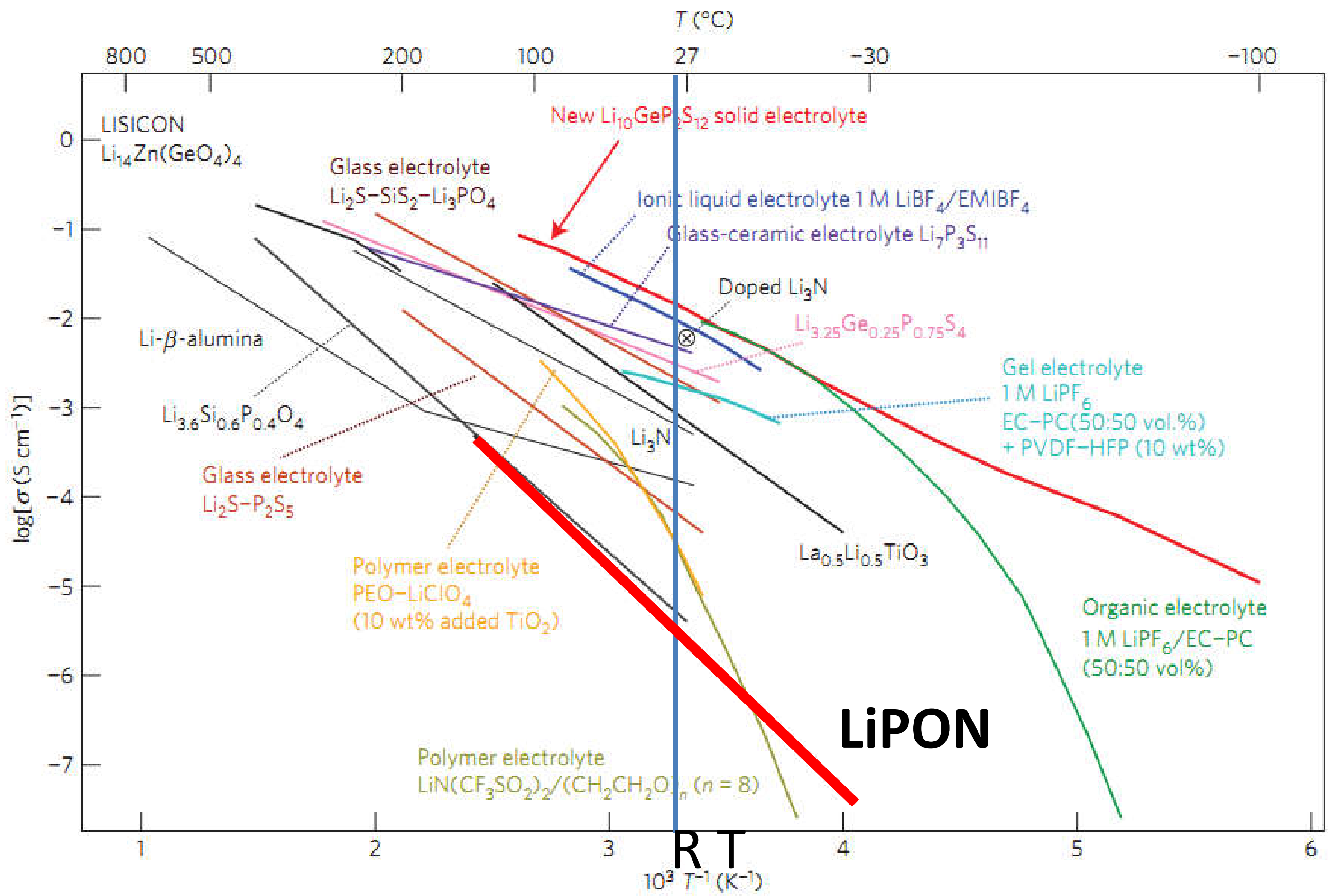

Figure 3 | Thermal evolution of ionic conductivity of the new $Li_{10}GeP_2S_{12}$ phase, together with those of other lithium solid electrolytes, organic liquid electrolytes, polymer electrolytes, ionic liquids and gel electrolytes[3-8,13-16,20,22]. The new $Li_{10}GeP_2S_{12}$ exhibits the highest lithium ionic conductivity (12 m S cm^{-1} at 27 °C) of the solid lithium conducting membranes of inorganic, polymer or composite systems. Because organic electrolytes usually have transport numbers below 0.5, inorganic lithium electrolytes have extremely high conductivities.

Motivation: Paper by N. Kamaya, *et. al* in ***Nature Materials*** **10**, 682-686 (2011)

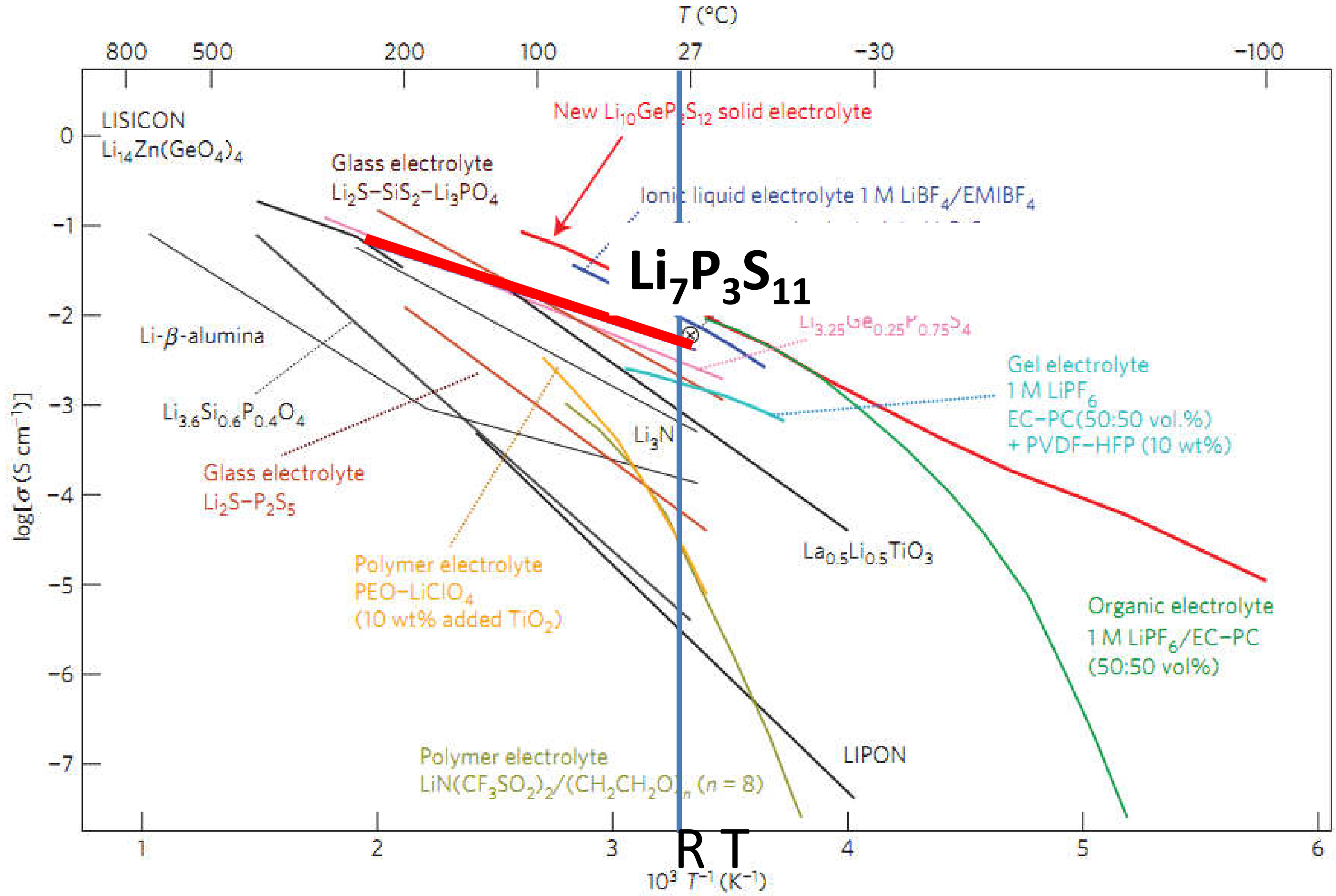

Figure 3 | Thermal evolution of ionic conductivity of the new $Li_{10}GeP_2S_{12}$ phase, together with those of other lithium solid electrolytes, organic liquid electrolytes, polymer electrolytes, ionic liquids and gel electrolytes[3-8,13-16,20,22]. The new $Li_{10}GeP_2S_{12}$ exhibits the highest lithium ionic conductivity ($12\ \mathrm{m\ S\ cm^{-1}}$ at 27 °C) of the solid lithium conducting membranes of inorganic, polymer or composite systems. Because organic electrolytes usually have transport numbers below 0.5, inorganic lithium electrolytes have extremely high conductivities.

Motivation: Paper by N. Kamaya, *et. al* in ***Nature Materials* 10**, 682-686 (2011)

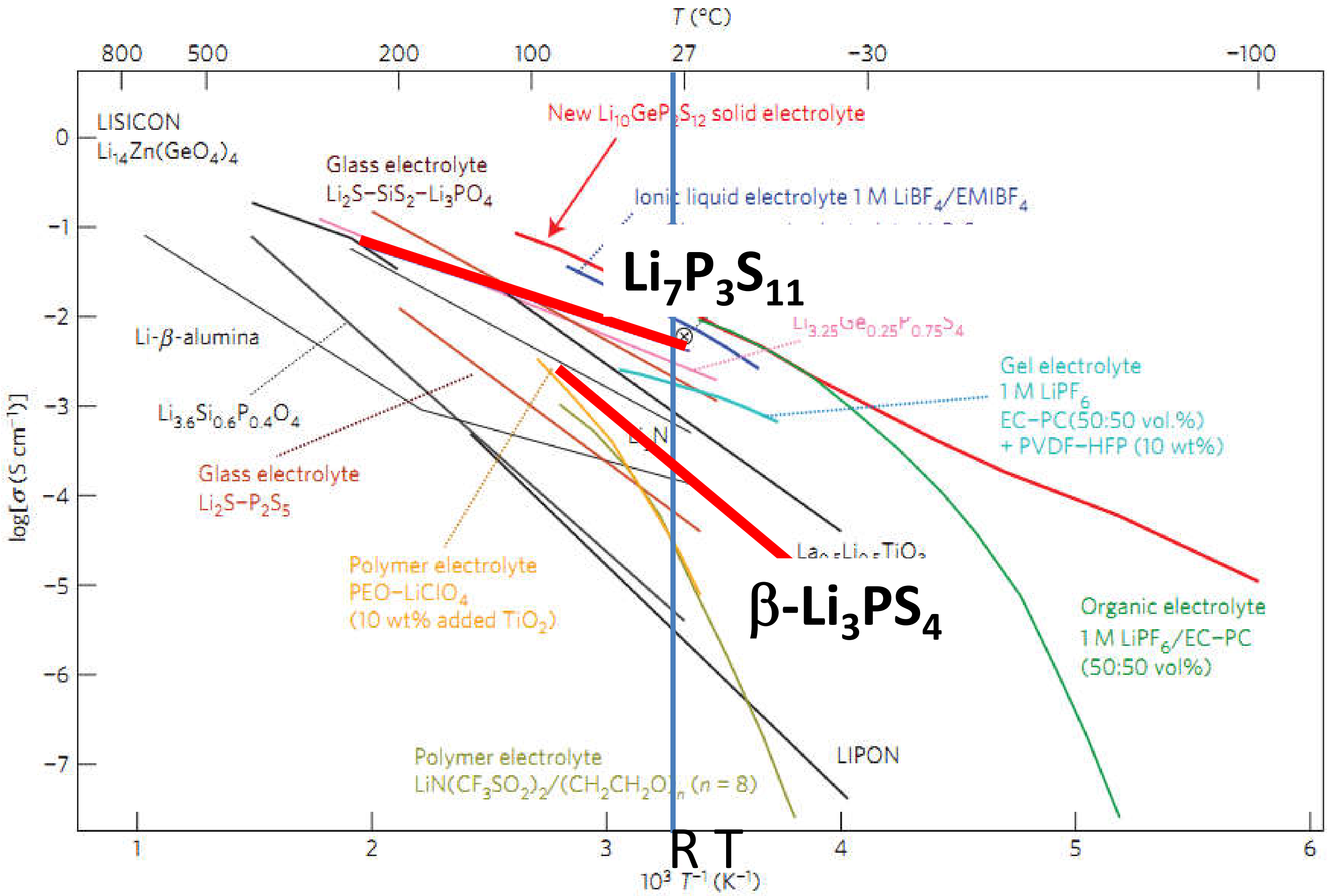

Figure 3 | Thermal evolution of ionic conductivity of the new $Li_{10}GeP_2S_{12}$ phase, together with those of other lithium solid electrolytes, organic liquid electrolytes, polymer electrolytes, ionic liquids and gel electrolytes[3-8,13-16,20,22]. The new $Li_{10}GeP_2S_{12}$ exhibits the highest lithium ionic conductivity (12 m S cm^{-1} at 27 °C) of the solid lithium conducting membranes of inorganic, polymer or composite systems. Because organic electrolytes usually have transport numbers below 0.5, inorganic lithium electrolytes have extremely high conductivities.

Motivation: Paper by N. Kamaya, *et. al* in ***Nature Materials*** **10**, 682-686 (2011)

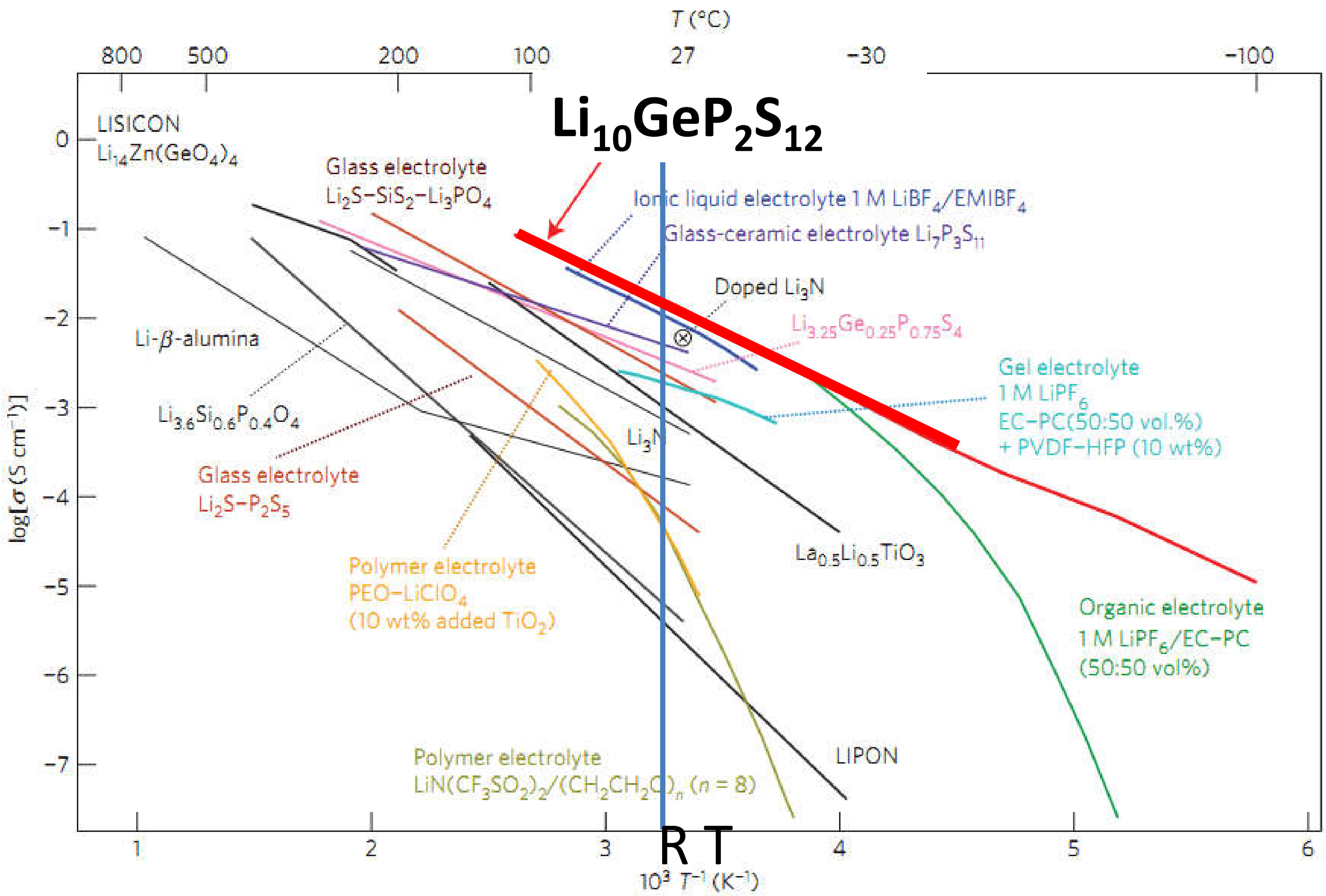

Figure 3 | Thermal evolution of ionic conductivity of the new $Li_{10}GeP_2S_{12}$ phase, together with those of other lithium solid electrolytes, organic liquid electrolytes, polymer electrolytes, ionic liquids and gel electrolytes[3-8,13-16,20,22]. The new $Li_{10}GeP_2S_{12}$ exhibits the highest lithium ionic conductivity (12 m S cm^{-1} at 27 °C) of the solid lithium conducting membranes of inorganic, polymer or composite systems. Because organic electrolytes usually have transport numbers below 0.5, inorganic lithium electrolytes have extremely high conductivities.

Solid Electrolyte Families Investigated in this Study:

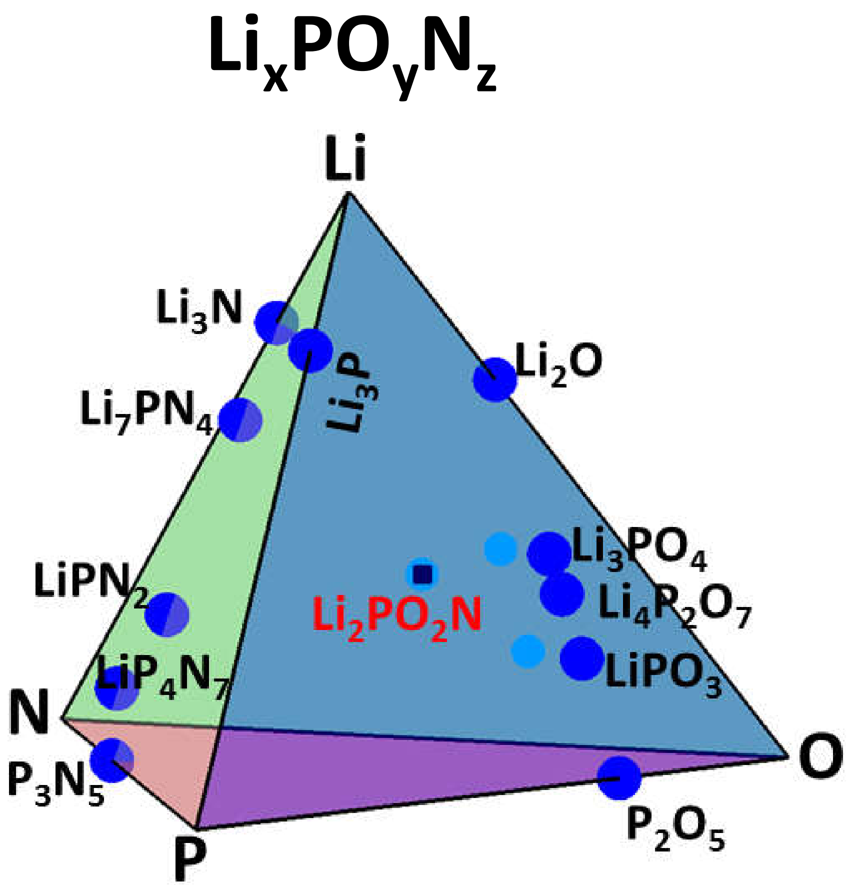

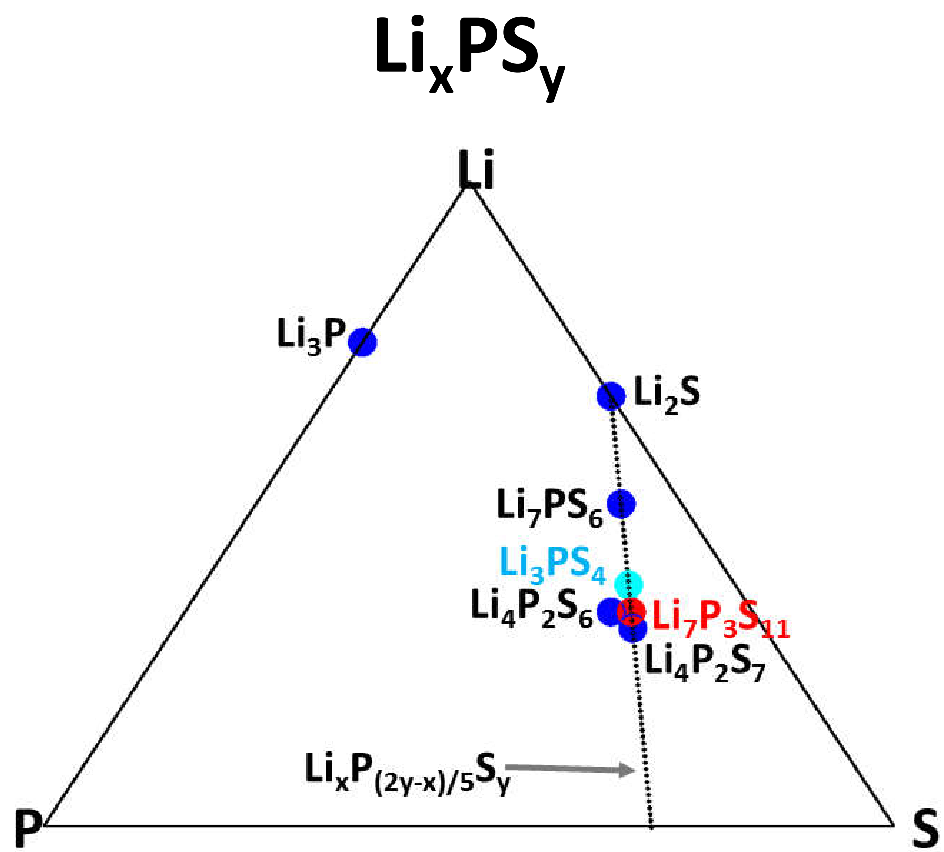

Computational tools

WAKE FOREST UNIVERSITY

Summary of "first-principles" calculation methods

Electronic coordinates

Atomic coordinates

Exact Schrödinger equation:

$$\mathcal{H}(\{\mathbf{r}_i\},\{\mathbf{R}^a\})\Psi_\alpha(\{\mathbf{r}_i\},\{\mathbf{R}^a\}) = E_\alpha \Psi_\alpha(\{\mathbf{r}_i\},\{\mathbf{R}^a\})$$

where

$$\mathcal{H}(\{\mathbf{r}_i\},\{\mathbf{R}^a\}) = \mathcal{H}^{\text{Nuclei}}(\{\mathbf{R}^a\}) + \mathcal{H}^{\text{Electrons}}(\{\mathbf{r}_i\},\{\mathbf{R}^a\})$$

Born-Oppenheimer approximation

Born & Huang, **Dynamical Theory of Crystal Lattices**, Oxford (1954)

Approximate factorization:

$$\Psi_\alpha(\{\mathbf{r}_i\},\{\mathbf{R}^a\}) = X_\alpha^{\text{Nuclei}}(\{\mathbf{R}^a\})\Upsilon_\alpha^{\text{Electrons}}(\{\mathbf{r}_i\},\{\mathbf{R}^a\})$$

Treated with classical mechanics

Treated with density functional theory

Electronic Schrödinger equation:

WAKE FOREST UNIVERSITY

$$\mathcal{H}^{\text{Electrons}}(\{\mathbf{r}_i\},\{\mathbf{R}^a\})\Upsilon_\alpha^{\text{Electrons}}(\{\mathbf{r}_i\},\{\mathbf{R}^a\}) = U_\alpha(\{\mathbf{R}^a\})\Upsilon_\alpha^{\text{Electrons}}(\{\mathbf{r}_i\},\{\mathbf{R}^a\})$$

$$\mathcal{H}^{\text{Electrons}}(\{\mathbf{r}_i\},\{\mathbf{R}^a\}) = -\frac{\hbar^2}{2m}\sum_i \nabla_i^2 - \sum_{a,i}\frac{Z^a e^2}{|\mathbf{r}_i - \mathbf{R}^a|} + \sum_{i<j}\frac{e^2}{|\mathbf{r}_i - \mathbf{r}_j|}$$

For electronic ground state: $\alpha \Rightarrow 0$

Density functional theory

Hohenberg and Kohn, *Phys. Rev.* **136** B864 (1964)

Kohn and Sham, *Phys. Rev.* **140** A1133 (1965)

Mean field approximation: $U_0(\{\mathbf{R}^a\}) \Rightarrow U_0(\{\rho(\mathbf{r})\},\{\mathbf{R}^a\})$

Electron density

Kohn-Sham construction: $\rho(\mathbf{r}) \approx \rho_{KS}(\mathbf{r}) = \sum_n |\psi_n(\mathbf{r})|^2$

$$\mathcal{H}_{\text{KS}}^{\text{Electrons}}(\mathbf{r},\rho(\mathbf{r}),\{\mathbf{R}^a\})\psi_n(\mathbf{r}) = \varepsilon_n\psi_n(\mathbf{r})$$

Independent electron wavefunction

WAKE FOREST UNIVERSITY

More computational details:

$$\mathcal{H}_{KS}^{\text{Electrons}}(\mathbf{r},\rho(\mathbf{r}),\{\mathbf{R}^a\}) = -\frac{\hbar^2\nabla^2}{2m} + \underbrace{\sum_a \frac{-Z^a e^2}{|\mathbf{r}-\mathbf{R}^a|}}_{\text{electron-nucleus}} + \underbrace{e^2\int d^3r' \frac{\rho(\mathbf{r}')}{|\mathbf{r}-\mathbf{r}'|}}_{\text{electron-electron}} + \underbrace{V_{xc}(\rho(\mathbf{r}))}_{\text{exchange-correlation}}$$

Exchange-correlation functionals:

LDA: J. Perdew and Y. Wang, Phys. Rev. B **45**, 13244 (1992)

GGA: J. Perdew, K. Burke, and M. Ernzerhof, PRL **77**, 3865 (1996)

HSE06: J. Heyd, G. E. Scuseria, and M. Ernzerhof, JCP **118**, 8207 (2003)

Numerical methods:

“Muffin-tin” construction: Augmented Plane Wave developed by Slater → “linearized” version by Andersen:

J. C. Slater, Phys. Rev. **51** 846 (1937)

O. K. Andersen, Phys. Rev. B **12** 3060 (1975) (LAPW)

Pseudopotential methods:

J. C. Phillips and L. Kleinman, Phys. Rev. **116** 287 (1959) -- original idea

P. Blöchl, Phys. Rev. B. 50 17953 (1994) – Projector Augmented Wave (PAW) method

Outputs of calculations:

Ground state energy:

$U_0(\{\rho(\mathbf{r})\},\{\mathbf{R}^a\})$ $\Rightarrow$ Determine formation energies

$\min\big|_{\{\mathbf{R}^a\}}\left(U_0(\{\rho(\mathbf{r})\},\{\mathbf{R}^a\})\right)$ $\Rightarrow$ Determine structural parameters

$\Rightarrow$ Stable and meta-stable structures

$\rho_{KS}(\mathbf{r})=\sum_n|\psi_n(\mathbf{r})|^2$ $\Rightarrow$ Self-consistent electron density

$\{\varepsilon_n\}$ $\Rightarrow$ One-electron energies; densities of states

Nuclear Hamiltonian (usually treated classically)

$$\mathcal{H}^{\text{Nuclei}}\left(\{\mathbf{R}^a\}\right)=\sum_a\frac{\mathbf{P}^{a2}}{2M^a}+U_0(\{\rho(\mathbf{r})\},\{\mathbf{R}^a\})$$

➔ Normal modes of vibration

WAKE FOREST UNIVERSITY

Codes used for calculations

Function	Code	Website
Generate atomic datasets	ATOMPAW	http://pwpaw.wfu.edu
DFT; optimize structure	PWscf abinit	http://www.quantum-espresso.org http://www.abinit.org
Structural visualization	XCrySDen VESTA	http://ww.xcrysden.org http://jp-minerals.org/vesta/en/

WAKE FOREST UNIVERSITY

ATOMPAW Code for generating atomic datasets for PAW calculations

Holzwarth, Tackett, and Matthews, CPC 135 329 (2001) http://pwpaw.wfu.edu

- ATOMPAW
- INFO
- DATASETS
- CONTRIBUTERS
- CONTACT INFO
- NAWH Web
- PHYSICS Web
- WFU Web

ATOMPAW

Download source code and example files:

- atompaw-4.0.0.13.tar.gz (5.4mb) 2/15/2016 Marc Torrent introduced improvements to XML output for abinit and new option for command line determination of version. MT also prepared some notes in text format or in PDF format to install atompaw under MacOS. In addition, NH made some slight changes to the UPF output for Quantum Espresso towards compatibility with libxc.
- atompaw-3.1.0.3.tar.gz (3.8mb) - January 2014 - Older version of atompaw with contributions from Marc Torrent and Francois Jollet as well as several others.
- pwpaw_2.4.tgz (0.2 mb) Updated 05/12/2010 version of *pwpaw* with very minor changes to accomodate changes to input files generated by new *atompaw* output files; also includes a BSD license file.

Atomic PAW datasets:
Comparison with LAPW results for binding energy curves --

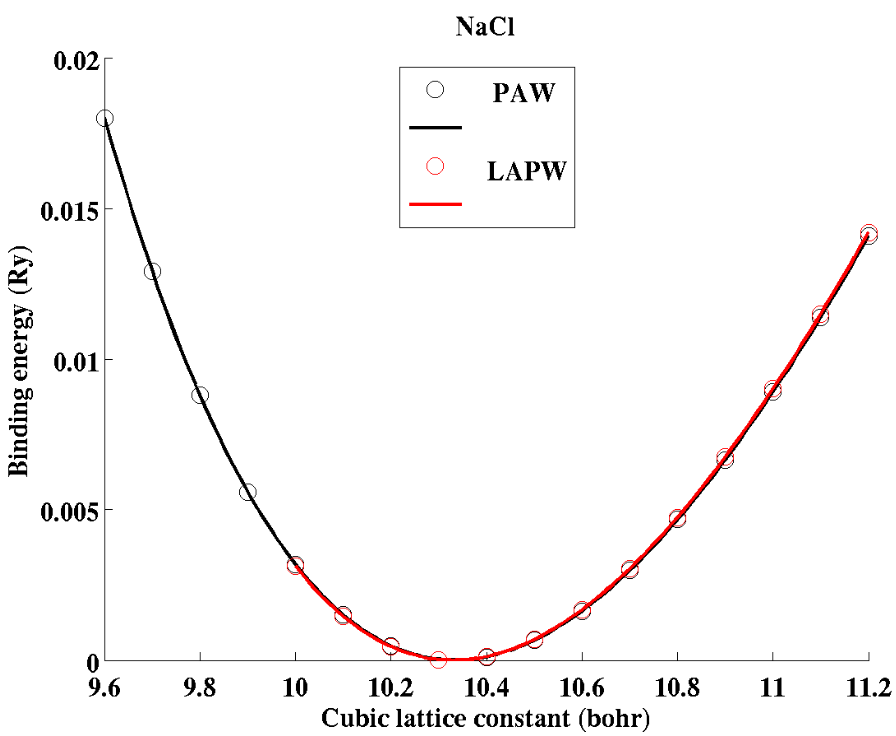

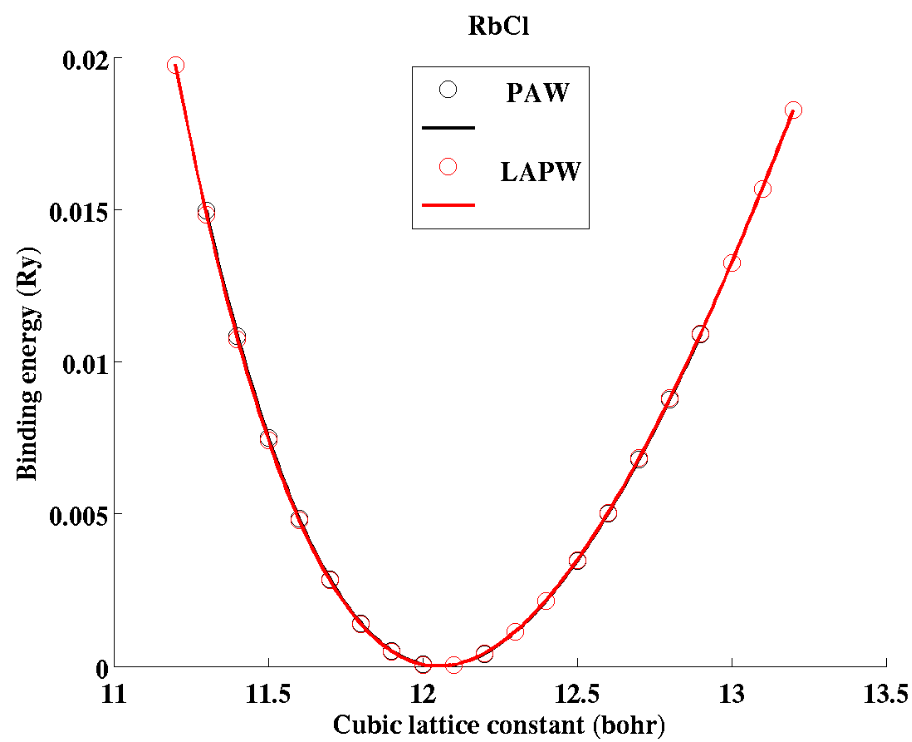

Validation

Li_3PO_4 crystals

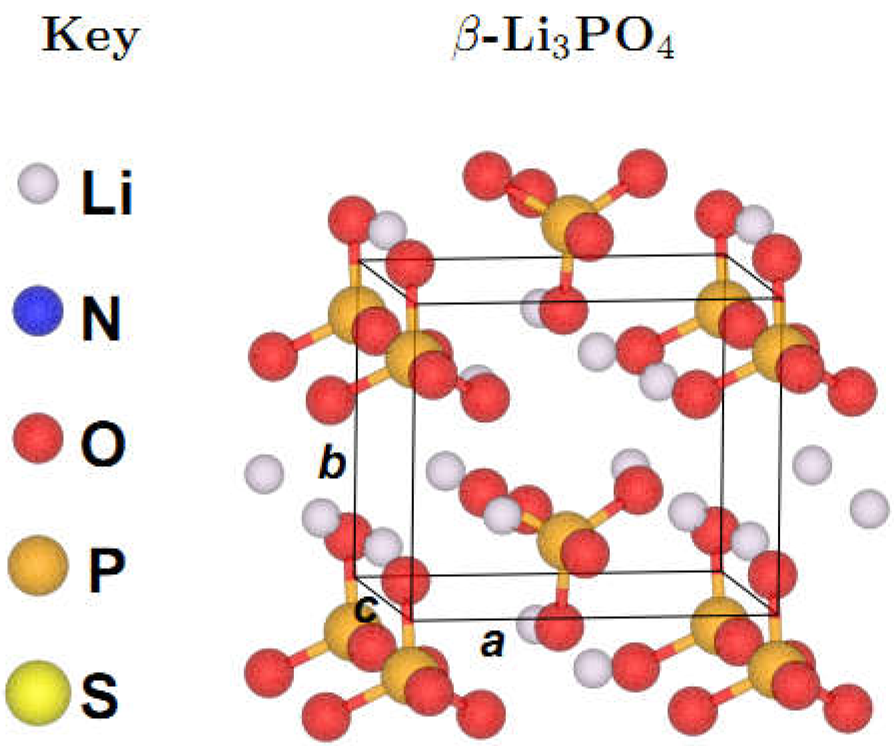

($Pmn2_1$)

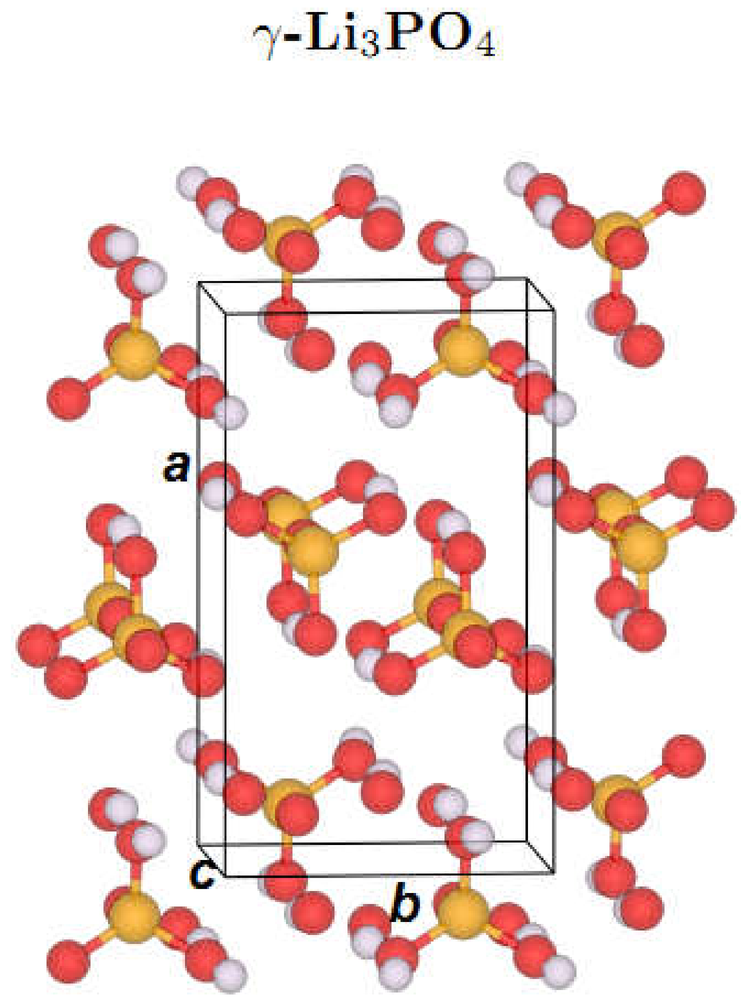

(Pnma)

Validation of calculations

Raman spectra – Experiment & Calculation

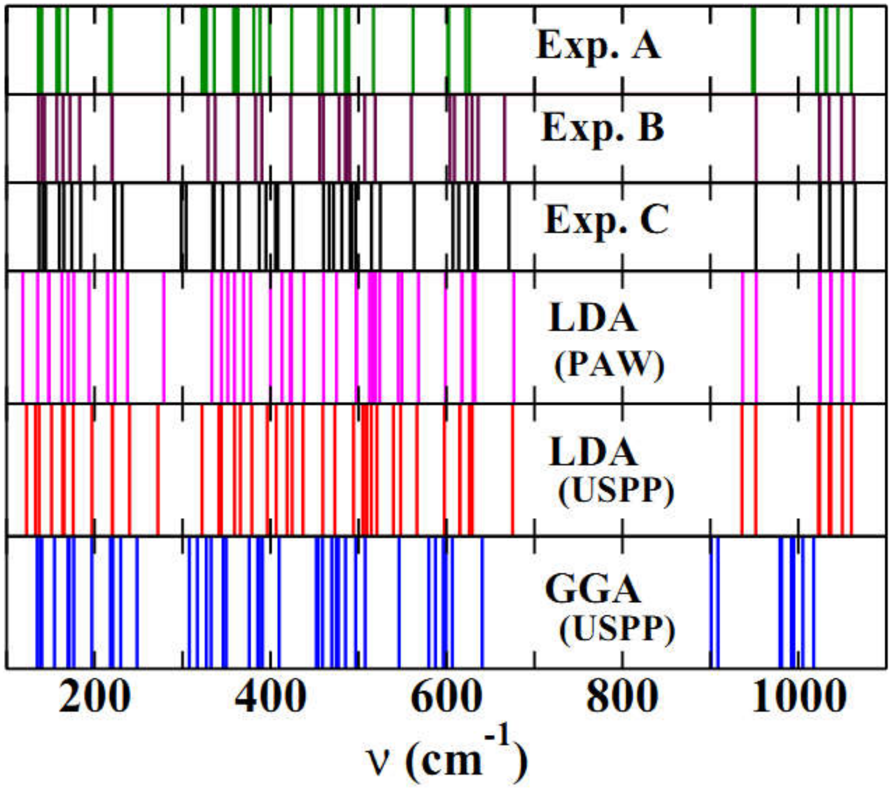

γ-Li_3PO_4

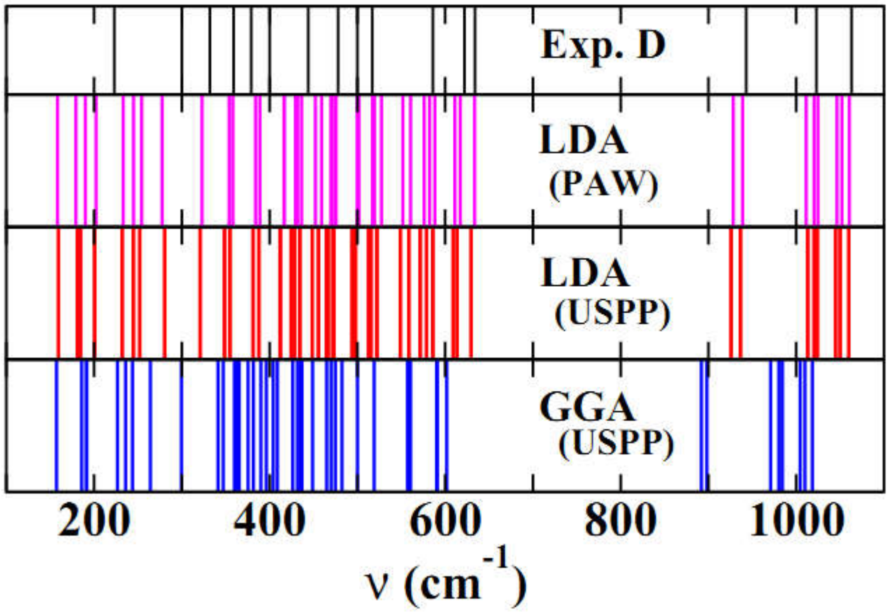

β-Li_3PO_4

A: B. N. Mavrin et al, J. Exp. Theor. Phys. **96**,53 (2003); B: F. Harbach and F. Fischer, Phys. Status Solidi B **66**, 237 (1974) – room temp. C: Ref. B at liquid nitrogen temp.; D: L. Popović et al, J. Raman Spectrosc. **34**,77 (2003).

Heats of formation – Experiment & Calculation

WAKE FOREST UNIVERSITY

Table 1. Calculated heats of formation for Li phosphates, phospho-nitrides, and thiophosphates and related materials. The structural designation uses the the notation defined in the International Table of Crystallography[85] based on structural information reported in the International Crystal Structure Database.[86] The heats of formation ΔH (eV/FU) are given in units of eV per formula unit. When available from Ref. [31] and [32] experiment values are indicated in parentheses. Those indicated with "*" were used fitting the O and N reference energies as explained in the text.

Material	Structure	ΔH (eV/FU)
β-Li_3PO_4	$Pmn2_1$ (#31)	-21.23
γ-Li_3PO_4	$Pnma$ (#62)	-21.20 (-21.72*)
γ-Li_3PS_4	$Pmn2_1$ (#31)	- 8.37
β-Li_3PS_4	$Pnma$ (#62)	- 8.28
$Li_4P_2O_6$	$P\bar{3}1m$ (#162)	-29.72
$Li_4P_2O_7$	$P\bar{1}$ (#2)	-33.97
$Li_5P_2O_6N$	$P\bar{1}$ (#2)	-33.18
$Li_4P_2S_6$	$P\bar{3}1m$ (#162)	-12.42
$Li_4P_2S_7$	$P\bar{1}$ (#2)	-11.59
$Li_7P_3O_{11}$	$P\bar{1}$ (#2)	-54.84
$Li_7P_3S_{11}$	$P\bar{1}$ (#2)	-20.01
$LiPO_3$	$P2/c$ (#13)	-12.75
$LiPN_2$	$I\bar{4}2d$ (#122)	- 3.65
$s1$-Li_2PO_2N	$Pbcm$ (#57)	-12.35
SD-Li_2PO_2N	$Cmc2_1$ (#36)	-12.47
SD-Li_2PS_2N	$Cmc2_1$ (#36)	- 5.80

Material	Structure	ΔH (eV/FU)
N_2O_5	$P6_3/mmc$ (#194)	- 0.94 (- 0.45*)
P_3N_5	$C2/c$ (#15)	- 3.02 (- 3.32*)
h-P_2O_5	$R3c$ (#161)	-15.45 (-15.53*)
o-P_2O_5	$Fdd2$ (#43)	-15.78
P_2S_5	$P\bar{1}$ (#2)	- 1.93
P_4S_3	$Pnma$ (#62)	- 2.45 (- 2.33)
SO_3	$Pna2_1$ (#33)	- 4.84 (- 4.71*)
Li_3N	$P6/mmm$ (#191)	- 1.60 (- 1.71*)
Li_2O	$Fm\bar{3}m$ (#225)	- 6.10 (- 6.20*)
Li_2O_2	$P6_3/mmc$ (#194)	- 6.35 (- 6.57*)
Li_3P	$P6_3/mmc$ (#194)	- 3.47
Li_2S	$Fm\bar{3}m$ (#225)	- 4.30 (- 4.57)
Li_2S_2	$P6_3/mmc$ (#194)	- 4.09
$LiNO_3$	$R\bar{3}c$ (#167)	- 5.37 (- 5.01*)
Li_2SO_4	$P2_1/c$ (#14)	-14.63 (-14.89*)

Estimate of ionic conductivity assuming activated hopping

Schematic diagram of minimal energy path

Approximated using NEB algorithm[a]
– "Nudged Elastic Band"

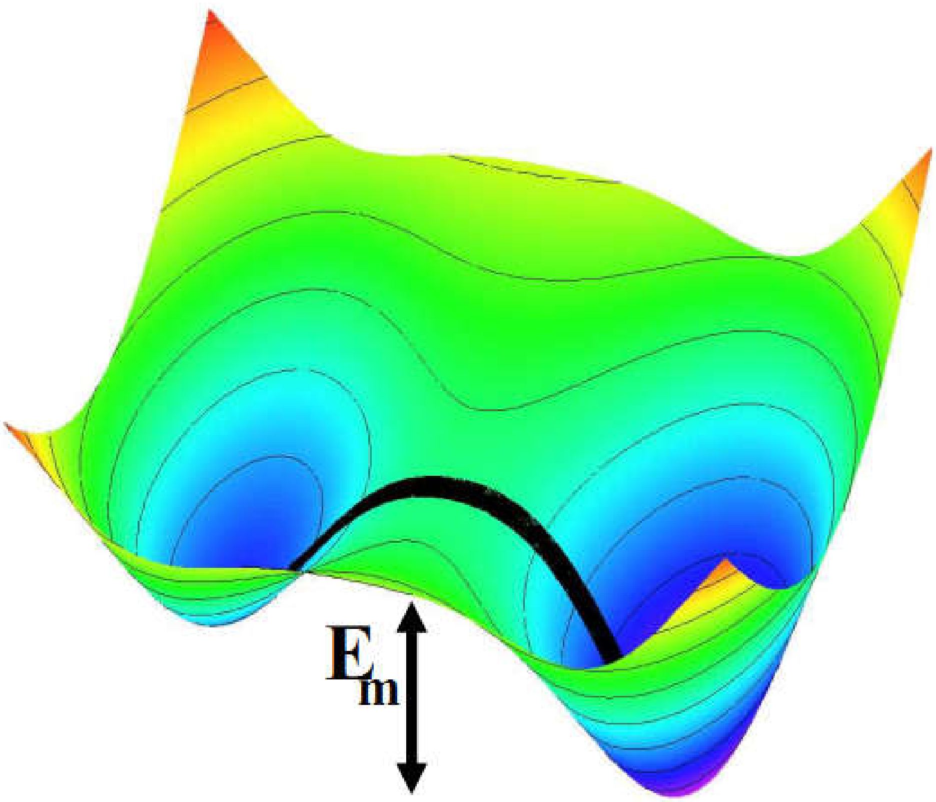

[a]Henkelman and Jónsson, *JCP* **113**, 9978 (2000)

Arrhenius relation

$$\sigma \cdot T = K e^{-E_A/kT}$$

From: Ivanov-Shitz and co-workers, *Cryst. Reports* **46**, 864 (2001):

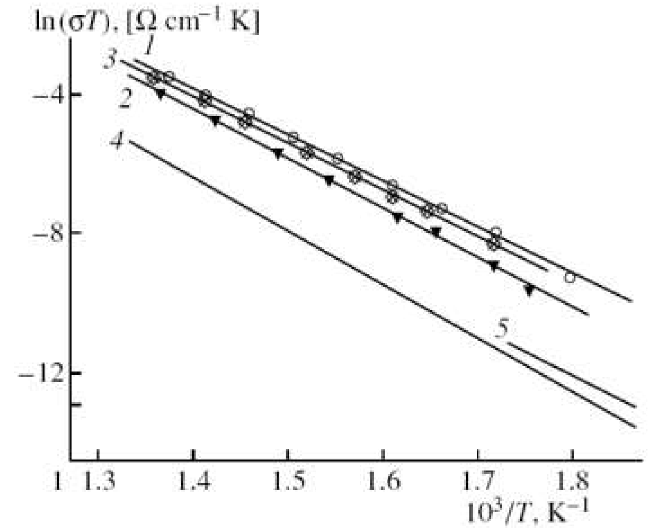

Fig. 2. Temperature dependences of conductivity in γ-Li_3PO_4: (*1–3*) for single crystals measured along the (*1*) *a*-axis, (*2*) *b*-axis, (*3*) *c*-axis and (*4*, *5*) for a polycrystal (*4*) according to [4, 5] and (*5*) according to [7].

E_A = 1.14, 1.23, 1.14, 1.31, 1.24 eV for 1,2,3,4,5, respectively.

Arrhenius activation energies – Experiment and Calculation

Table 3. Calculated migration energies (E_m^{cal}) for Li ion vacancies (vac) and interstitials (int), vacancy-interstitial formation energies (E_f^{cal}), and corresponding the activation energies (E_A^{cal}) for crystalline materials computed using the NEB method in idealized supercells. When available, experimental activation energies E_A^{exp} are also listed together with additional information including the literature reference indicated in [ ] brackets. For γ-Li_3PO_4, results for different crystallographic directions are quoted to compare with single crystal experiment; in other cases, only the minimum energies are given. All energies are given in eV.

$$E_A^{cal} \approx E_m^{cal} + \frac{1}{2}E_f^{cal}$$

Material	vac E_m^{cal}	int E_m^{cal}	E_f^{cal}	E_A^{cal}	E_A^{exp}	Reference
β-Li_3PO_4	0.7	0.4	2.1	1.4		
γ-Li_3PO_4	0.7, 0.7	0.4, 0.3	1.7	1.3, 1.1	1.23, 1.14	(sngl. cryst.) [100]
$Li_{2.88}PO_{3.73}N_{0.14}$					0.97	(poly cryst.) [58]
$Li_{3.3}PO_{3.9}N_{0.17}$					0.56	(amorphous) [58]
$Li_{1.35}PO_{2.99}N_{0.13}$					0.60	(amorphous) [101]
$LiPO_3$	0.6	0.7	1.2	1.2	1.4	(poly cryst.) [97]
					0.76-1.2	(amorphous) [97]
$LiPN_2$	0.4		2.5	1.7	0.6	(poly cryst.) [99]
SD-Li_2PO_2N	0.4	0.8	2.0	1.4	0.6	(poly cryst.) [52]
γ-Li_3PS_4	0.3		0.8	0.7	0.5	(poly cryst.) [102]
β-Li_3PS_4	0.2		0.0	0.2	0.4	(nano cryst.) [103]
$Li_7P_3S_{11}$	0.2	0.5	0.0	0.2	0.1	(poly cryst.) [76]

WAKE FOREST UNIVERSITY

➢What is meant by "first principles"?

A series of well-controlled approximations

- ❑ Born-Oppenheimer Approximation
- ❑ Density Functional Approximation
- ❑ Local density Approximation (LDA)
- ❑ Numerical method: Projector Augmented Wave

Validation

- ❑ Lattice vibration modes
- ❑ Heats of formation
- ❑ Activation energies for lattice migration

How can computer simulations contribute to the development of materials?

- Computationally examine known materials and predict new materials and their properties
  - Structural forms
  - Relative stabilities
  - Direct comparisons of simulations and experiment
  - Investigate properties that are difficult to realize experimentally

Of particular interest in battery materials --

- Model ion migration mechanisms
  - Vacancy migration
  - Interstitial migration
  - Vacancy-interstitial formation energies
- Model ideal electrolyte interfaces with anodes

Systematic study of LiPON materials – $Li_xPO_yN_z$ –
(Yaojun A. Du and N. A. W. Holzwarth, Phys. Rev. B 81, 184106 (2010))

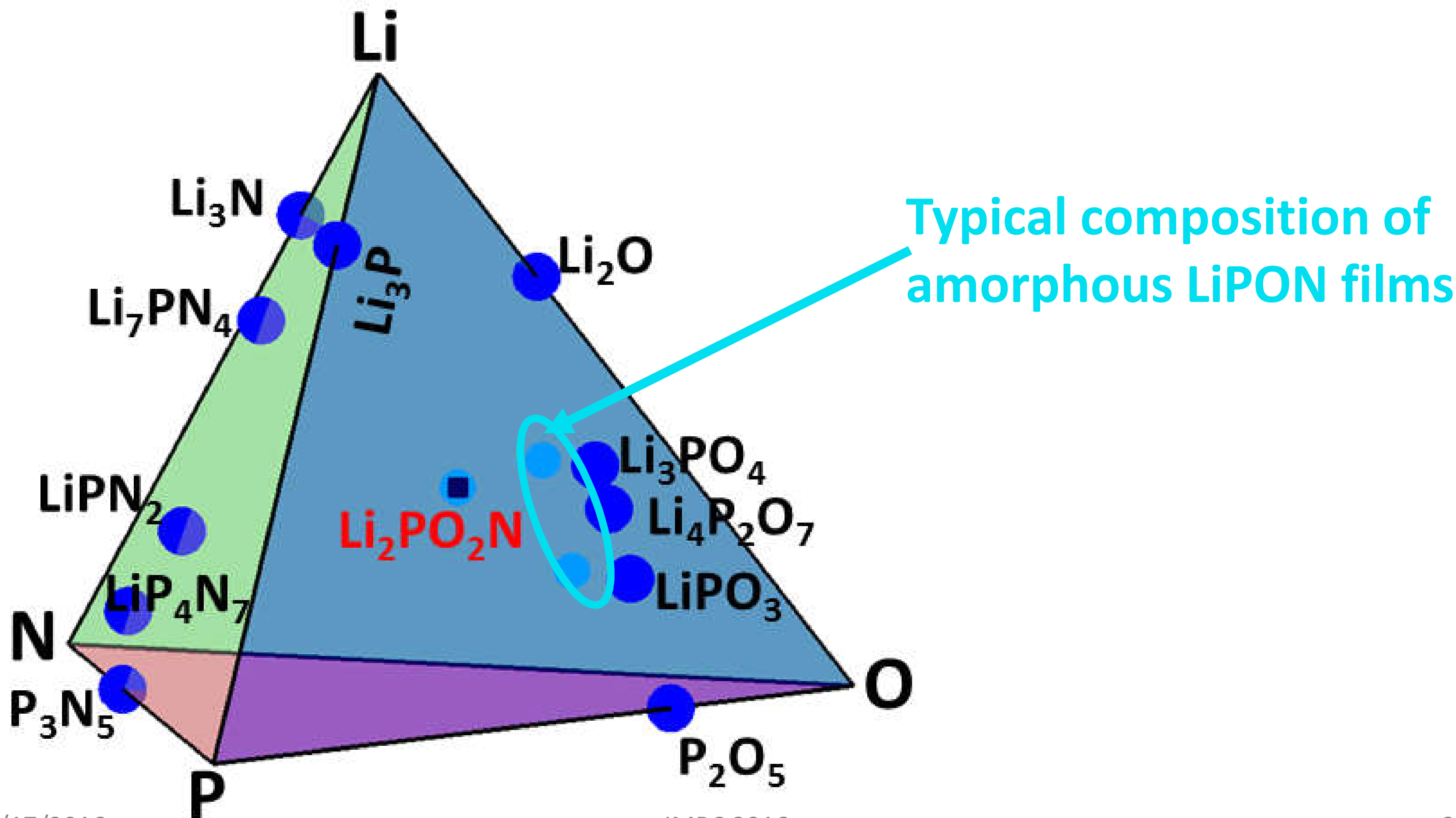

Experimentally known structure

Computationally predicted structure

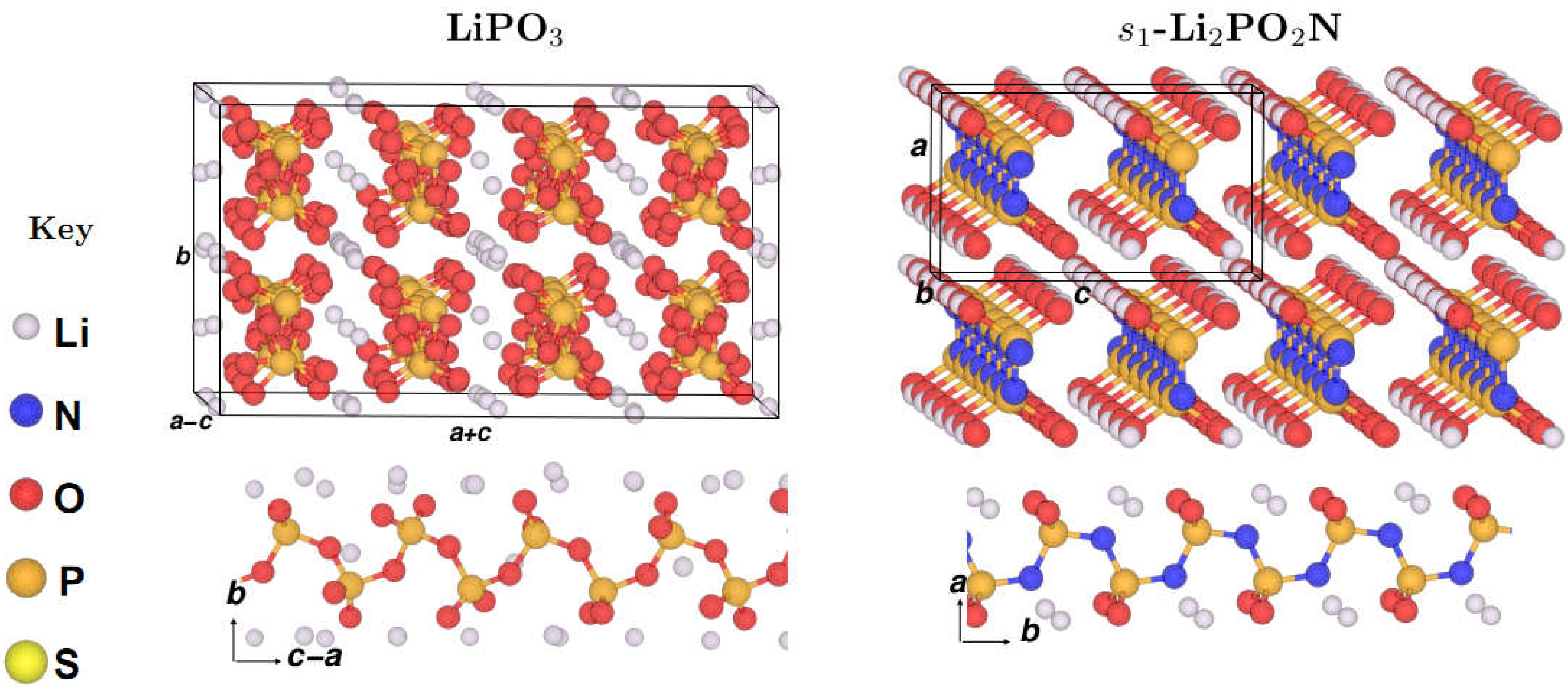

Fig. 7. Ball and stick diagrams for $LiPO_3$ in the $P2/c$ structure (20 formula units per unit cell) and $s1$-Li_2PO_2N in the $Pbcm$ structure (4 formula units per unit cell) from the calculated results. For each crystal diagram, a view of a horizontal chain axis is also provided for a single phosphate or phospho-nitride chain.

Computationally predicted structure

Key

s_1-Li_2PO_2N ***Pbcm***

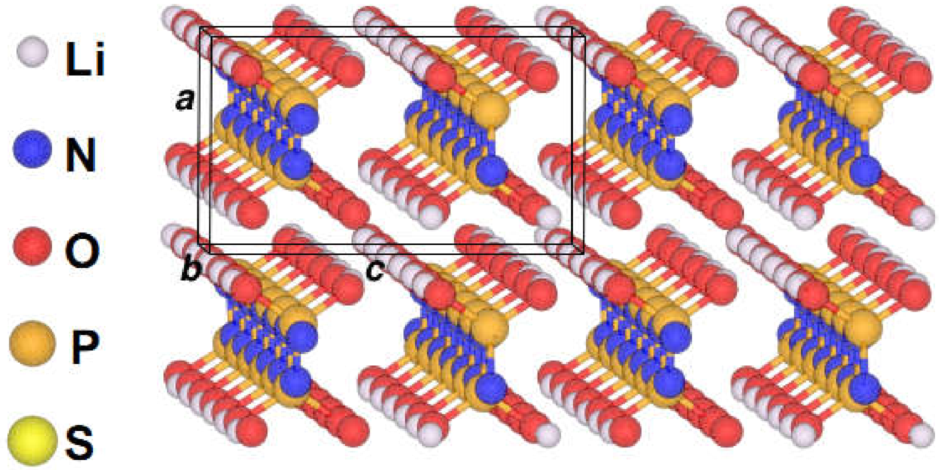

Calculations have now verified that the *SD* structure is more stable than the s_1 structure by 0.1 eV/FU.

Experimentally realized structure

SD*-Li_2PO_2N** ***$Cmc2_1$

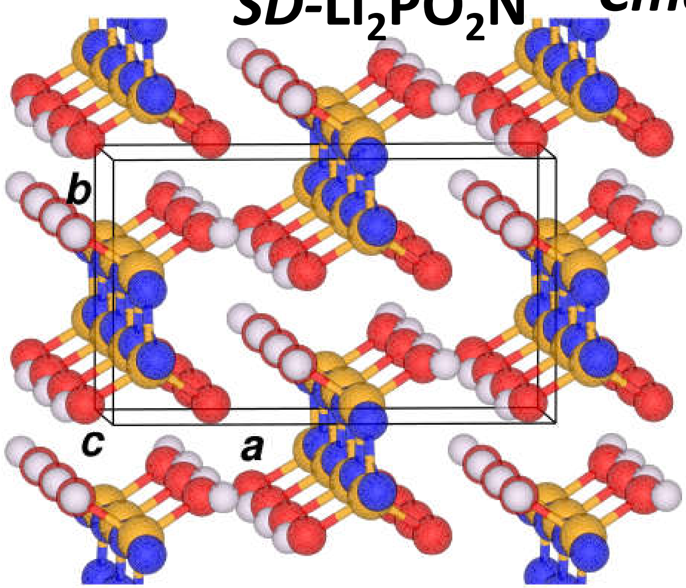

Synthesis of Li_2PO_2N by Keerthi Senevirathne, Cynthia Day, Michael Gross, and Abdessadek Lachgar (*SSI* 233, 95-101 (2013)**)**

High temperature solid state synthesis using reaction:

$$Li_2O + \tfrac{1}{5}P_2O_5 + \tfrac{1}{5}P_3N_5 \rightarrow Li_2PO_2N$$

Comparison of synthesized Li_2PO_2N with Li_2SiO_3

SD-Li_2PO_2N *($Cmc2_1$)*	Li_2SiO_3 *($Cmc2_1$)*

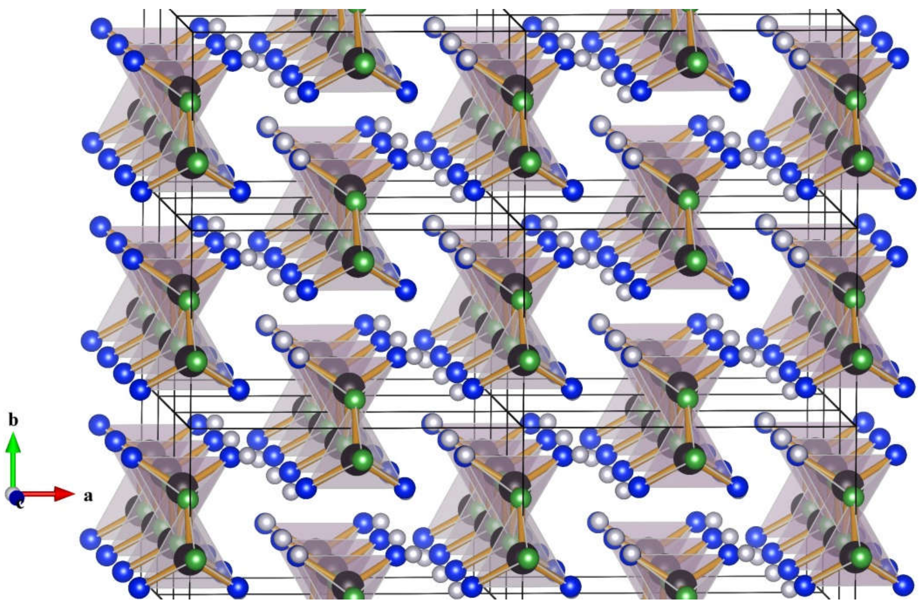

a=9.07 Å, b=5.40 Å, c=4.60 Å

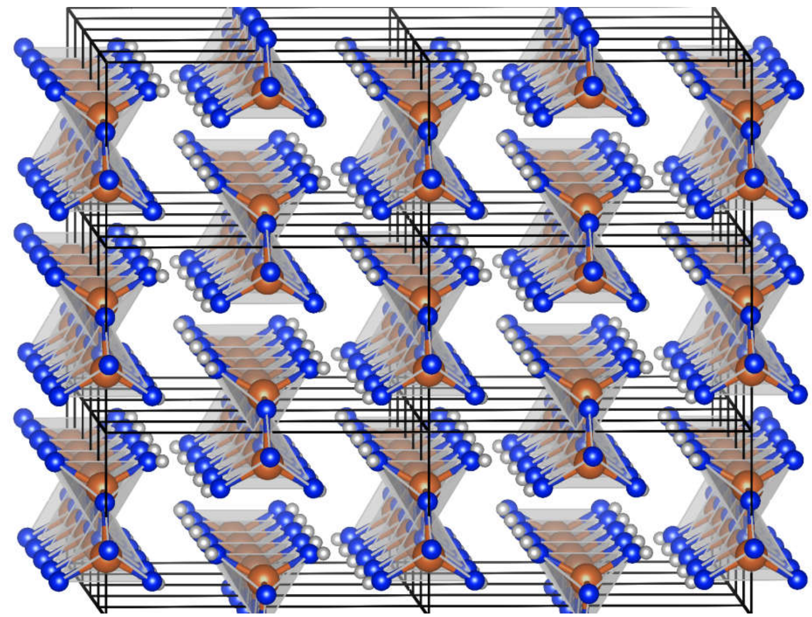

a=9.39 Å, b=5.40 Å, c=4.66 Å

K.-F. Hesse, Acta Cryst. B33, 901 (1977)

Li **P** **O** **N** **Si**

Electronic band structure of *SD*-Li_2PO_2N

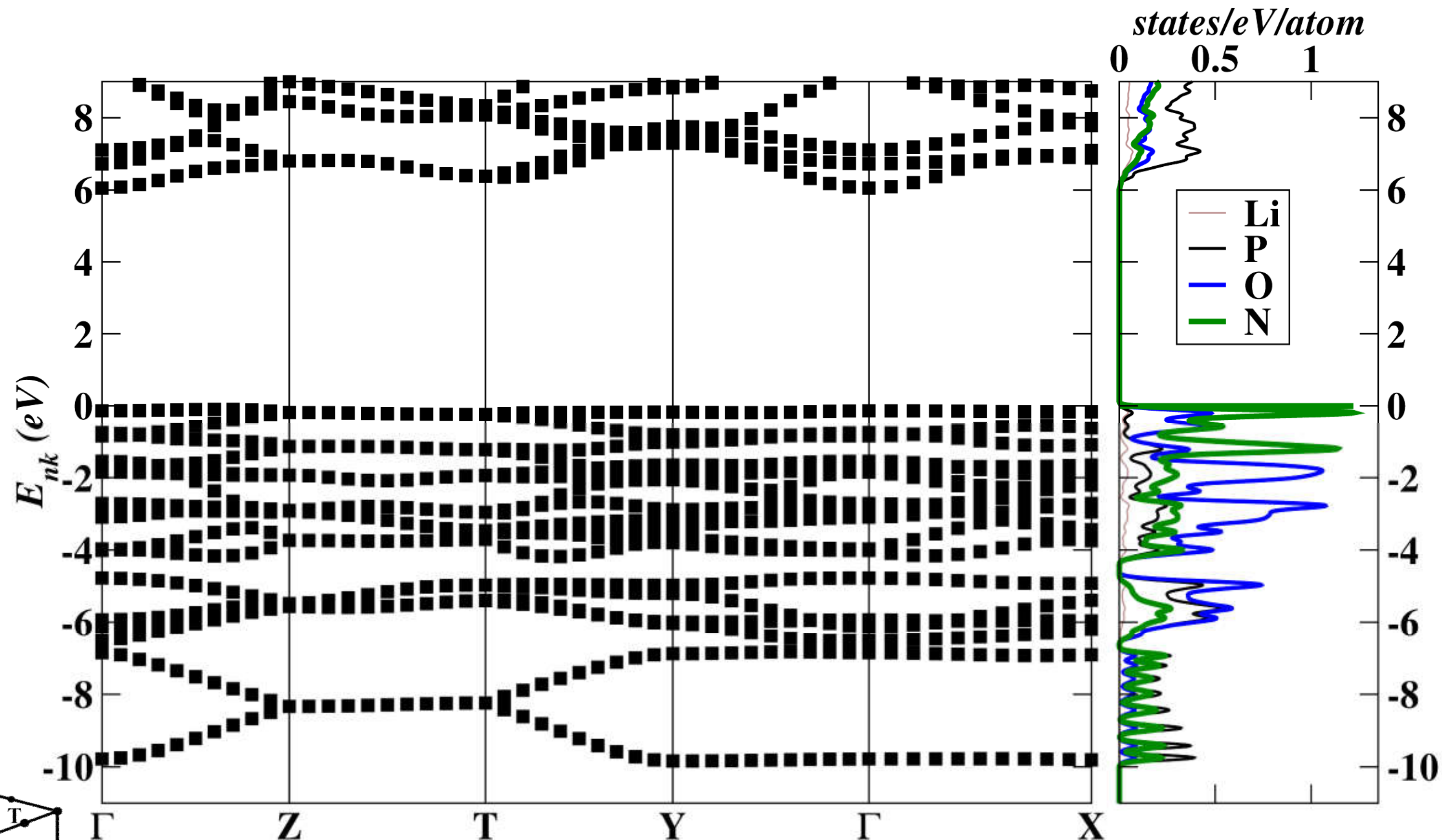

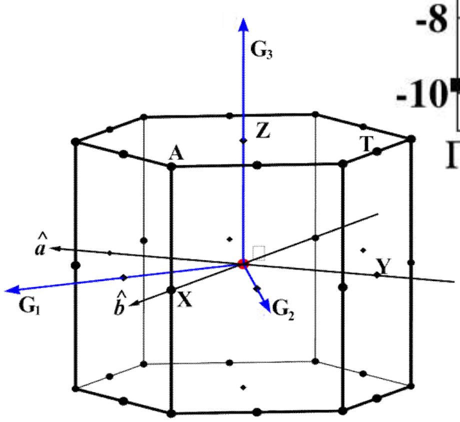

More details of *SD*-Li_2PO_2N structure

Ball and stick model

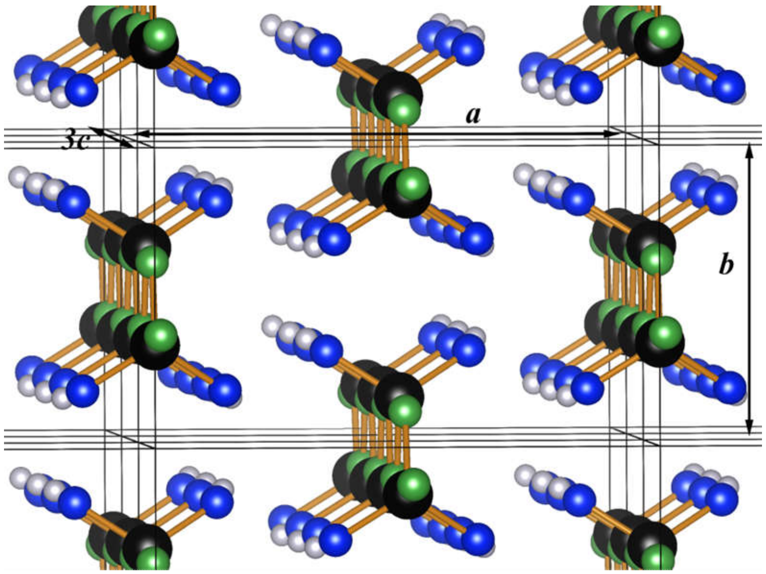

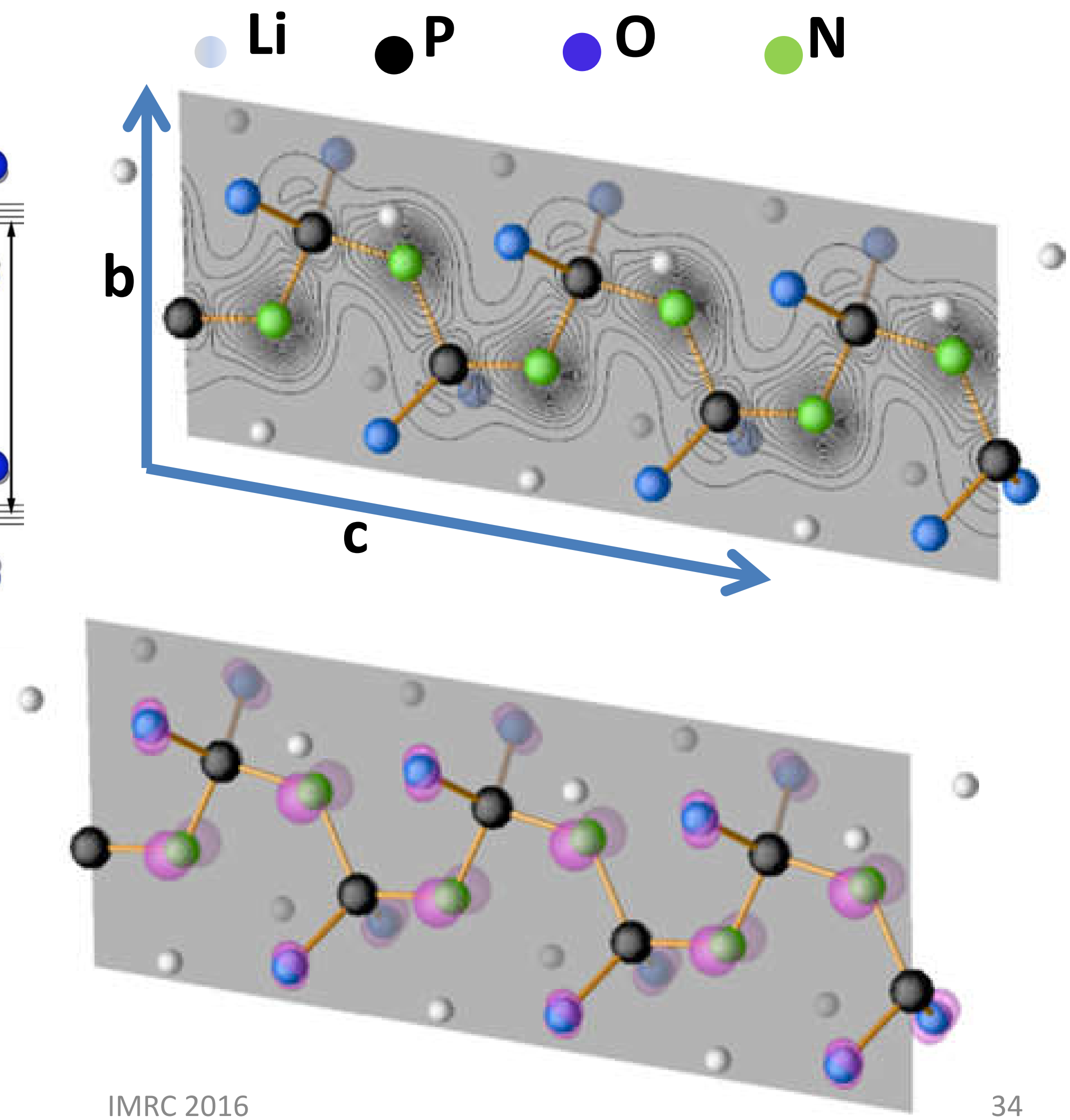

Isosurfaces (maroon) of charge density of states at top of valence band, primarily π states on N.

Vibrational spectrum of *SD*-Li_2PO_2N

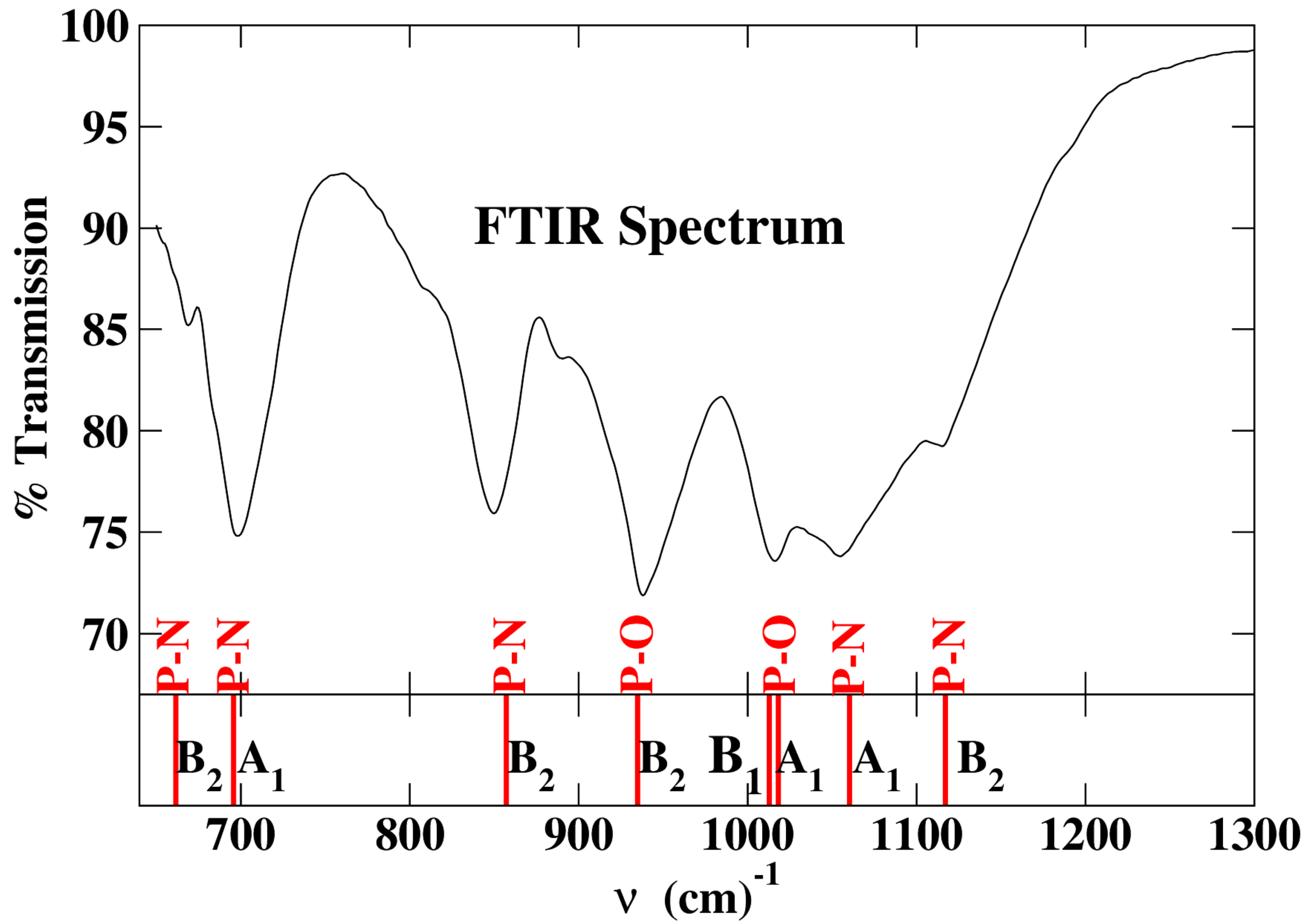

Stability of *SD*-Li_2PO_2N in air

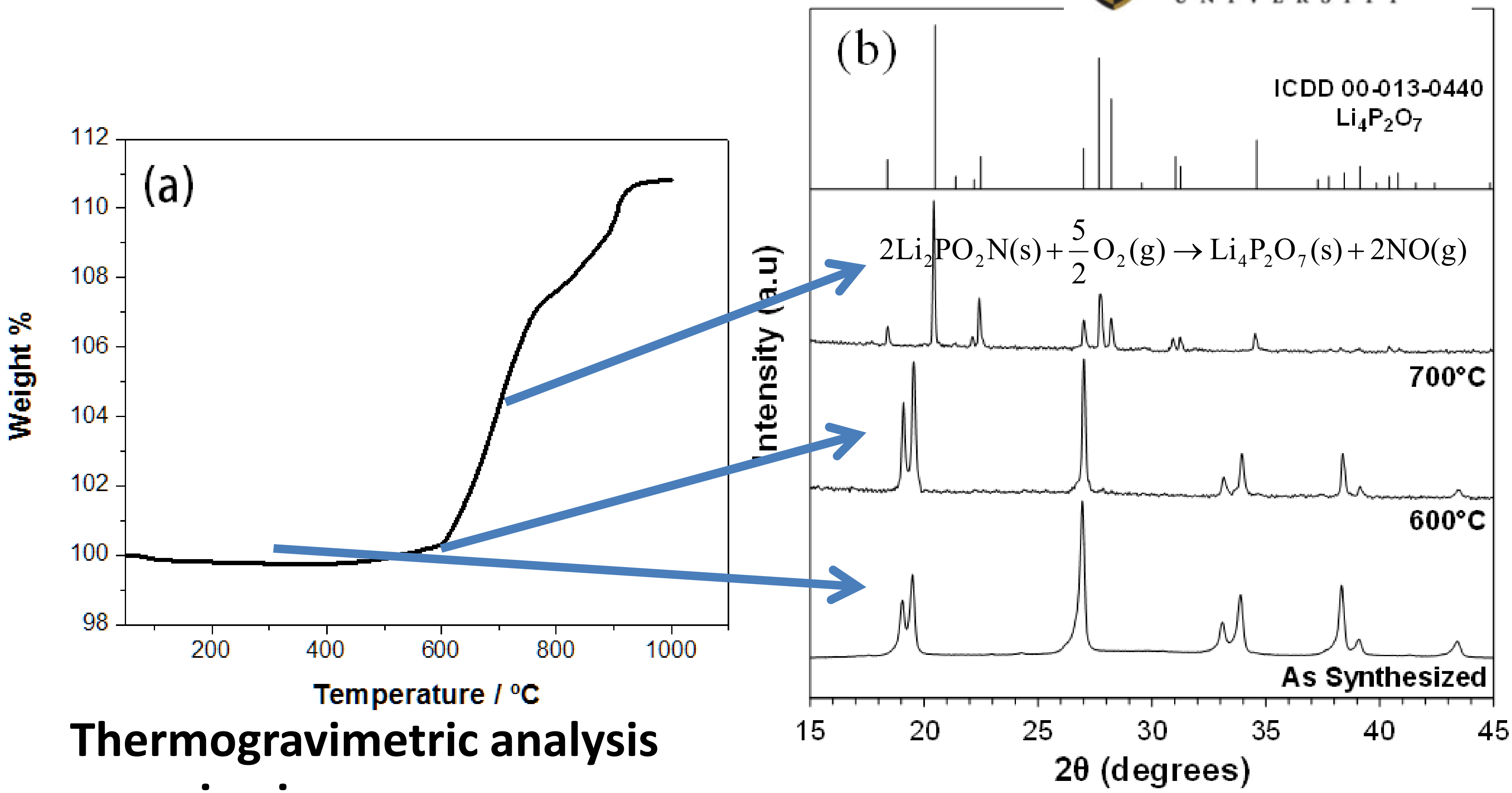

Thermogravimetric analysis curve in air

Note: no structural changes were observed while heating in vacuum up to 1050^{o} C.

Wake Forest University

Ionic conductivity of *SD*-Li_2PO_2N

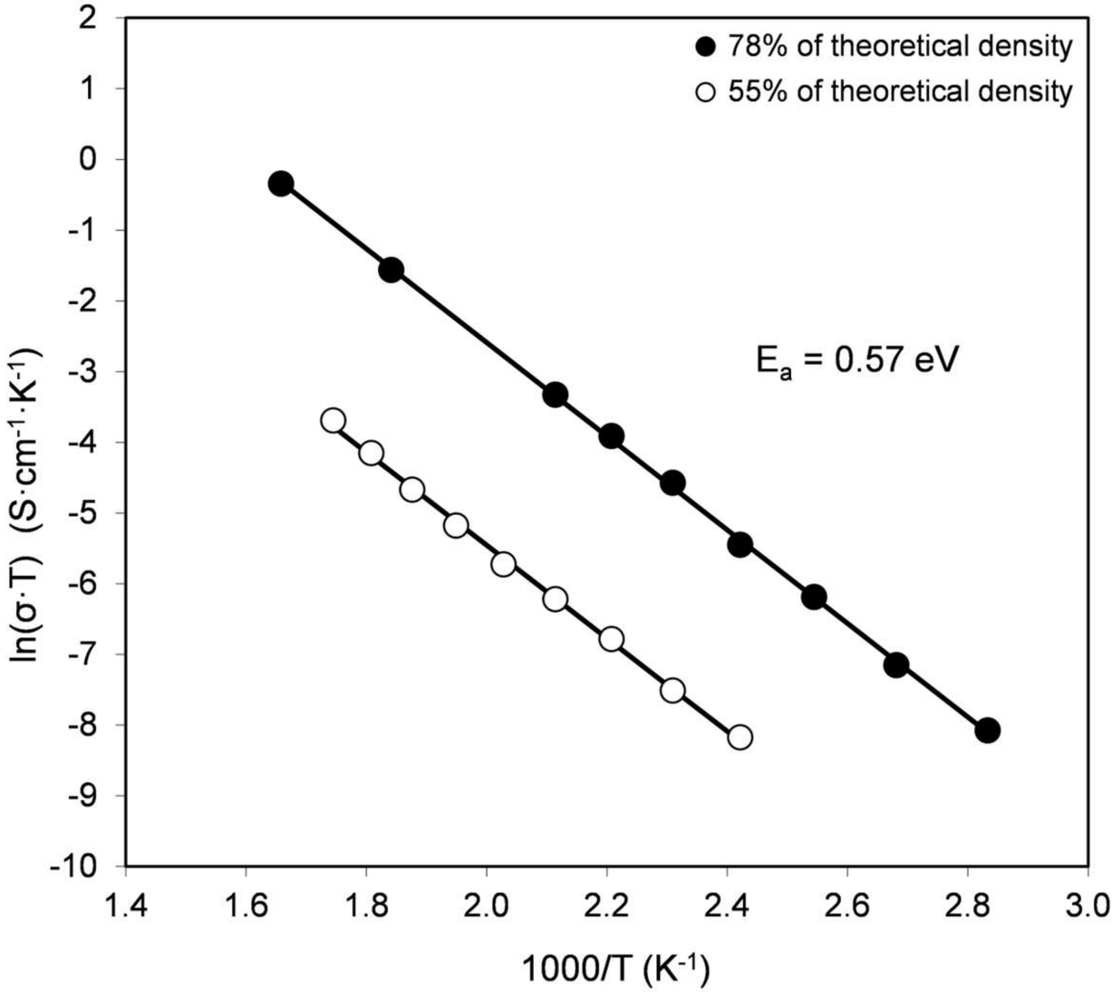

$$\sigma \approx 10^{-6}\ \text{S/cm} \quad \text{at } 80^o\ \text{C}$$

NEB analysis of E_m (vacancy mechanism)

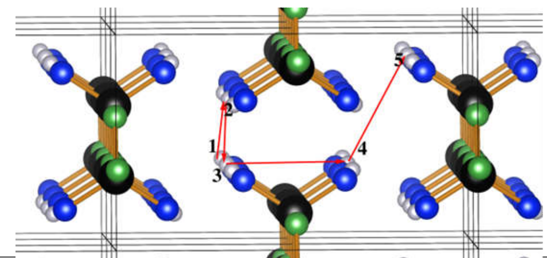

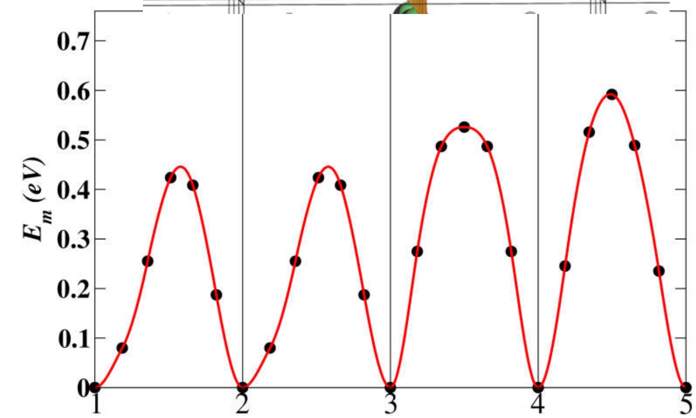

$$E_m \approx 0.4\ \text{eV}; E_f \approx 2\ \text{eV}$$

$$\Rightarrow E_A = E_m + \tfrac{1}{2}E_f \approx 1.4\ \text{eV}$$

➔Sample has appreciable population of vacancies

Summary of the Li_2PO_2N story

- Predicted on the basis of first principles theory
- Subsequently, experimentally realized by Keerthi Seneviranthe and colleagues;   generally good agreement between experiment and theory
- Ion conductivity properties not (yet) competitive
- Crystalline *SD*-Li_2PO_2N *($Cmc2_1$)* is quite different from the amorphous LiPON electrolyte developed at ORNL

WAKE FOREST UNIVERSITY

LiPON and LiS_2-P_2S_5 conductivities

X. Yu, J. B. Bates, G. E. Jellison, Jr., and F. X. Hart, J. Electrochem. Soc. **144** 524-532 (1997):

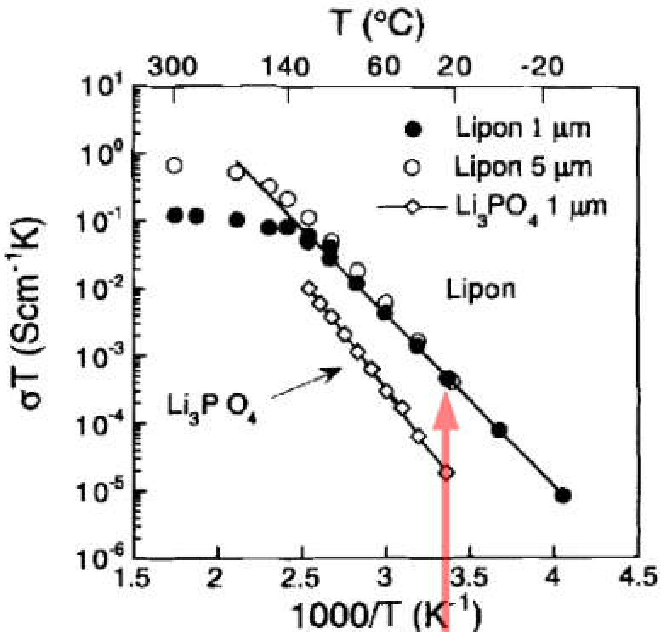

Fig. 3. Arrhenius plot of ionic conductivity of Lipon and Li_3PO_4 vs. temperature.

$\sigma = 2 \times 10^{-6}$ S/cm
$E_a = 0.5$ eV

M. Tatsumisago and A. Hayashi, J. Non-Cryst. Solids **354** 1411-1417 (2008):

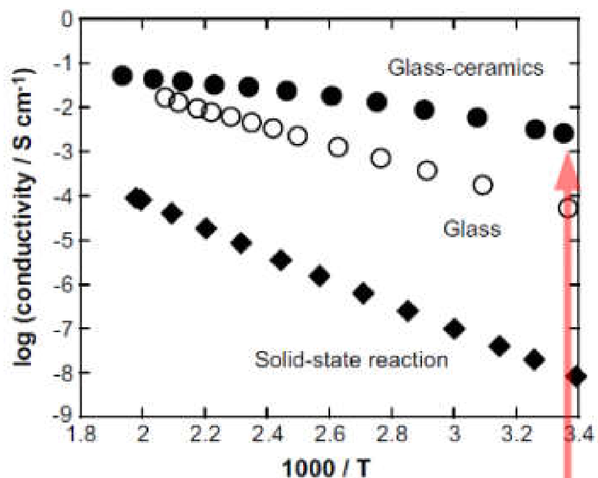

Fig. 5. Temperature dependences of the conductivities for the $70Li_2S \cdot 30P_2S_5$ glass and glass-ceramics. The conductivity data for the sample prepared by solid-state reaction are also shown.

$\sigma = 3 \times 10^{-3}$ S/cm
$E_a = 0.1$ eV

Systematic study of Li_xPS_y materials – (N. D. Lepley and N. A. W. Holzwarth, J. Electrochem. Soc. 159, A538 (2012), Phys. Rev. B 88, 104103 (2013))

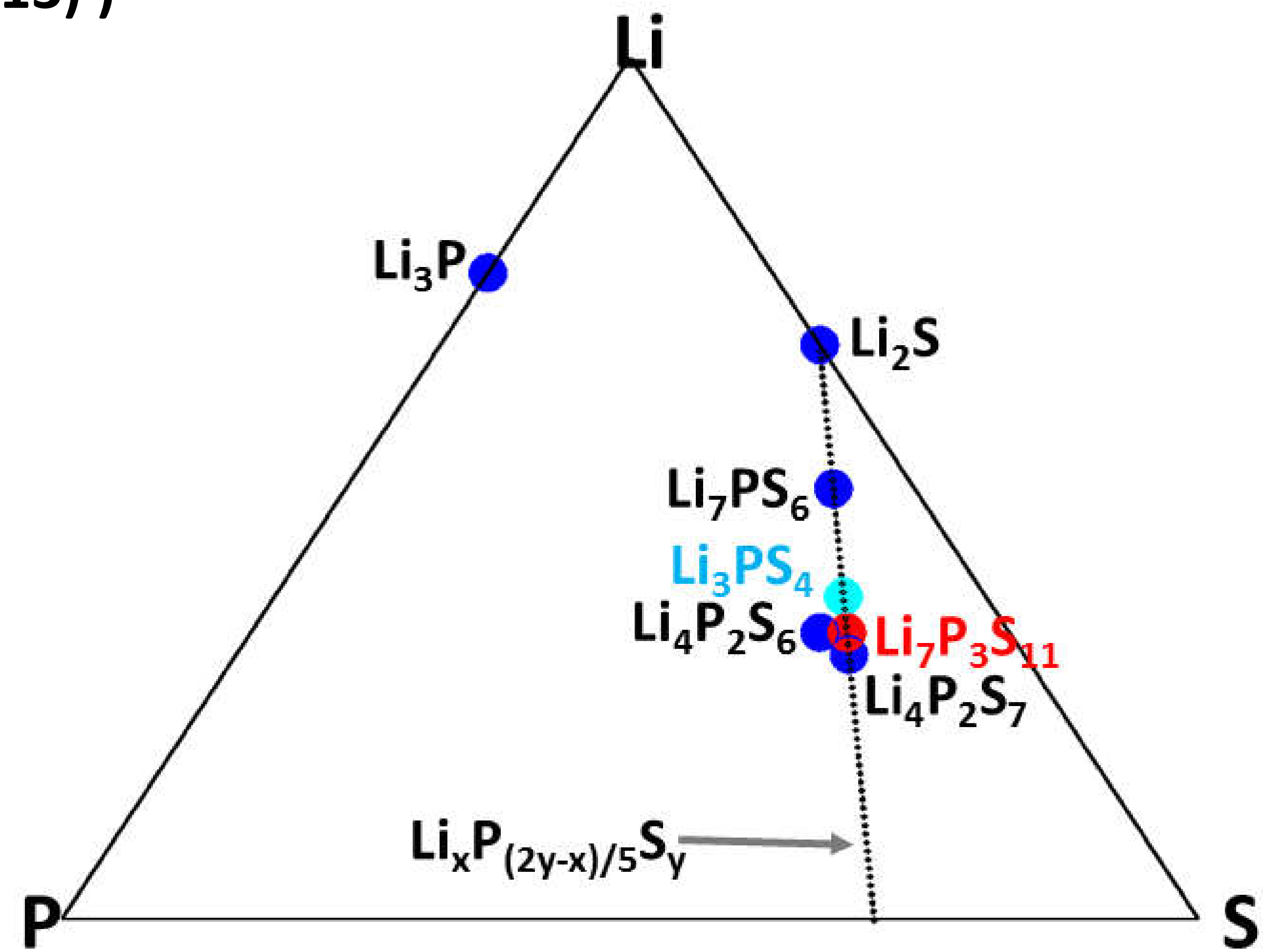

Comparison of some lithium phosphates and thiophosphates

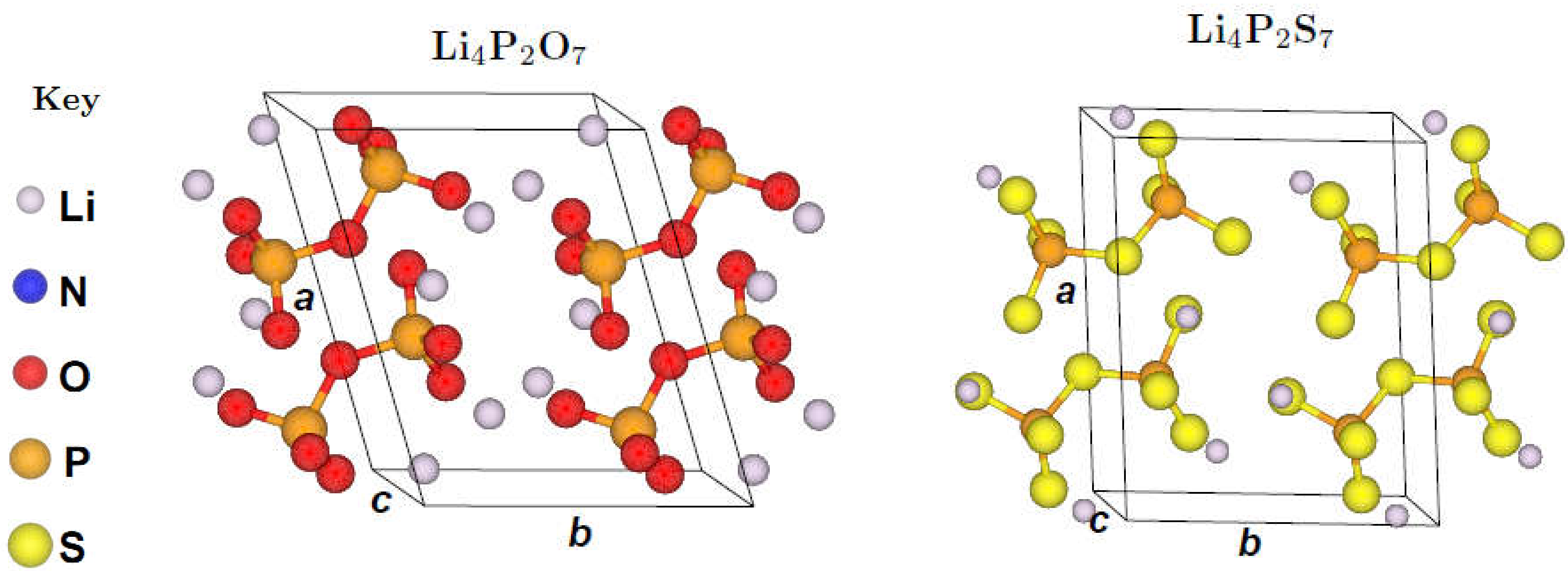

Crystallizes (experimentally and computationally) into $P\bar{1}$ structure

Experimentally amorphous; computationally metastable in $P\bar{1}$ structure

Some lithium thiophosphate crystal structures

$Li_4P_2S_7$

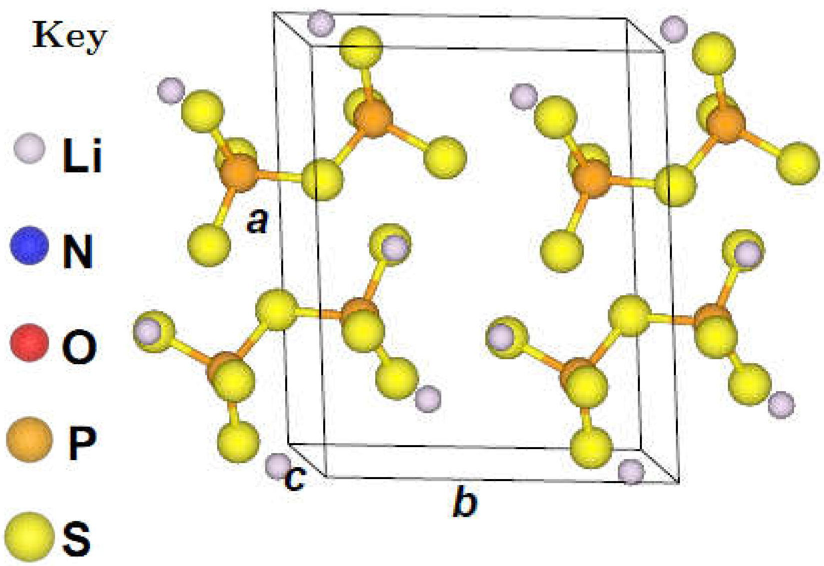

Experimentally amorphous; computationally metastable in $P\bar{1}$ structure

$Li_7P_3S_{11}$

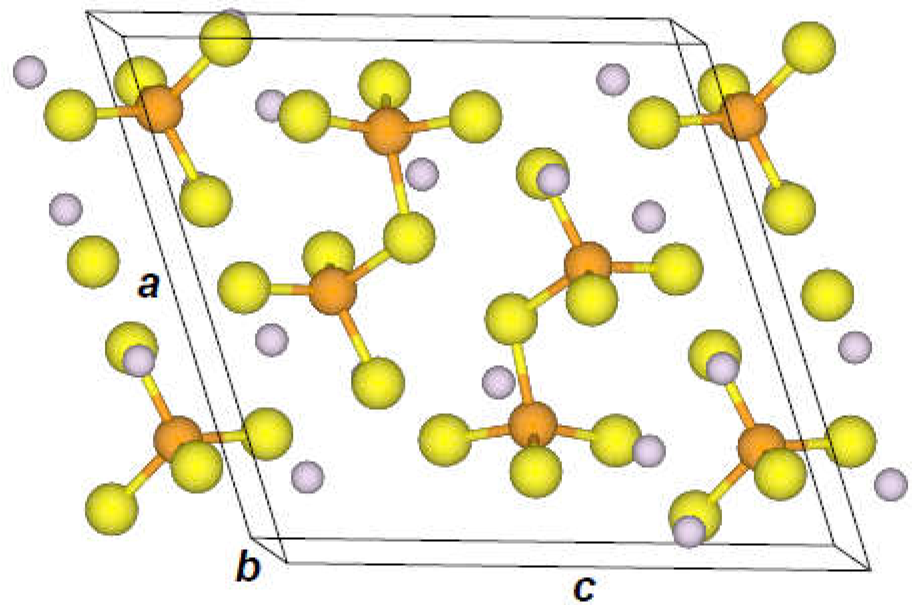

Experimentally and computationally metastable in $P\bar{1}$ structure

Vacancy migration analysis from NEB results

for $Li_7P_3S_{11}$: Lepley & Holzwarth, *JECS* **159**, A538-A547 (2012)

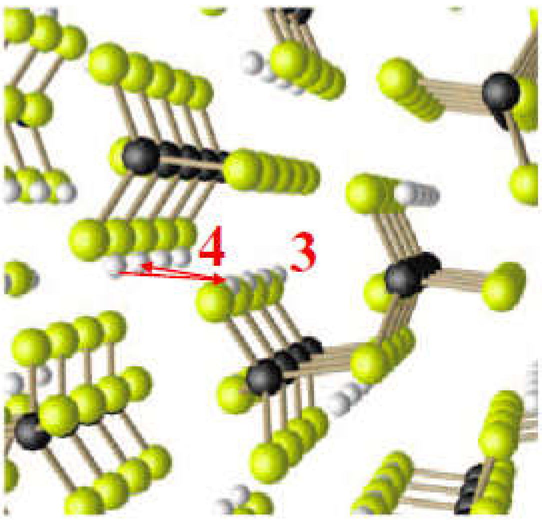

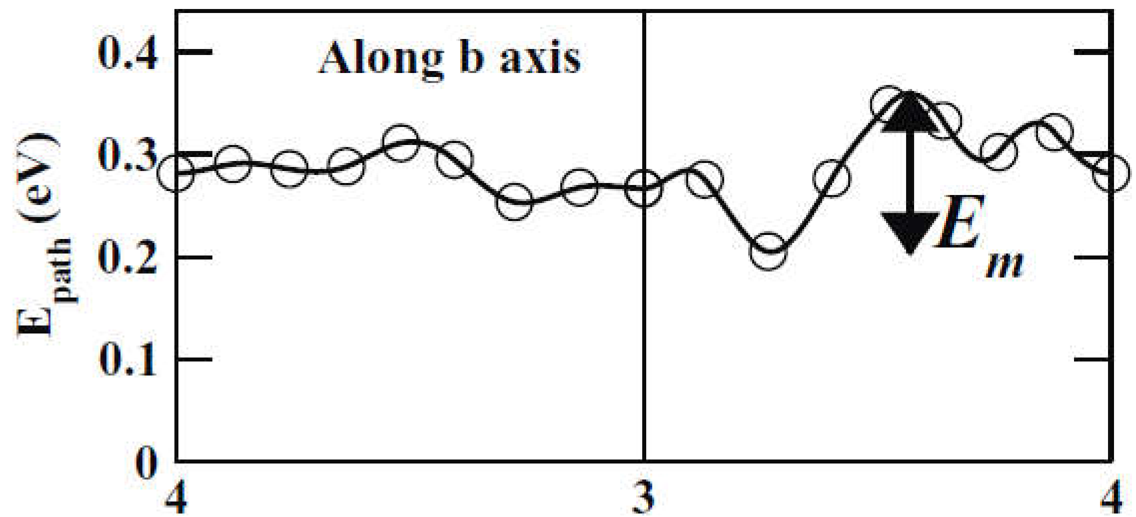

● **Li** ● **P** ● **S**

$$E_m \approx 0.15 \text{ eV}; E_f \approx 0 \text{ eV}$$

$$\Rightarrow E_A = E_m + \tfrac{1}{2} E_f \approx 0.15 \text{ eV}$$

Experiment -- A Hayashi *et al.,* J. Solid State Electrochem. **14**, 1761 (2010):

$$\sigma \approx 2 - 3 \times 10^{-3} \text{ S/cm} \qquad \text{E}_A \approx 0.12 - 0.18 \text{ eV}$$

From ORNL: Experiment on electrolyte Li_3PS_4

WAKE FOREST UNIVERSITY

JACS JOURNAL OF THE AMERICAN CHEMICAL SOCIETY

Communication

pubs.acs.org/JACS

Anomalous High Ionic Conductivity of Nanoporous β-Li_3PS_4

Zengcai Liu,[†] Wujun Fu,[†] E. Andrew Payzant,[†,‡] Xiang Yu,[†] Zili Wu,[†,§] Nancy J. Dudney,[‡] Jim Kiggans,[‡] Kunlun Hong,[†] Adam J. Rondinone,[†] and Chengdu Liang*[,†]

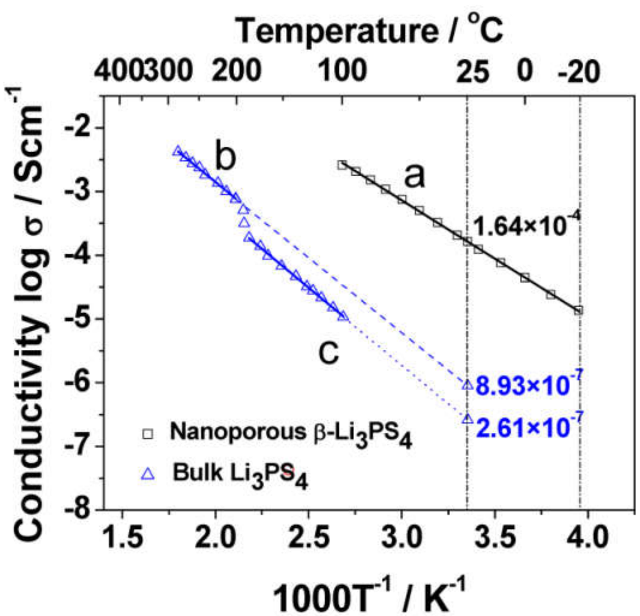

Figure 1. Arrhenius plots for nanoporous β-Li_3PS_4 (line a), bulk β-Li_3PS_4 (line b), and bulk γ-Li_3PS_4 (line c). The conductivity data for bulk Li_3PS_4 are reproduced from the work of Tachez.[10].

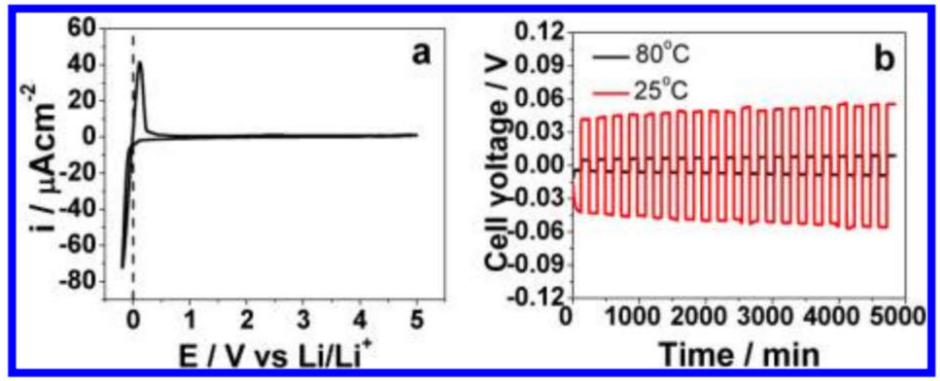

Figure 5. Electrochemical stability of β-Li_3PS_4 and cycling stability with metallic lithium electrodes. (a) CV of a Li/β-Li_3PS_4/Pt cell, where Li and Pt serve as the reference/counter and working electrodes, respectively. (b) Lithium cyclability in a symmetric Li/β-Li_3PS_4/Li cell. The cell was cycled at a current density of 0.1 mA cm^{-2} at room temperature and 80 °C.

β-Li_3PS_4

● Li ● P ● S

WAKE FOREST UNIVERSITY

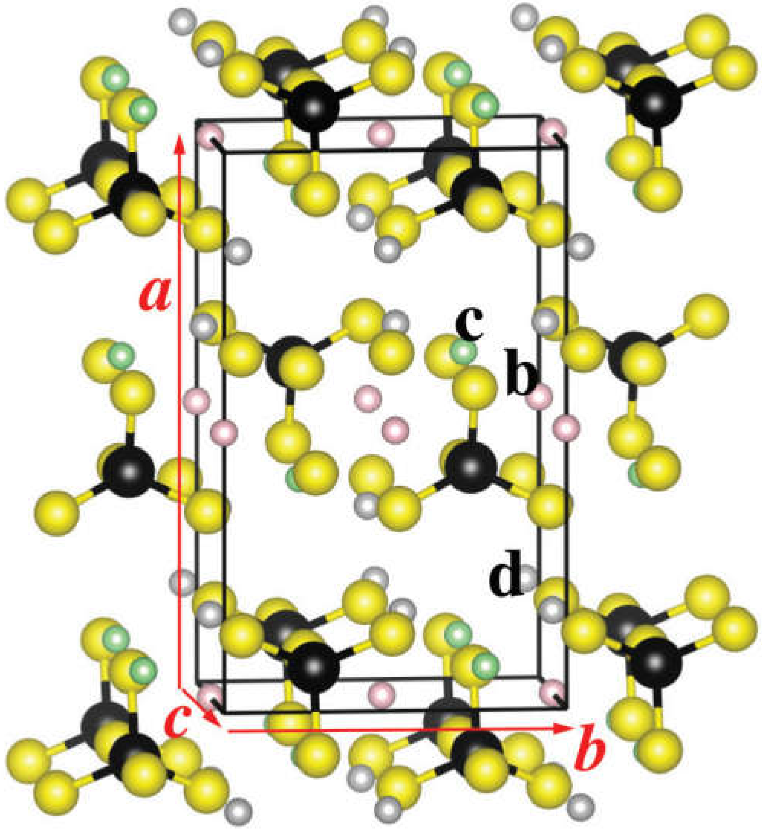

$$E_m \approx 0.3 \text{ eV}; \; E_f \approx 0.0 \text{ eV}$$

$$E_A = E_m + \tfrac{1}{2} E_f \approx 0.3 \text{ eV}$$

$$E_{exp} = 0.4 - 0.5 \text{ eV}$$

γ-Li_3PS_4

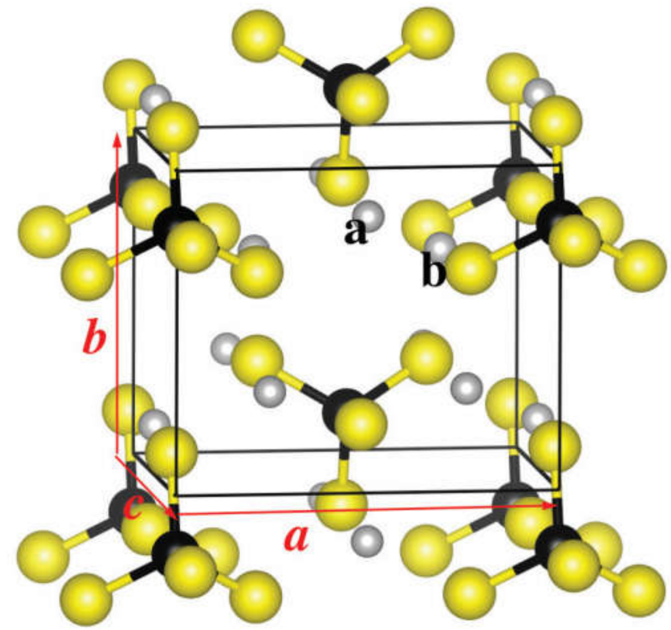

$$E_m \approx 0.3 \text{ eV}; \; E_f \approx 0.8 \text{ eV}$$

$$E_A = E_m + \tfrac{1}{2} E_f \approx 0.7 \text{ eV}$$

$$E_{exp} = 0.5 \text{ eV}$$

Lepley, Du, and Holzwarth, *PRB* **88**, 104103 (2013)

Summary of the Li_xPS_y story

- Simulations verify that thiophosphates have better ion mobility properties than their phosphate analogs
- Meta-stable crystalline $Li_7P_3S_{11}$ has been shown to have particularly favorable ion migration pathways
- γ- and β-Li_3PS_4 have very similar structures, but simulations show their ion mobilities to be different.

Models of Idealized Interfaces

Crystal structure of bulk Li_3PS_4 – γ-form Pmn2_1 (#31)

Note: Li_3PS_4 is also found in the β-form with Pnma (#62) structure

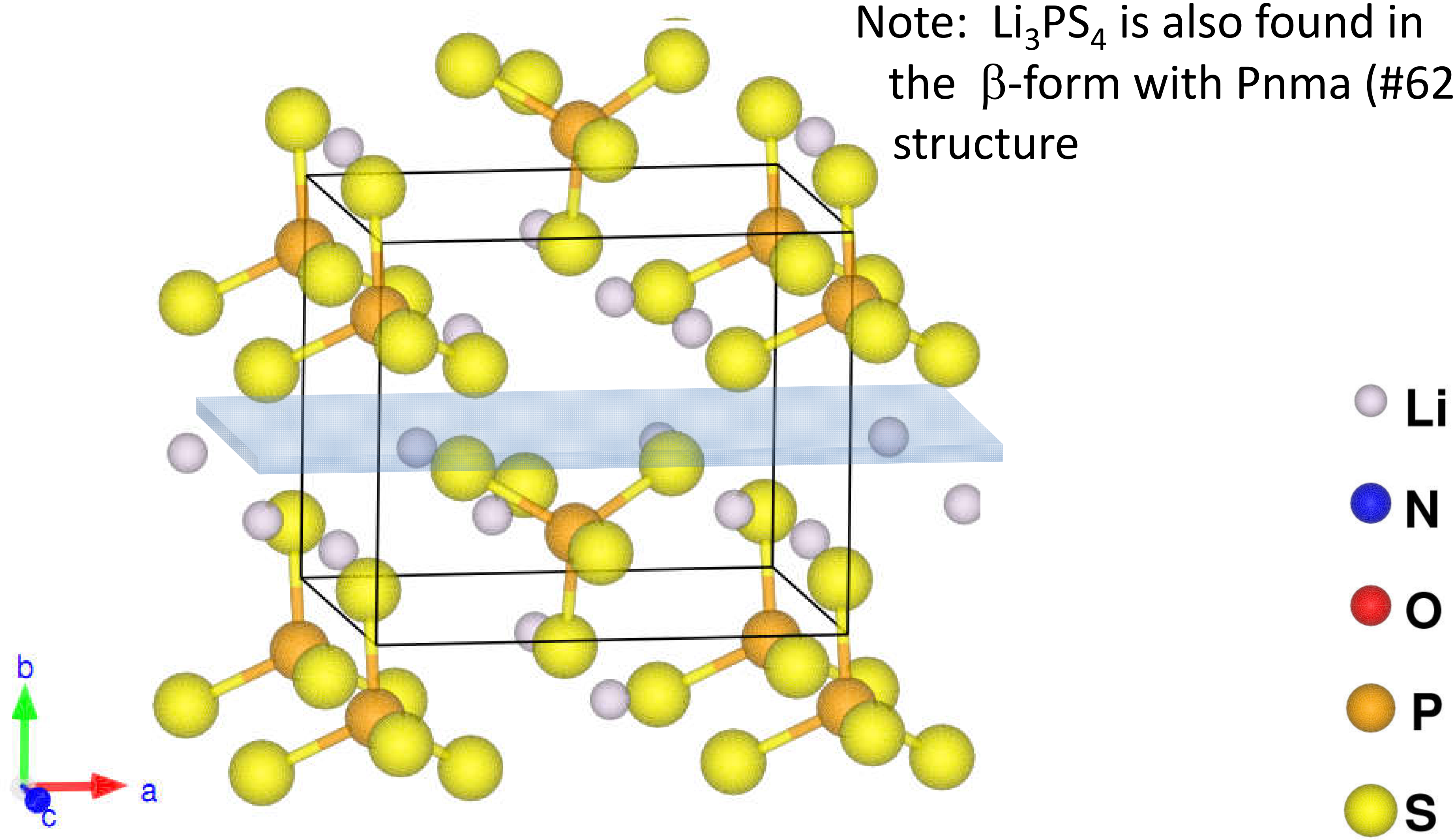

γ-Li_3PS_4 [0 1 0] surface

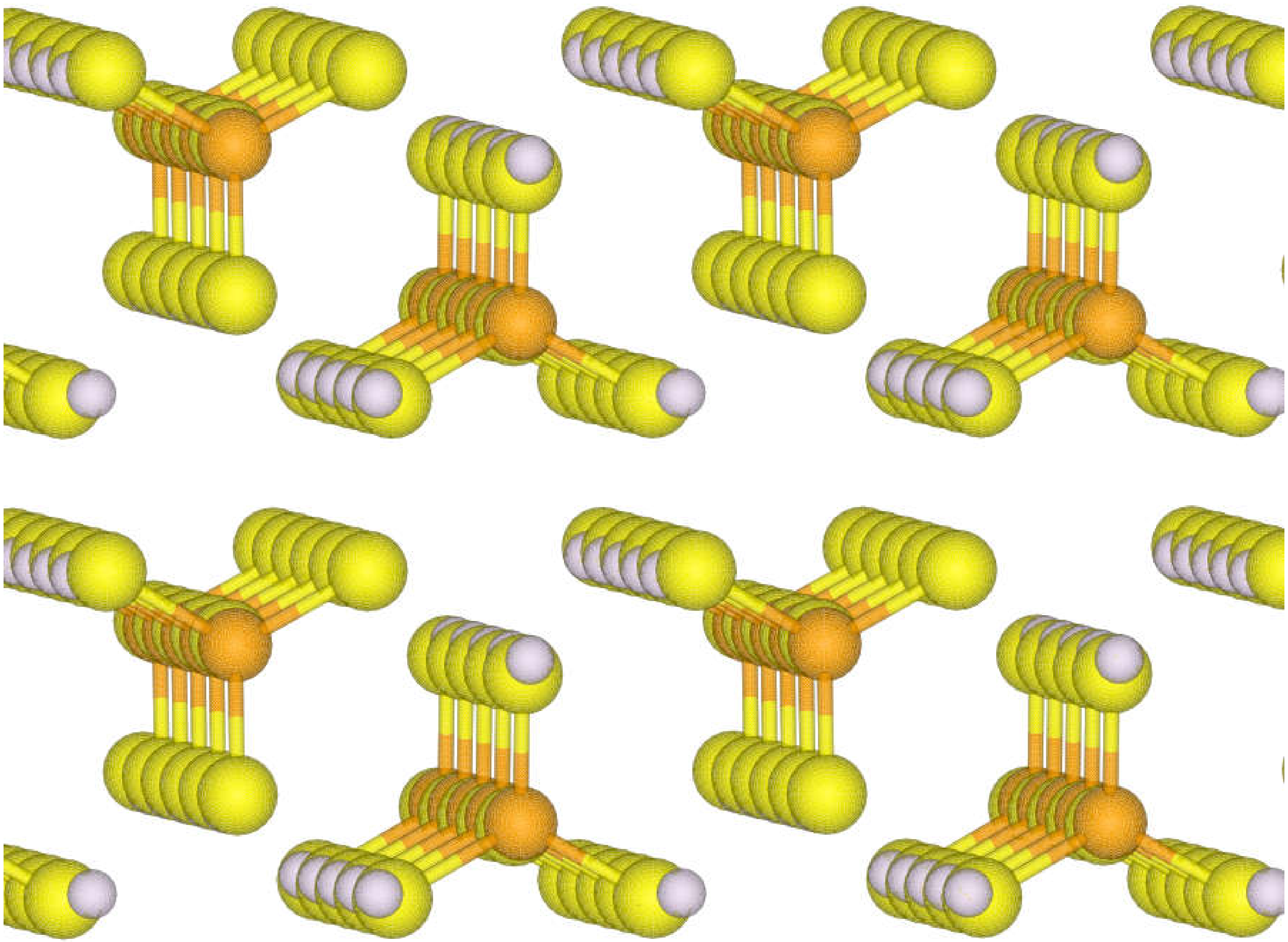

Simulations of ideal γ-Li_3PS_4 [0 1 0] surface in the presence of Li

Initial configuration:

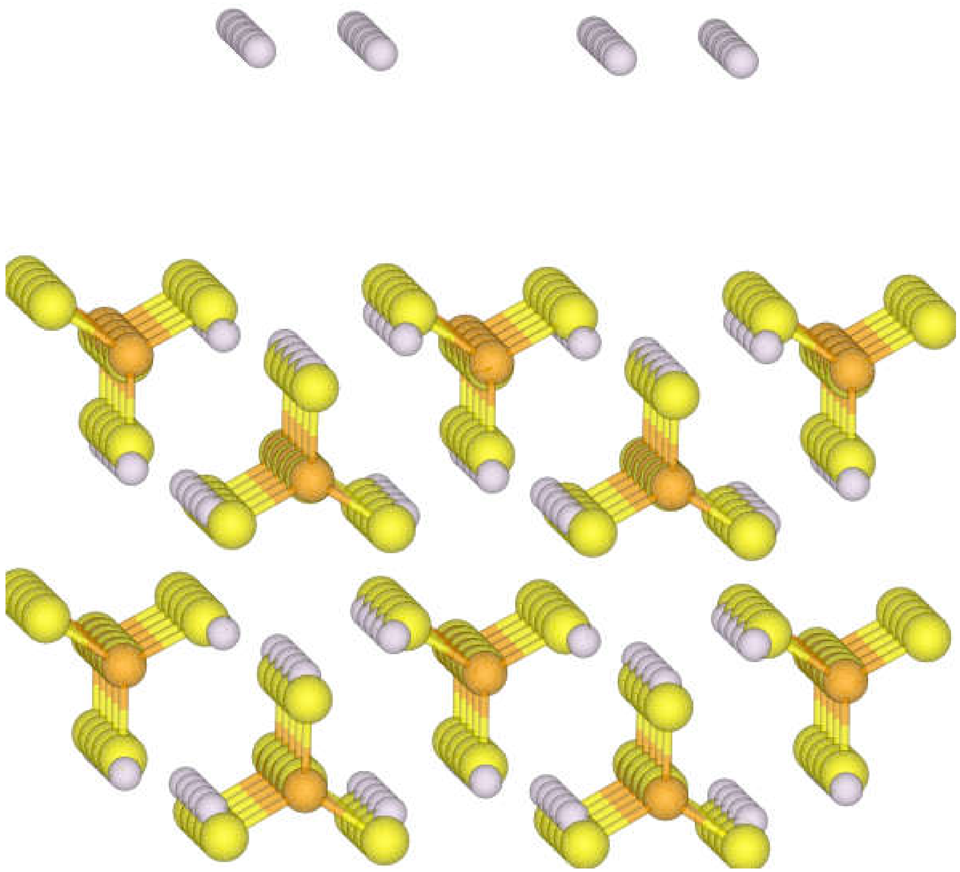

Computed optimized structure:

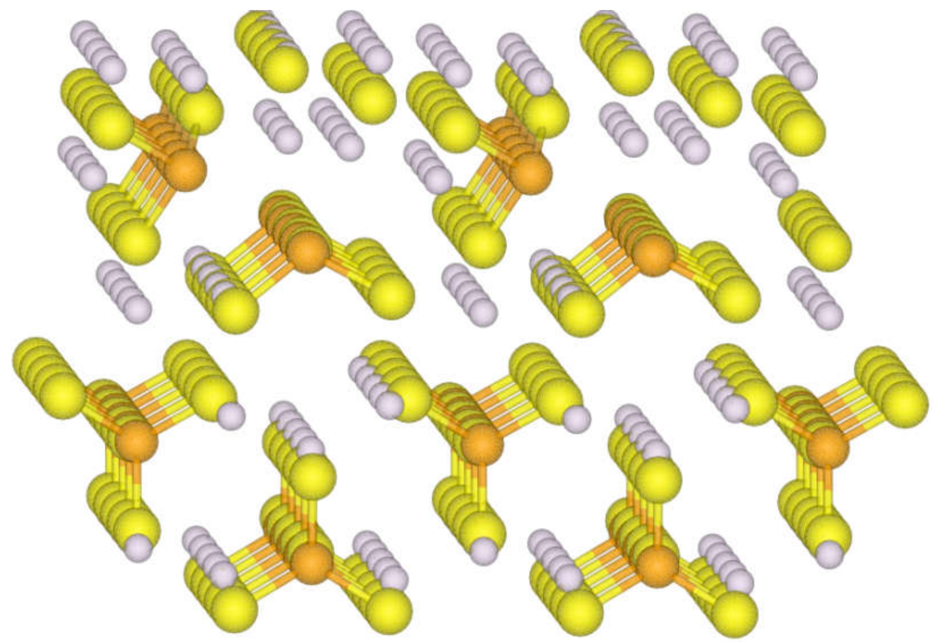

Computational counter example – stable interface: Li/β-Li_3PO_4

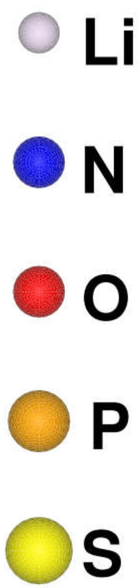

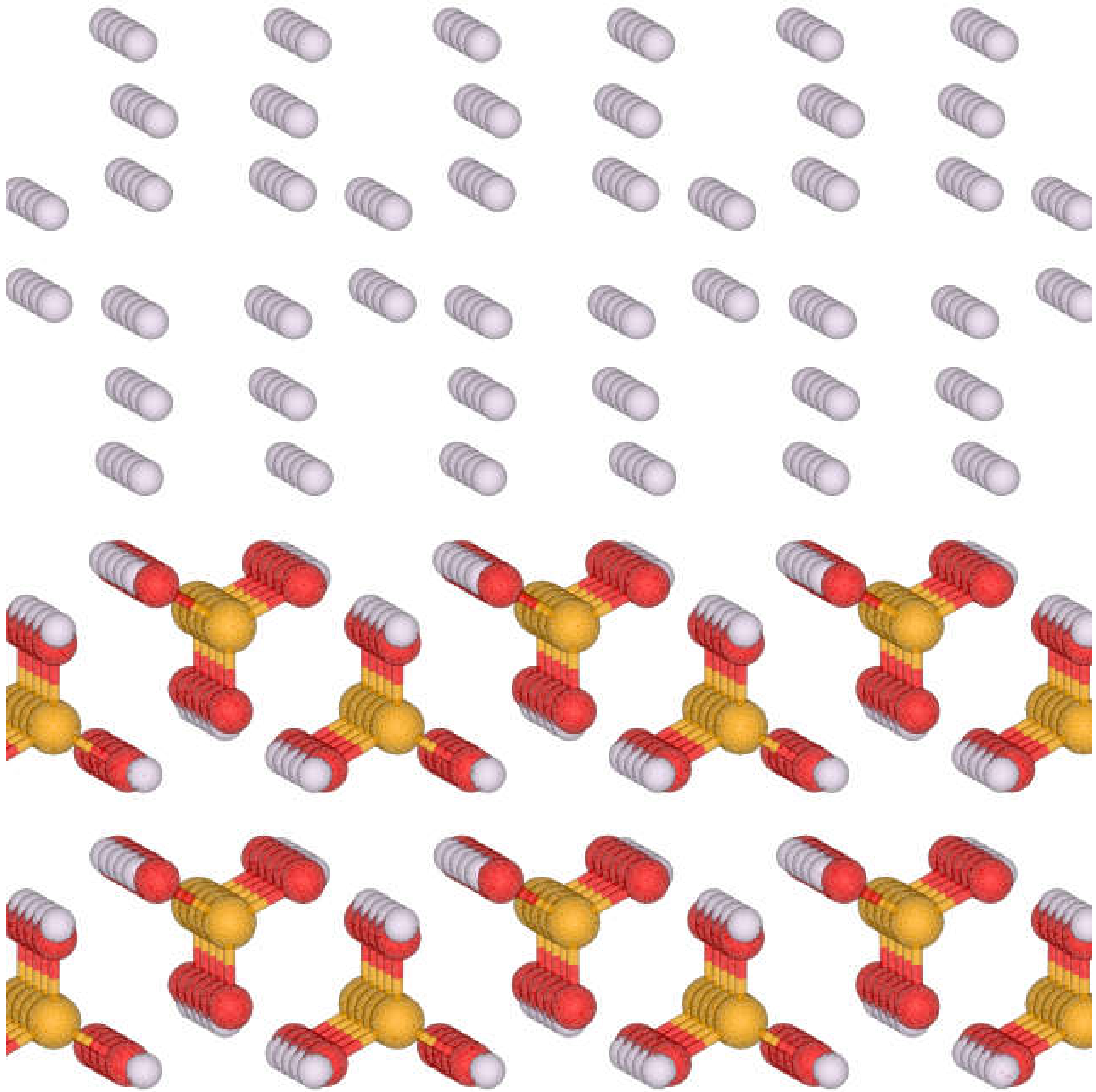

Computational counter example – stable interface: Li/*SD*-Li_2PO_2N

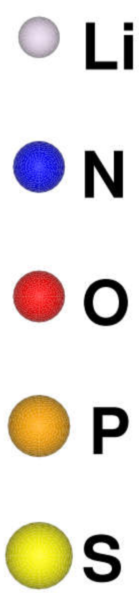

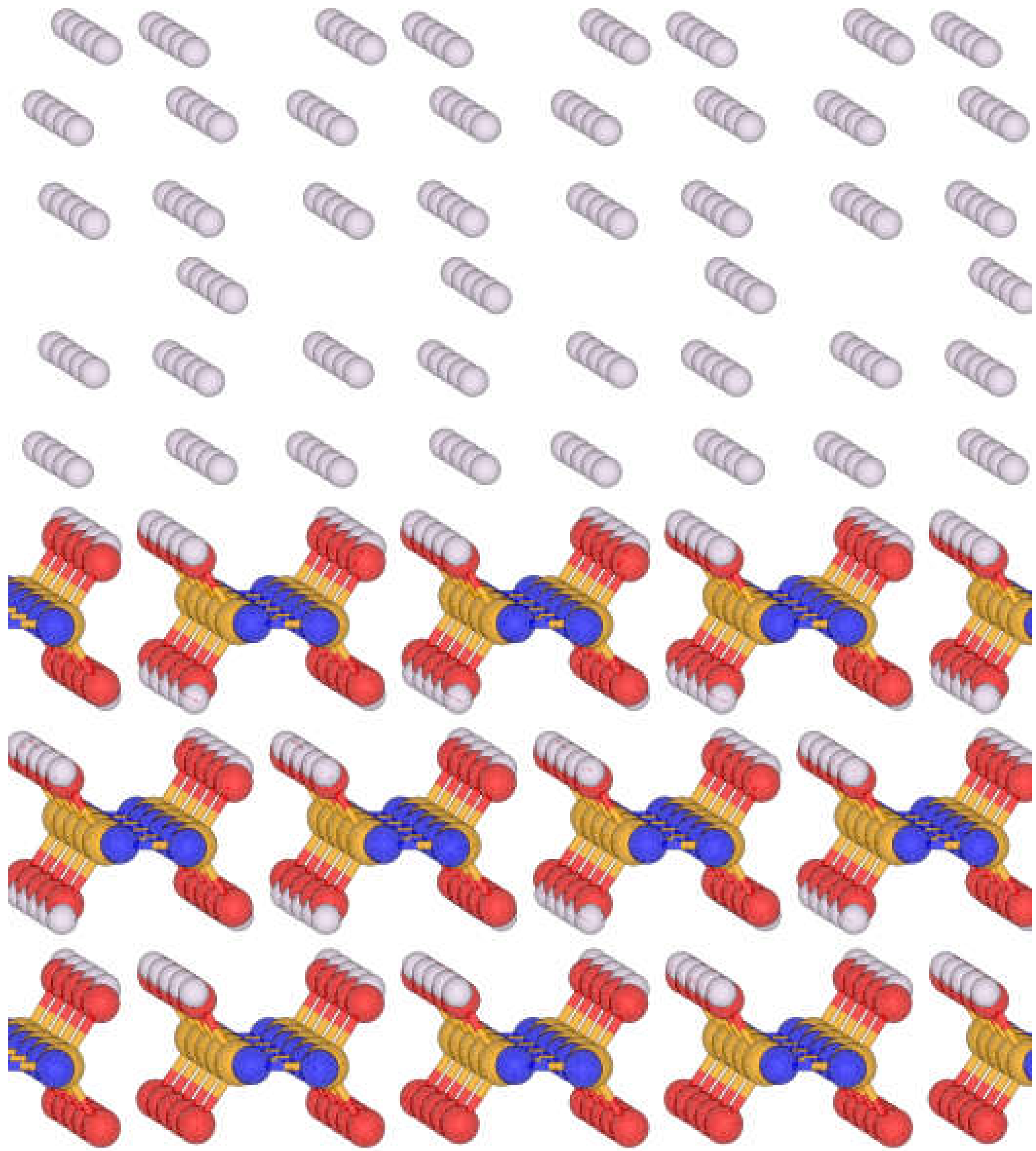

Quantitative study of interfaces – (Lepley & Holzwarth, *PRB* **92** 214201 (2015))

Within any given periodic simulation cell with n_a units of material a and with n_b units of material b, we can define an interface energy:

$$\tilde{\gamma}_{ab}\left(\tilde{\Omega}, n_a, n_b\right) = \frac{\tilde{E}_{ab}\left(\tilde{\Omega}, A, n_a, n_b\right) - n_a E_a - n_b E_b}{A}$$

area of interface within supercell

bulk energies

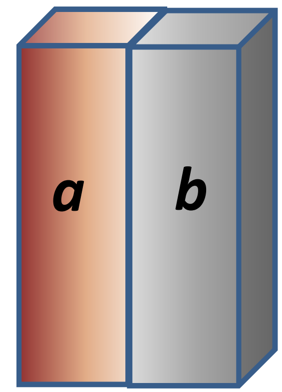

In order approximately remove the effects of lattice strain:

- Design the supercell to be commenserate with lattice a
- Now the strain will scale with the amount of material b

$$\Rightarrow \tilde{\gamma}_{ab}\left(\tilde{\Omega}, n_a, n_b\right) = \tilde{\gamma}_{ab}^{\lim}\left(\tilde{\Omega}\right) + n_b \sigma$$

It is convenient to model the interface between a solid electrolyte and solid electrode in the slab geometry using a periodic simulation cell:

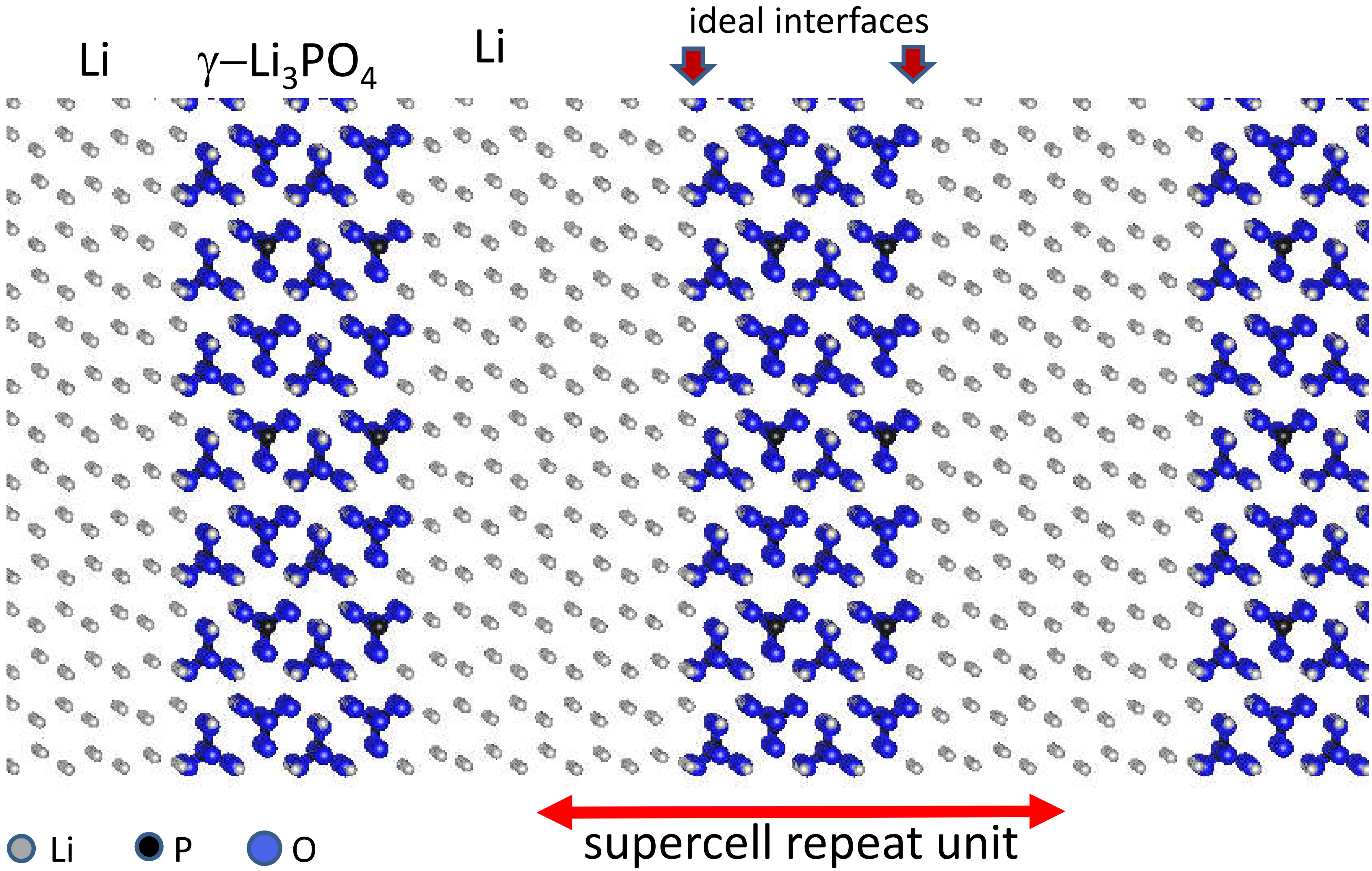

Lepley's linear equation for the interface energy: $\tilde{\gamma}_{ab}\left(\tilde{\Omega}, n_a, n_b\right) = \tilde{\gamma}_{ab}^{\lim}\left(\tilde{\Omega}\right) + n_b \sigma$

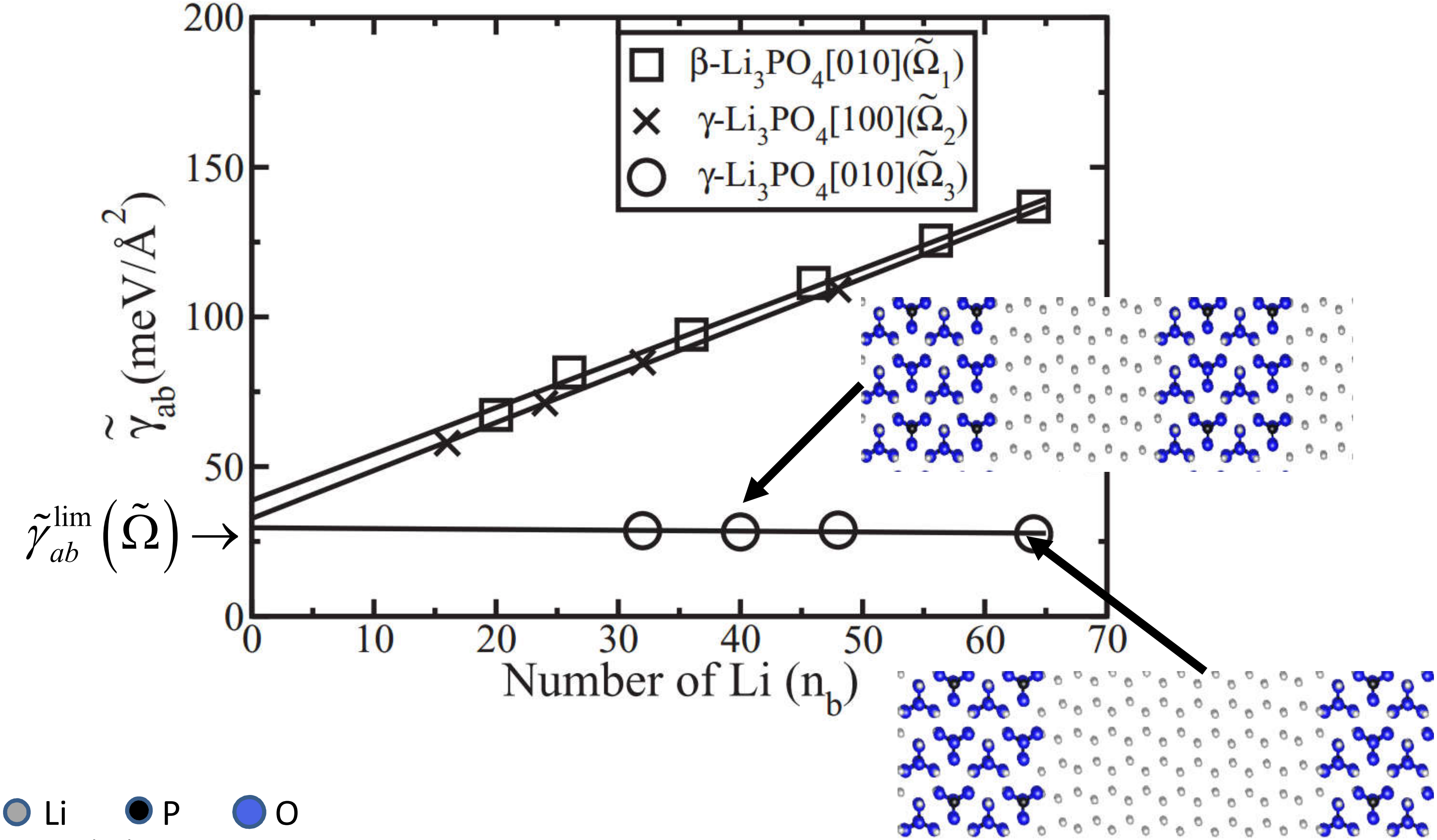

Li P O

Some interface energy results

System	$\tilde{\gamma}_{ab}^{\lim}$ (meV/Å²)	σ (meV/Å²)
Li_2O[110]/Li(Ω_1)	30	6.1
Li_2O[110]/Li(Ω_2)	26	0.2
Li_2S[110]/Li(Ω_3)	19	0.2
Li_2S[100]/Li(Ω_4)	19	0.0
γ–Li_3PO_4 [010]/Li(Ω_3)	31	0.0
γ–Li_3PS_4 [010]/Li_2S [110]	16	1.0
γ–Li_3PS_4 [010]/Li	-216	-0.1

γ–Li_3PS_4 [010]/Li_2S [110]

Li P S

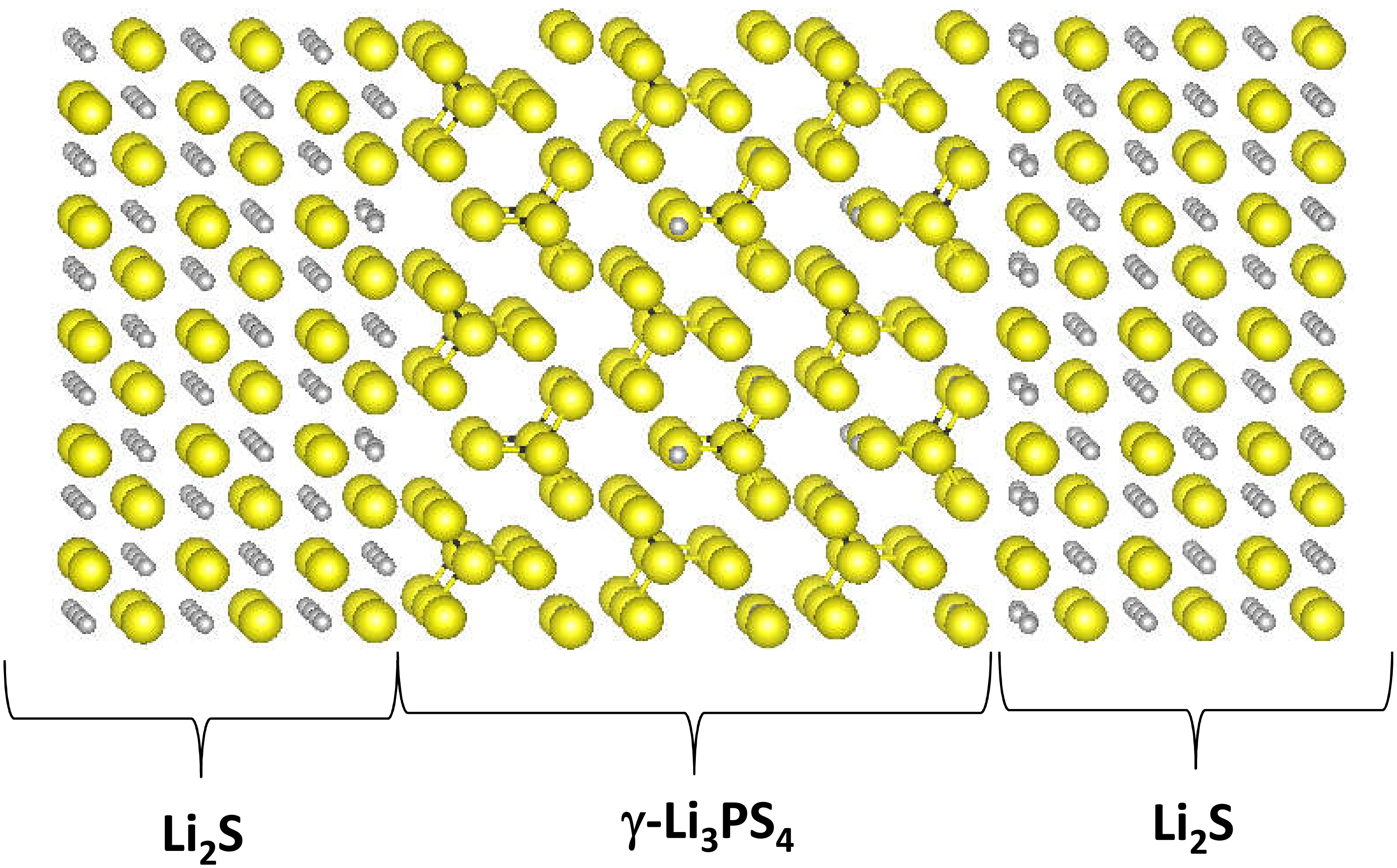

Stable interface; composite electrolyte system

γ–Li_3PS_4 [010]/Li

Li P S

WAKE FOREST UNIVERSITY

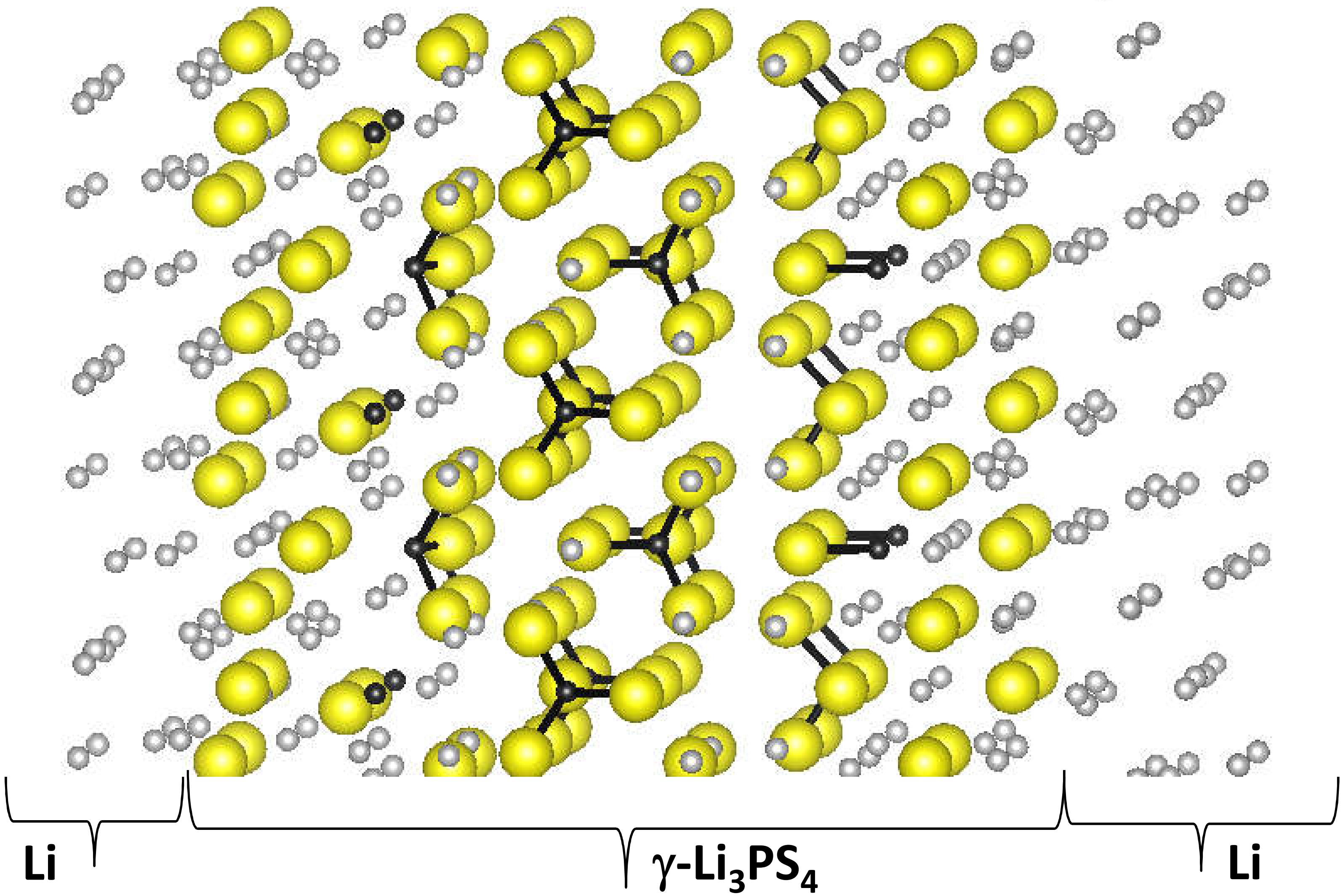

Initially unstable interface; (meta)-stable buffer layer formed

Partial density of states analysis of unstable Li_3PS_4/Li interface:

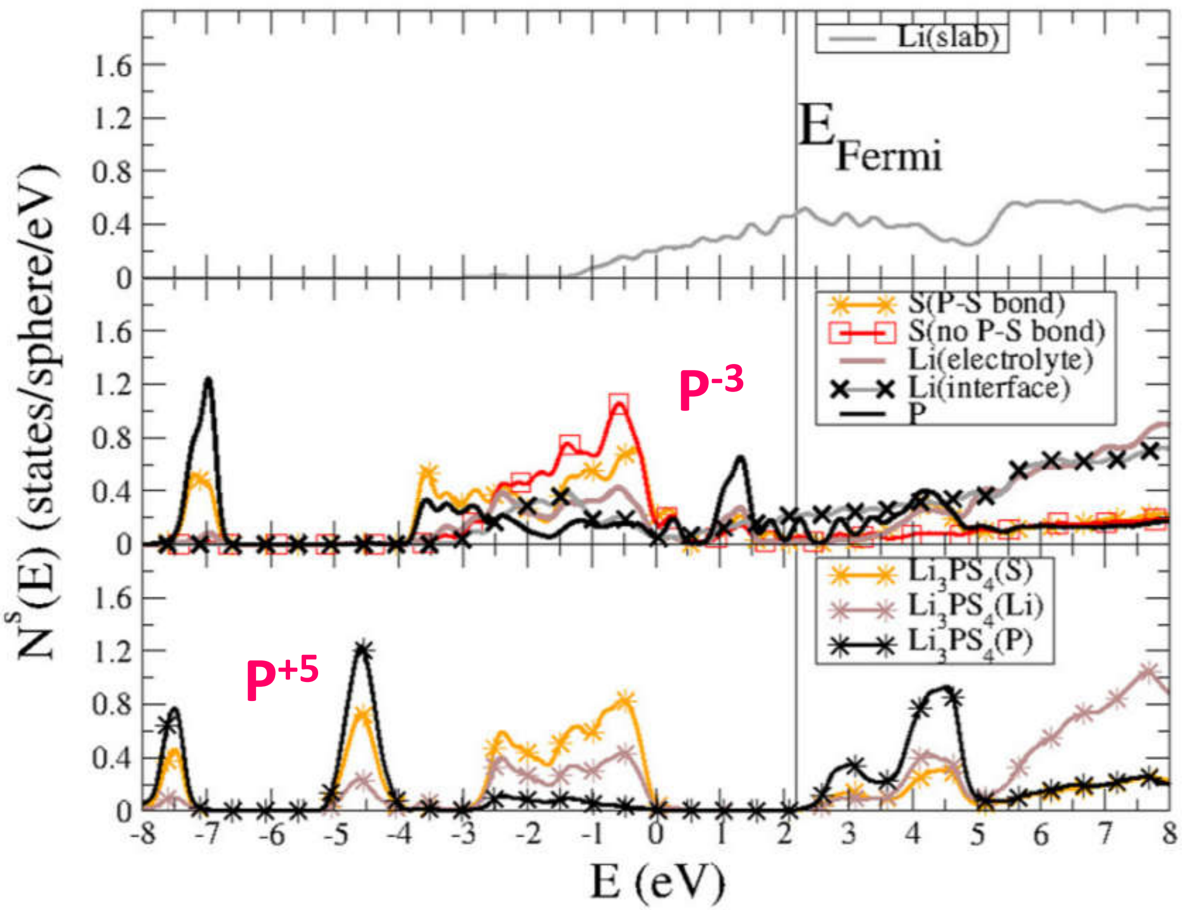

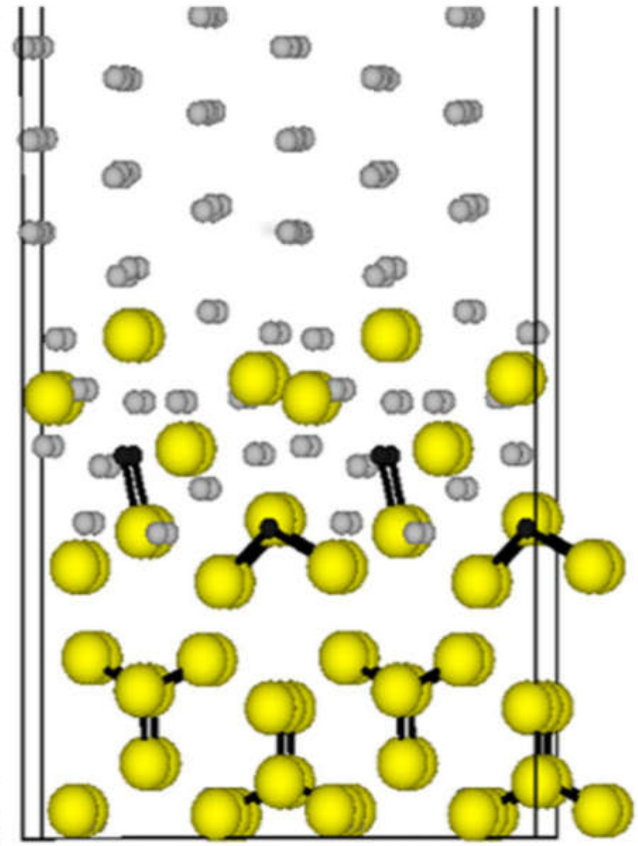

$$Li_3PS_4 + 8Li \longrightarrow Li_3P + 4Li_2S + 12.30\ eV$$

WAKE FOREST UNIVERSITY

Bulk reactions from estimated heats of formation

$$Li_3PS_4 + 8Li \longrightarrow Li_3P + 4Li_2S + 12.30\ eV$$

Decomposition at interface

$$Li_3PO_4 + 8Li \longrightarrow Li_3P + 4Li_2O + 6.64\ eV$$

(Meta-)stable interface

Evidence of kinetic barrier at Li_3PO_4/Li interface

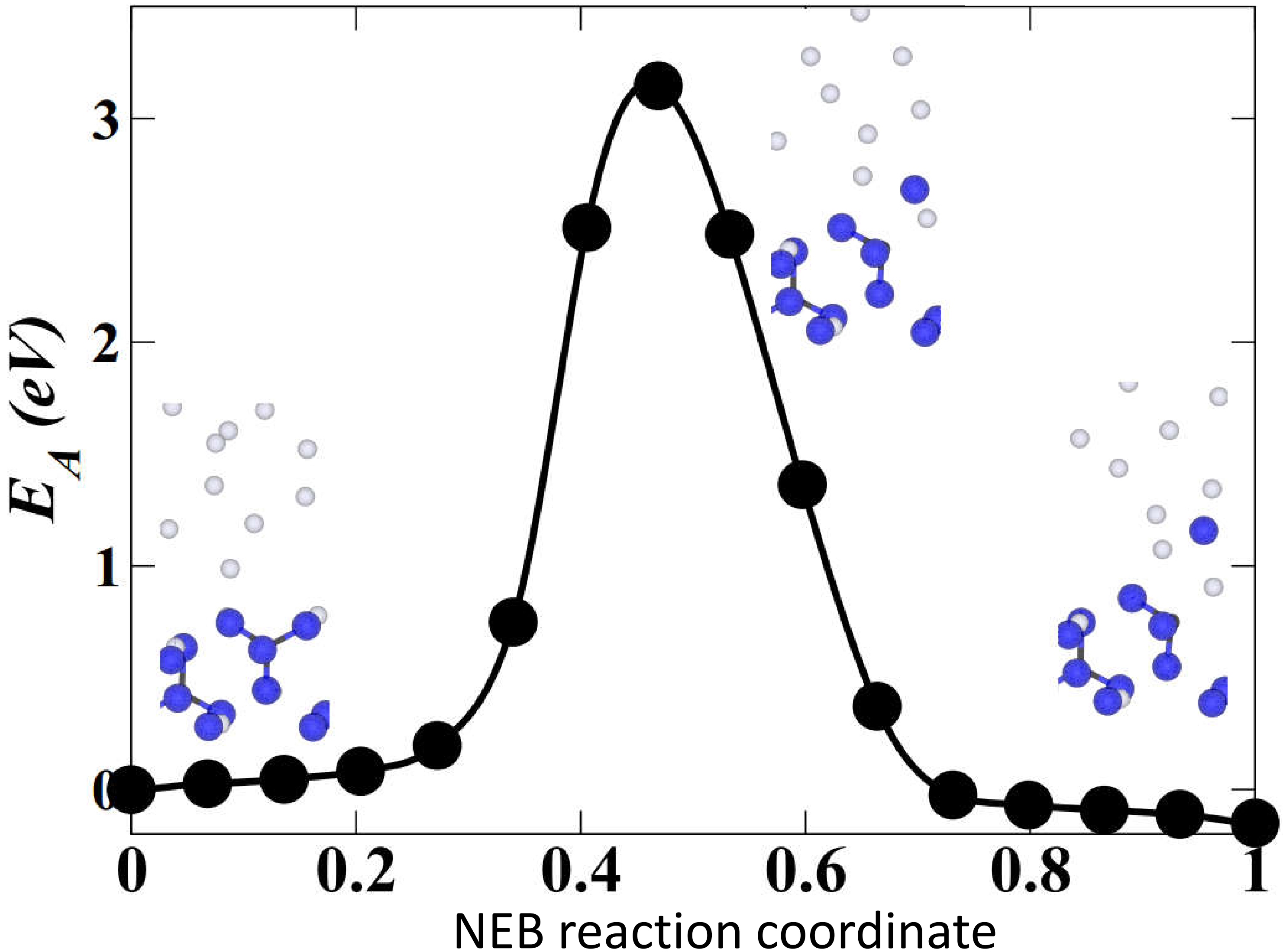

WAKE FOREST UNIVERSITY

Summary of ideal interface story

- A practical scheme was developed to compute an intensive measure of the interface interaction $\tilde{\gamma}_{ab}^{\mathrm{int}}$, explicitly accounting for the effects of lattice stain.
- Discussed bulk reactivity as related to the interface stability of the interfaces of
  - Li_3PO_4/Li (having a significant kinetic barrier to decomposition)
  - Li_3PS_4/Li (having localized decomposition).

Other thiophosphate compounds; comparison of $Li_4P_2S_6$ and $Na_4P_2S_6$

Zachary D. Hood, Cameron Kates, Melanie Kirkham, Shiba Adhikari, Chengdu Liang, and N. A. W. Holzwarth, *Solid State Ionics* **284**, 61-70 (2015)

Larry E. Rush Jr. and N.A.W. Holzwarth, *Solid State Ionics* **286**, 45-50 (2016)

High temperature processing of Li and Na thiophosphates have shown to produce dimer units $(P_2S_6)^{-4}$ (hexathiohypodiphosphates):

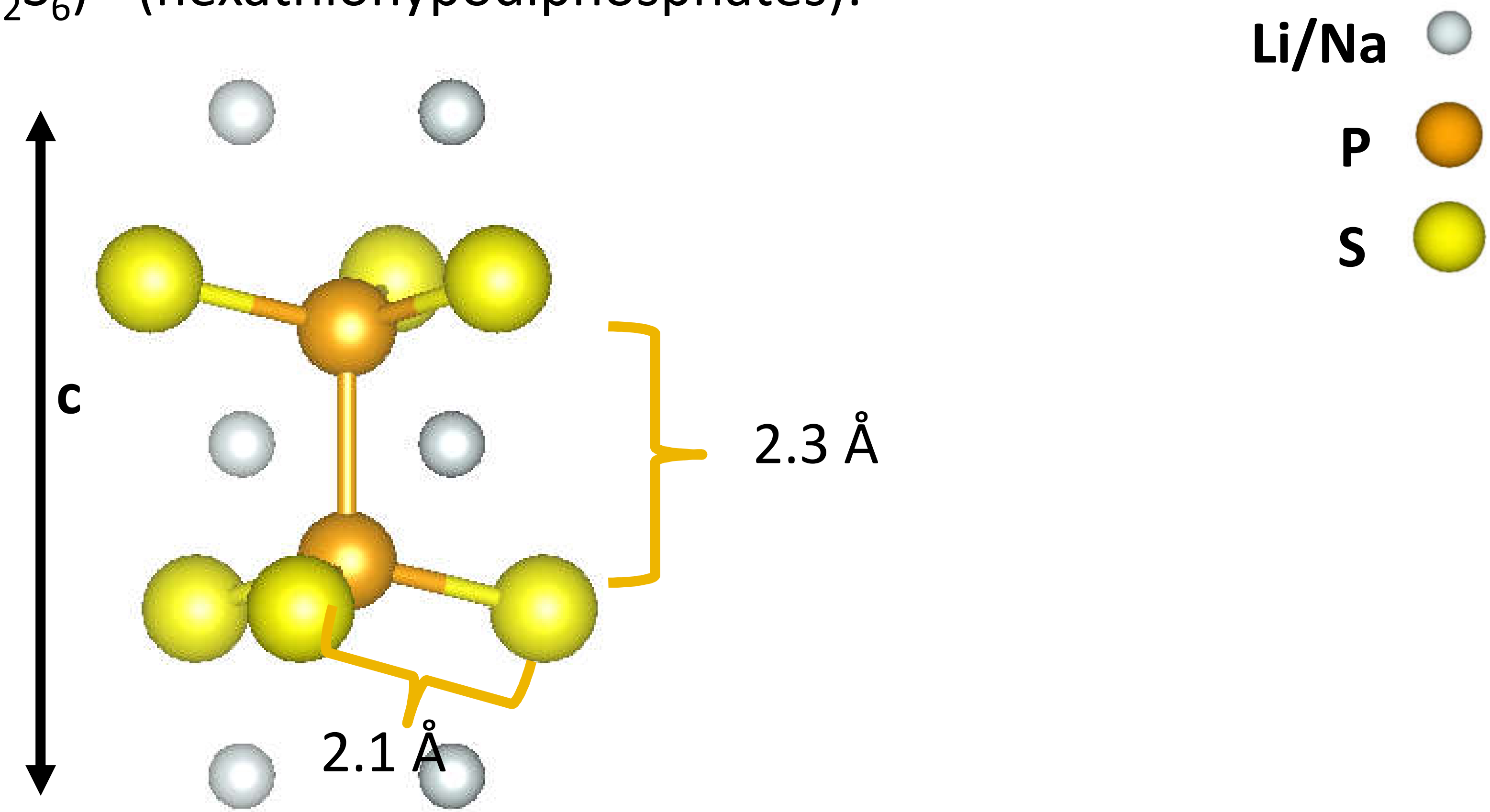

R. Mercier, J.P. Malugani, B. Fahys, J. Douglade, G. Robert, *J. Solid State Chem.* **43,** 151–162 (1982).
A. Kuhn, R. Eger, J. Nuss, B.V. Lotsch, *Z. Anorg. Allg. Chem.* **640,** 689–692 (2014).

Mercier's analysis of $Li_4P_2S_6$

-- disorder in P-P placements

Crystal Space Group *$P6_3/mcm$* (#193)

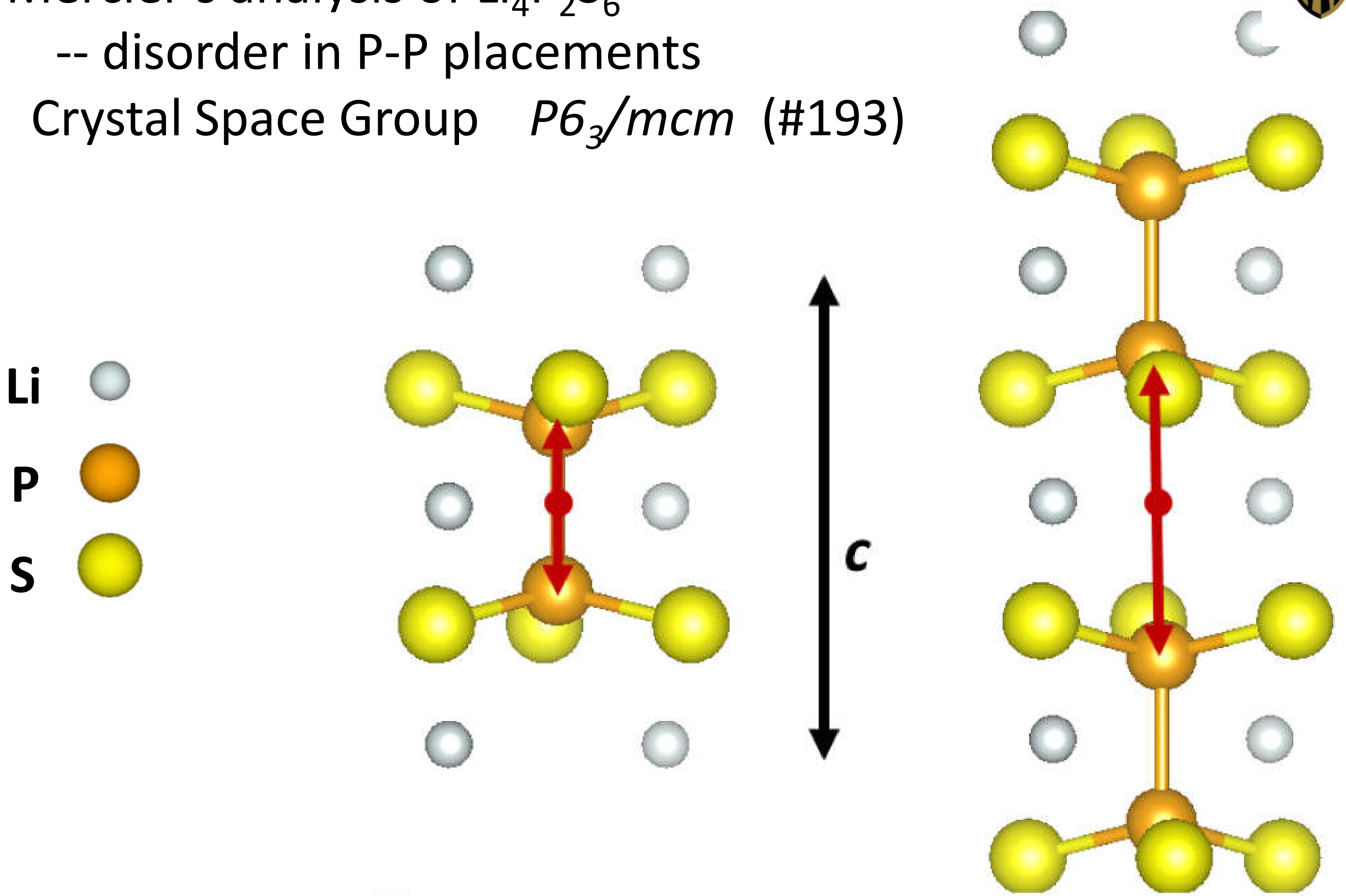

$$P_{\uparrow} \equiv \pm z_P c \quad P_{\downarrow} \equiv \pm\left(\frac{1}{2} - z_P\right)c$$

Structural variation can be mapped on to a two-dimensional hexagonal lattice with each P configuration taking P↑ or P↓ settings; Li and S configurations fixed

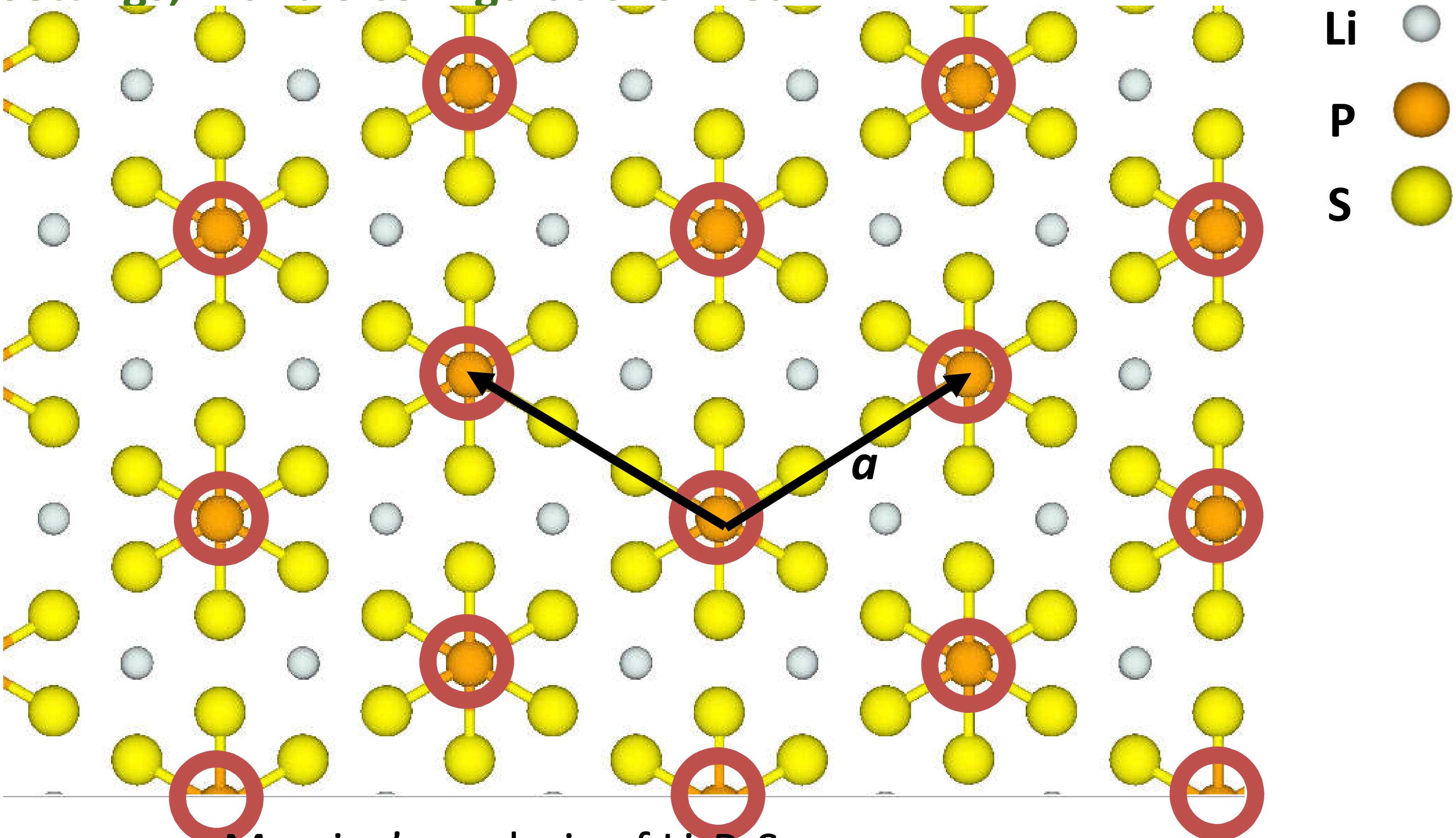

Mercier's analysis of $Li_4P_2S_6$

Examples: Mercier's analysis of $Li_4P_2S_6$

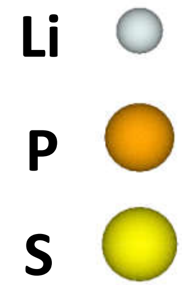

Structure "b"

$P\bar{3}1m$

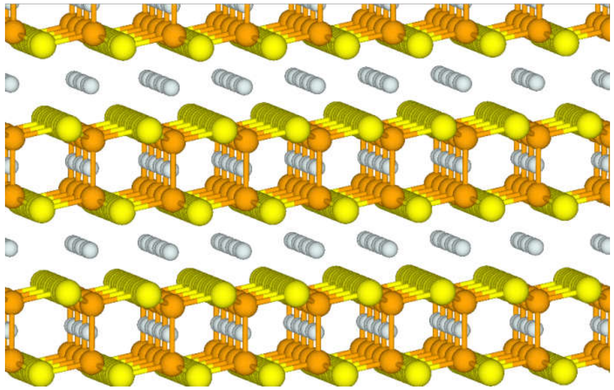

ΔE = 0.03 eV

100% P $\uparrow$

Structure "c"

Pnnm

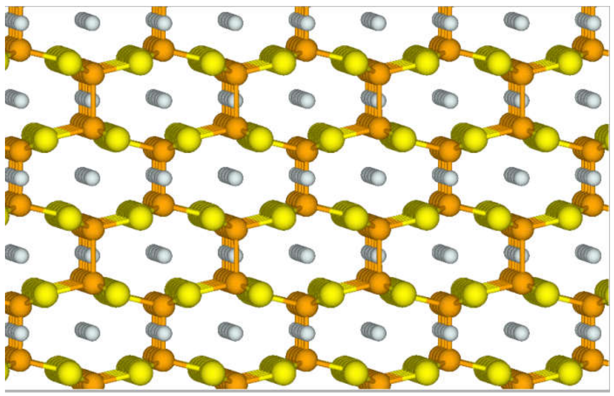

ΔE = 0

50% P $\uparrow$

50% P $\downarrow$

Structure "d"

Pnma

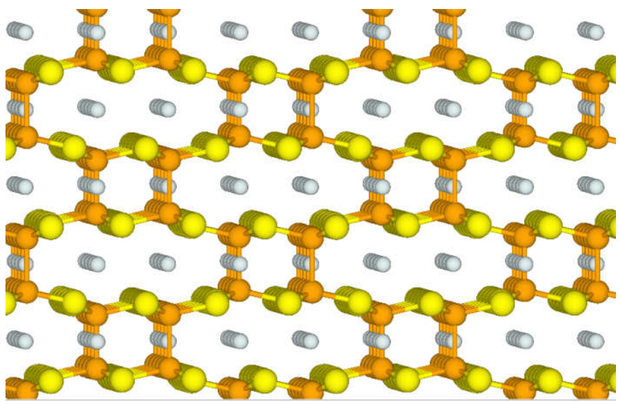

ΔE = 0

50% P $\uparrow$

50% P $\downarrow$

Two model configurations of disordered ground state structure

Structure of $Na_4P_2S_6$:

Kuhn et al., ZAAC **640**, 689-692 (2014) synthesized single crystals with a monoclinc structure having space group *C2/m* with similarities to the trigonal structure with $P\bar{3}1m$ space group

Structural comparison – *c*-axis projection

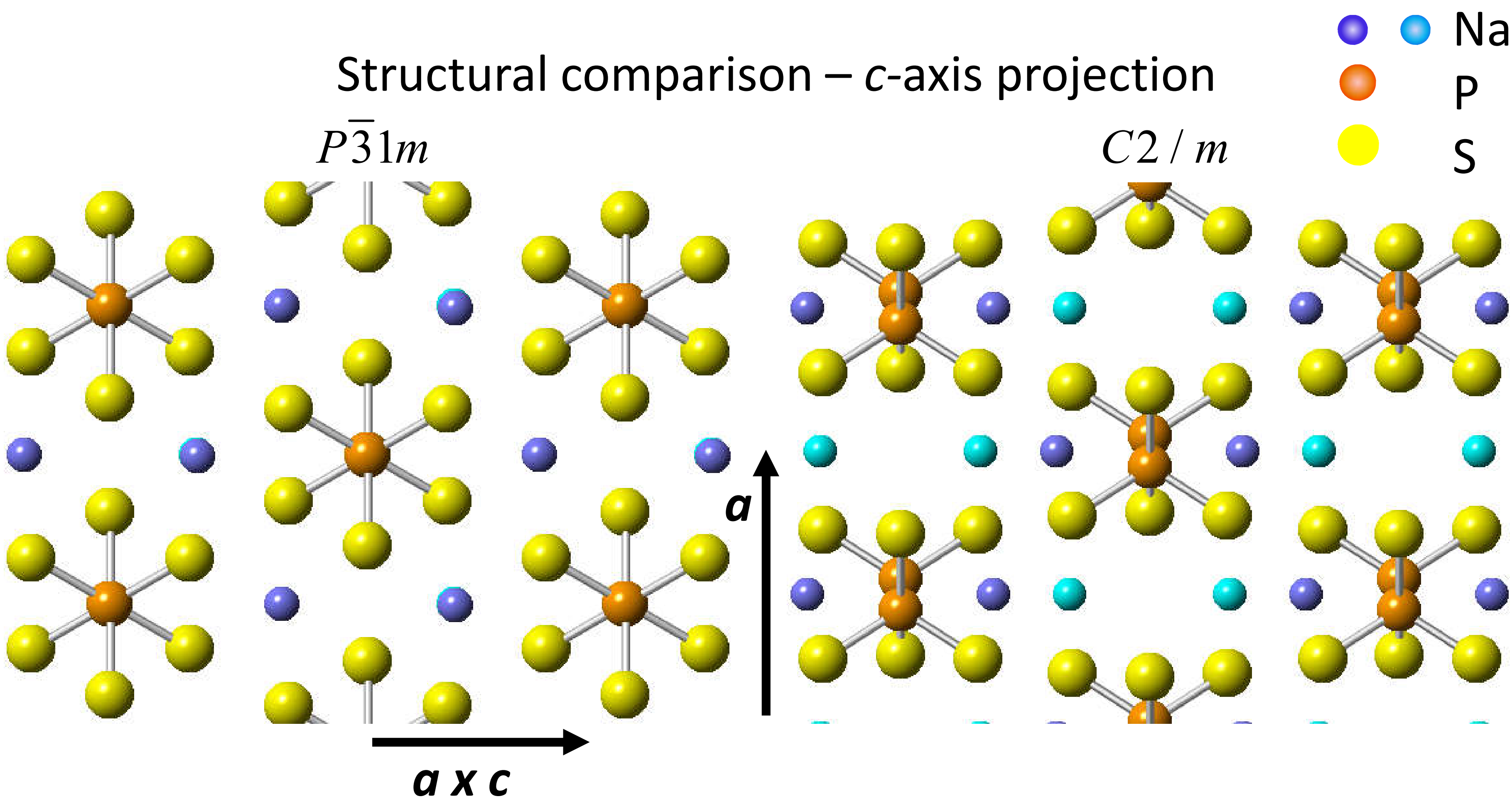

$Na_4P_2S_6$

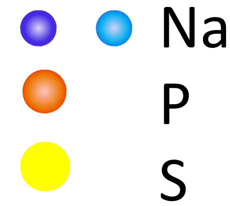

Structural comparison – view including *c*-axis

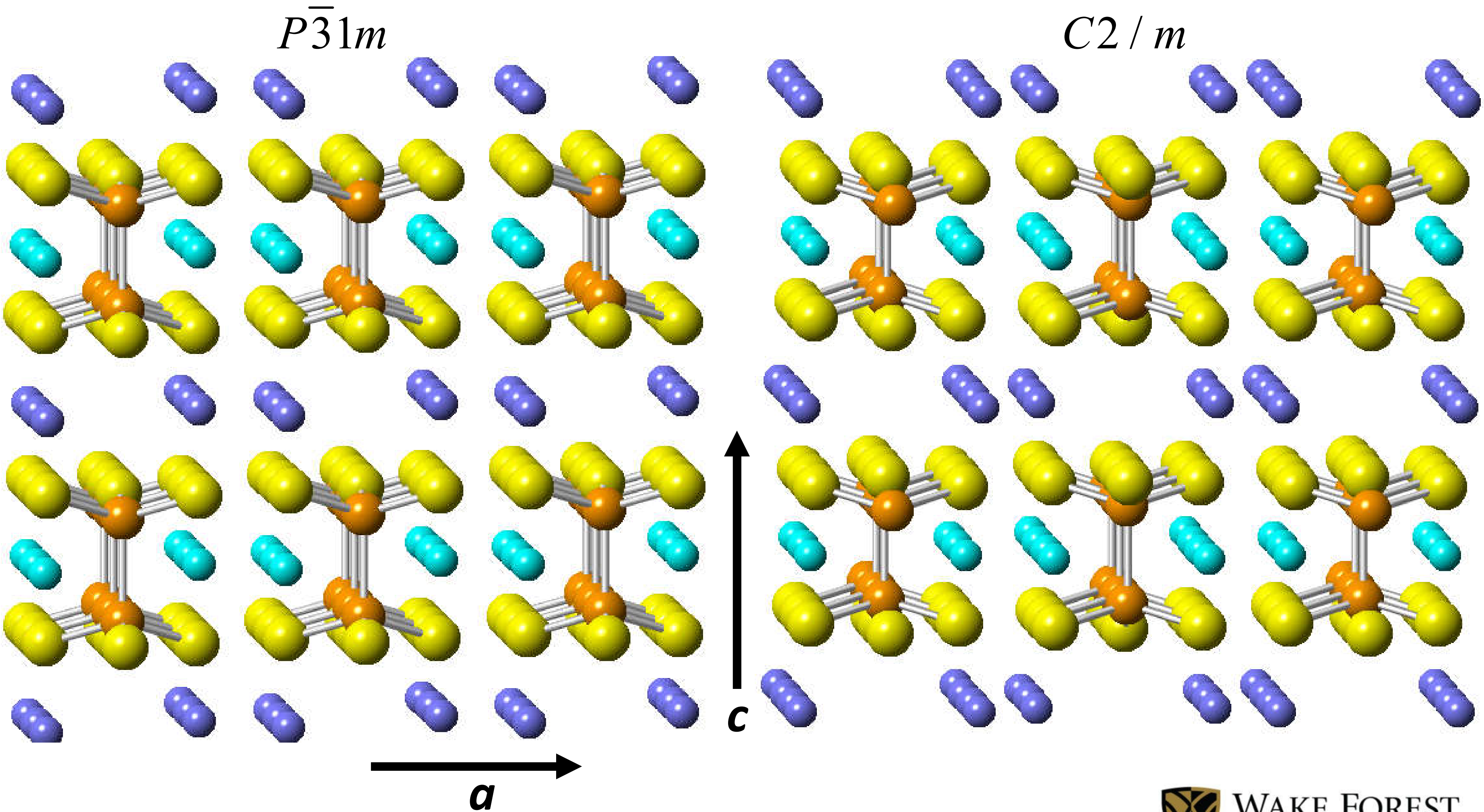

$Na_4P_2S_6$

WAKE FOREST UNIVERSITY

Structural comparison – view including *c*-axis

Na
P
S

$P\bar{3}1m$

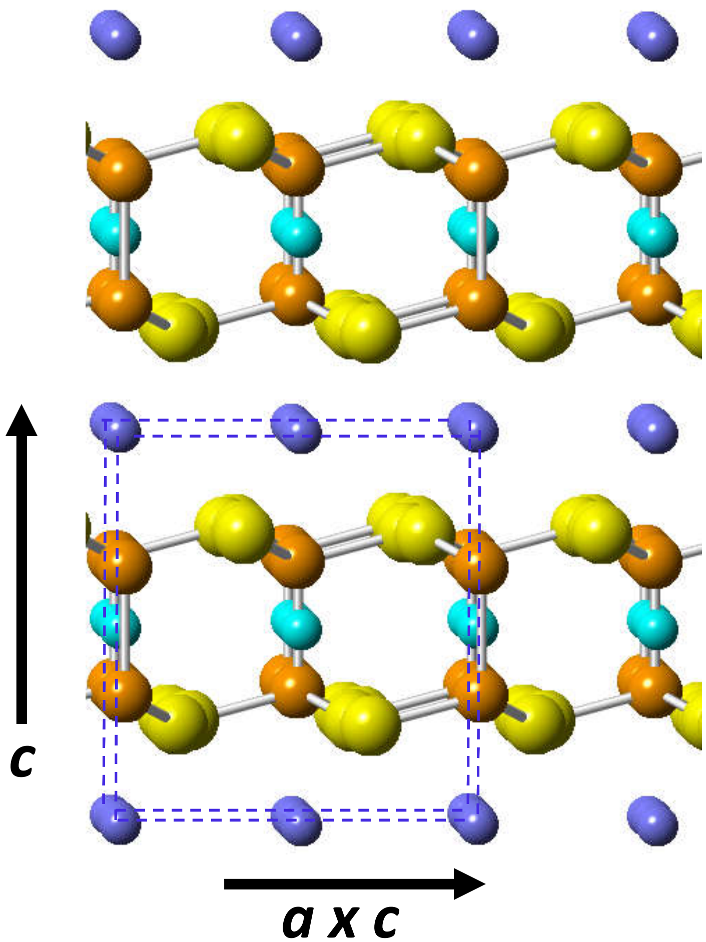

$C2/m$

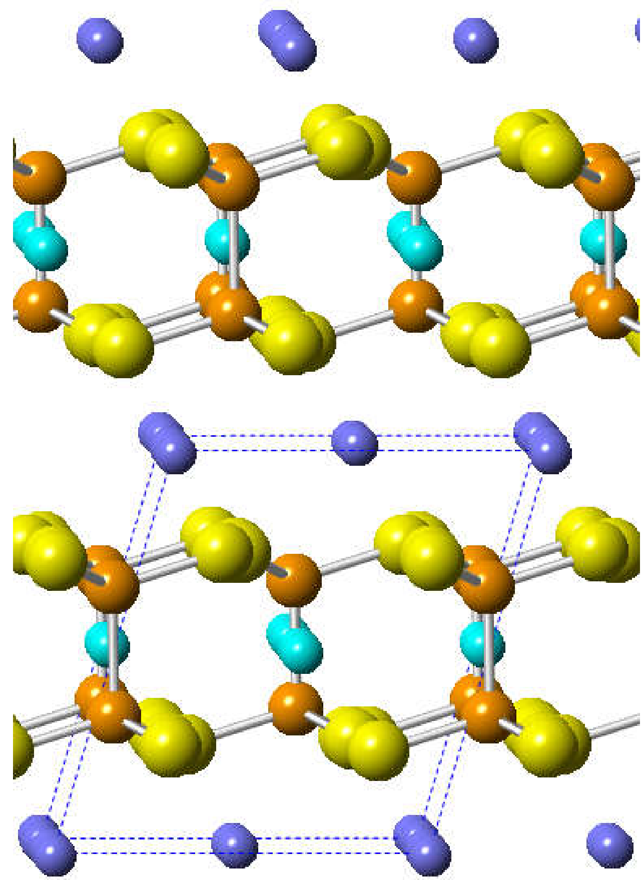

Results for $Na_4P_2S_6$:

Calculated heats of formation (eV per formula unit) for $Na_4P_2S_6$ and $Li_4P_2S_6$ in 4 structural models

	$Na_4P_2S_6$	$Li_4P_2S_6$
Kuhn structure	-11.47 eV	-12.07 eV
Structure "b"	-11.47 eV	-12.42 eV
Structure "c"	-11.56 eV	-12.46 eV
Structure "d"	-11.56 eV	-12.46 eV

Models of disordered Mercier structure

➔ Calculations find the most stable structure for both $Na_4P_2S_6$ and $Li_4P_2S_6$ to be the disordered Mercier structure, suggesting that the Kuhn structure is meta-stable.

Comparison of X-ray data for $Li_4P_2S_6$ with simulations

Note: simulations scaled by 102% to compensate for systematic LDA error.

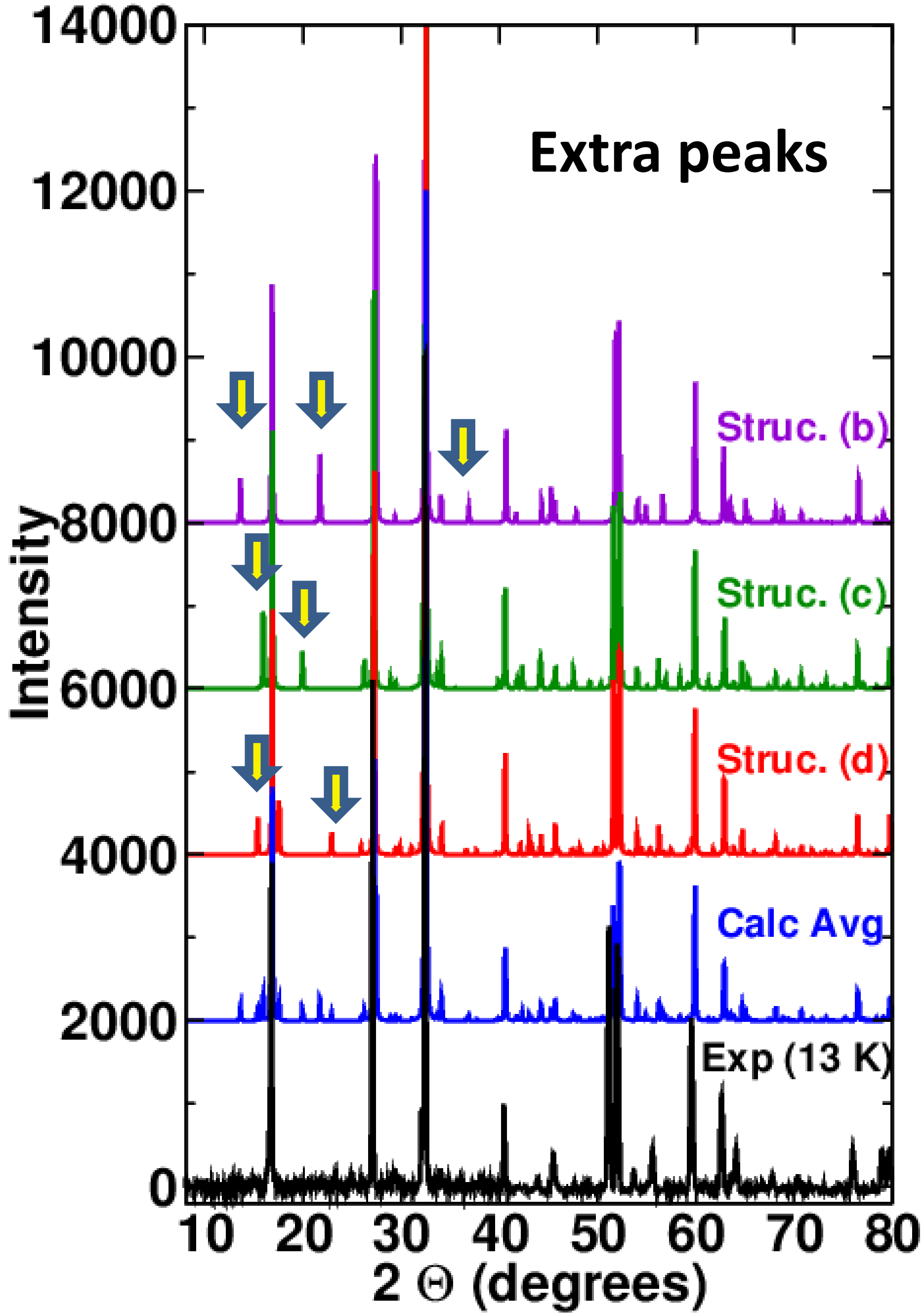

Simulations consistent with incoherent average over all P↑ and P↓ configurations

Ionic conductivity and Activation Energy for $Li_4P_2S_6$

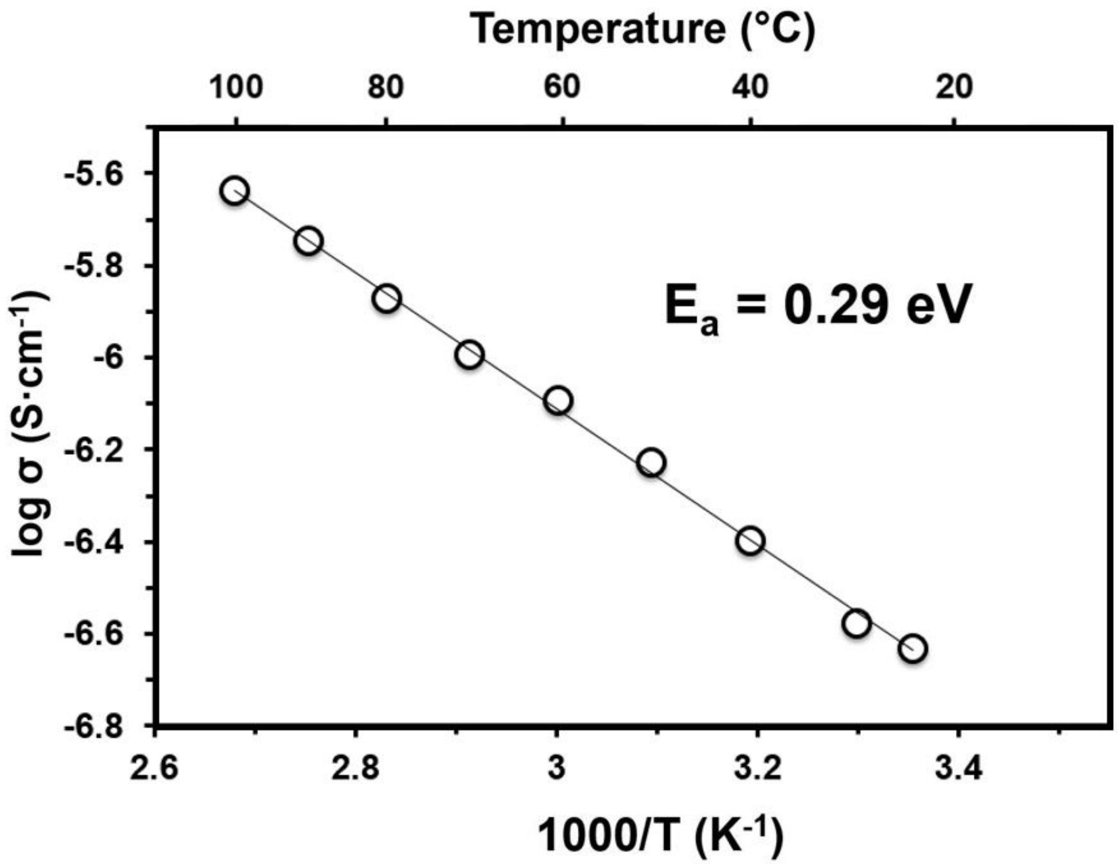

2.38 x 10^{-7} S/cm at 25˚C and 2.33 x 10^{-6} S/cm at 100˚C

$Li_4P_2S_6$ pressed pellets with blocking (Al/C) electrodes

Li/ $Li_4P_2S_6$ /Li cells could not be cycled

Comparison of vacancy migration of $Na_4P_2S_6$ and $Li_4P_2S_6$

$P\bar{3}1m$

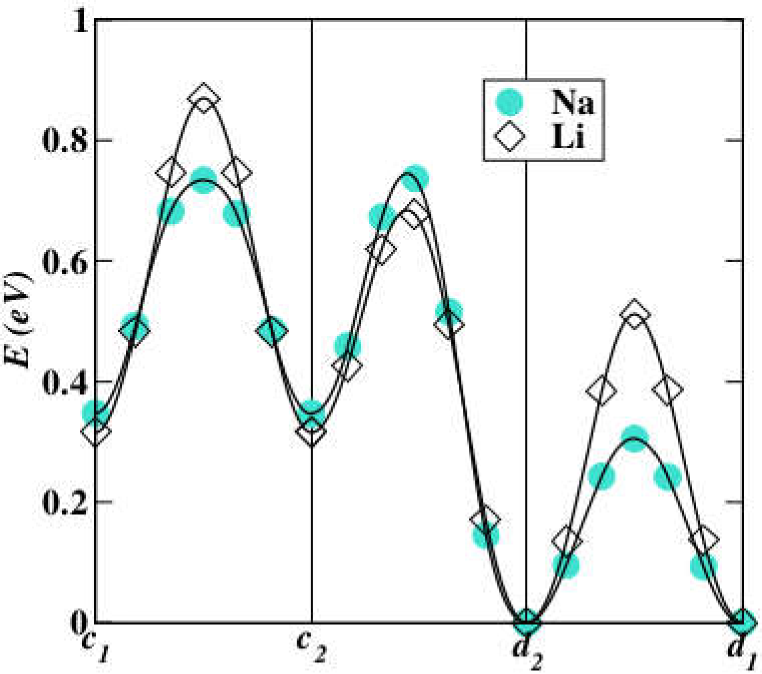

$C2/m$

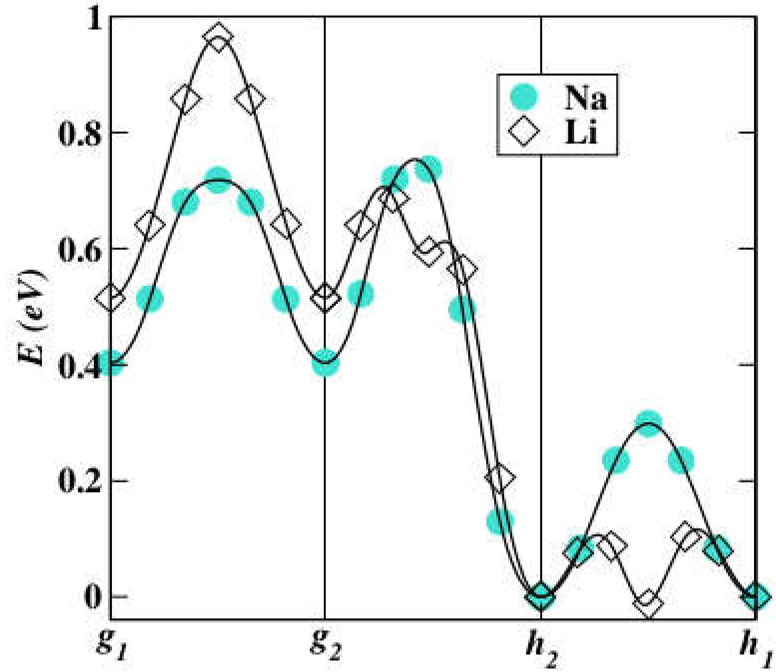

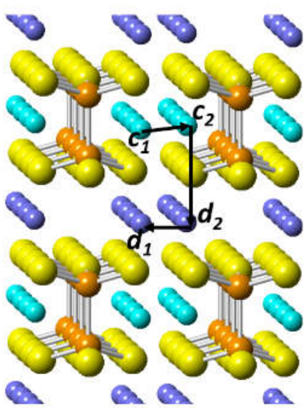

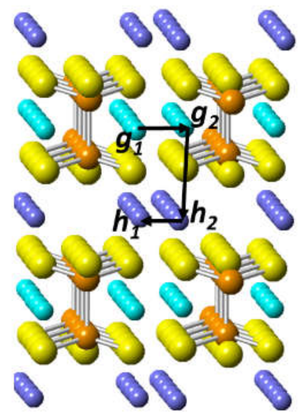

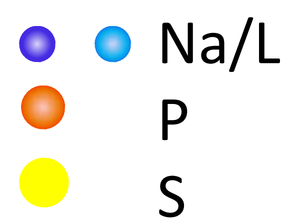

$P\bar{3}1m$ $C2/m$

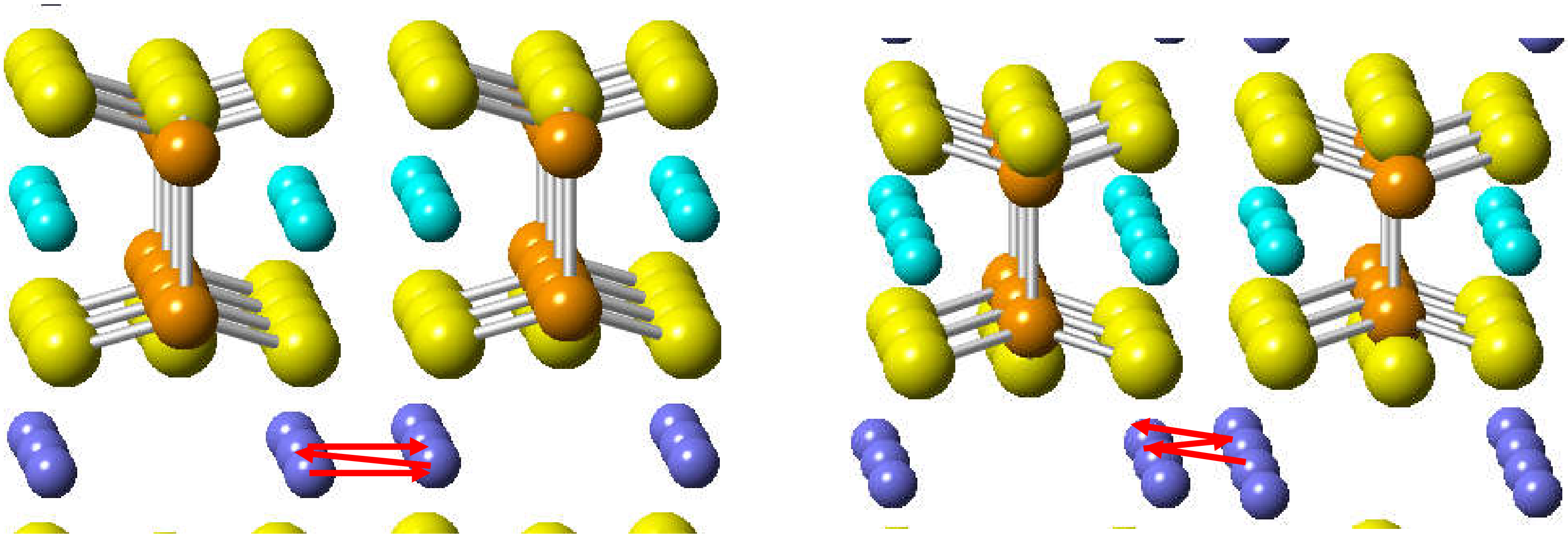

Minimum ion vacancy migration energies

Na/Li
P
S

	$P\bar{3}1m$	$C2/m$
$Na_4P_2S_6$	0.3 eV	0.3 eV
$Li_4P_2S_6$	0.5 eV	0.1 eV

Conclusions on studies of $Li_4P_2S_6$ and $Na_4P_2S_6$:

- $Li_4P_2S_6$ and $Na_4P_2S_6$ have interesting structural properties; simulations find the most stable structure for both to be the disordered Mercier structure, suggesting that the Kuhn structure is meta-stable.
- Experimental structural studies for $Li_4P_2S_6$ agree with the simulations; material is found to be remarkably temperature independent and thermally stable relative to other thio-phosphates.
- Measurements find $Li_4P_2S_6$ to have low ionic conductivity; simulations suggest that $Na_4P_2S_6$ may have more favorable ionic conductivity.
- Models of ideal $Li_4P_2S_6$/Li interfaces find broken P—S bonds; $Na_4P_2S_6$/Na interfaces in the Kuhn structure may be slightly more stable

WAKE FOREST UNIVERSITY

Additional thoughts

- Limitations of first principles modeling
  - Small simulation cells
  - Zero temperature
- Possible extensions
  - Develop approximation schemes for treatment of larger supercells
  - Use molecular dynamics and/or Monte Carlo techniques
- Ideal research effort in materials includes close collaboration of both simulations and experimental measurements.
- For battery technology, there remain many opportunities for new materials development.